UPHEAVAL BUCKLING OF BURIED PIPELINES

Master thesis at the University of Stavanger

Marius Loen Ommundsen

Stavanger, 29th of June 2009

Upheaval buckling simulation from an experiment

Universitetet i Stavanger

I·K·M Ocean Design AS

Summary

This thesis is divided into two parts. The first part consists of an introduction to theory and design aspects regarding the subject of thermal buckling with main focus on buried pipelines. The second part introduces the reader to the experiments performed in this thesis, including the analytical tests performed in ANSYS followed by a presentation of the derived results. Analysis of the results, conclusions and recommendations for further work is presented in the final chapter.

A lifting experiment was performed to detect and analyze the resistance provided by different soils. Upheaval buckling experiments were performed to detect a general behavior of a pipe in different upheaval buckling scenarios.

Several scenarios regarding upheaval buckling were tested including;

- Upheaval buckling over an imperfection with gravel, sand and clay as cover respectively
- Upheaval buckling with a trenched pipe without cover in granular soils
- Creep scenario simulating a pipeline going in and out of service while buried in clay
- Upheaval buckling with various imperfection heights while buried in clay

Most of the experiments provided interesting results, and some unforeseen happenings with the experiments in clay led to tough challenges. This also made some of the intended objectives for the thesis hard to fulfill.

All performed experiments are presented graphically in the appendix. A CD with videos from the experiments, analytical calculation summaries and measured data is attached to this thesis available for external overview and verification.

It is recommended that you watch the video before reading.

Preface

This thesis has been written in the spring of 2009 as the final examination before achieving my master degree in Offshore Systems – Marine and Subsea Technology at the University of Stavanger. The thesis has been defined in cooperation with IKM Ocean Design, Forus. The assembling and construction of the test rig was performed at the concrete lab at the University of Stavanger. The experiments were carried out at a barn at Nærbø, which during this period functioned as a test laboratory. IKM Ocean design provided office space at their location, where most of the writing and the analytical part of the thesis was performed.

During this period employees at the University of Stavanger and IKM Ocean Design has given useful advice and guidance to help me with the thesis. I have also received help from friends and family as some parts of the experiments could not be carried out alone. Persons who deserve a great thank you are;

Employees at the University of Stavanger;

- Professor Ove Tobias Gudmestad who has been my supervisor. He has given valuable guidance on design of the test rig, performing of the experiments and given continuously feedback on the writing of the report during the whole progression of the thesis.
- John Grønli, teacher, who has helped with funds and introduced me to the concrete lab where geotechnical tests were performed. He ordered the polycarbonate plates used in the test rig. He has also given useful advice on performing the experiments and preparation of the clay.
- Ahmad Yaseen Amith, teacher, for teaching me how to use the measuring equipment and mounting of strain gauges, scaling the load cell, using the Catman software and the Spider 8 amplifier.
- Samdar Kakay, employee, for being a great support as we both worked in the concrete lab with separate projects. He has also given me valuable guidance on how to perform geotechnical measures of the soils.

Employees at IKM Ocean Desing;

- Engineering manager Per Nystrøm for providing funds and office space, guidance on performing experiments and defining relevant problems.
- Kristin Sandvik, engineer, for advice on how to design the test rig, as she had experience in performing similar experiments. [4]
- Ingar Stava, engineer, for useful advice on performing the experiments and advice on mounting the strain gauges. He was also present at one of the first experiments carried out.
- Norman Vikse, engineer for introducing me into the scripts used for analytical calculations in ANSYS. He has used a lot of his time helping me with the analysis.
- Line Newermann, engineer, for helping me getting the analysis running.

- Juan Giong, engineer, for suggestions to get the analysis running properly.
- All employees at IKM Ocean Design`s location for showing interest in the thesis.

Stavanger 29.06.09

Marius Loen Ommundsen

Contents

Nomenclature and abbreviations

Abbrevations

ROV	Remotely Operated Vehicle
DNV	Det Norske Veritas
ULS	Ultimate Limit State
FEM	Finite Element Method
OD	Outside diameter
ID	Inside diamter
1D	One times Diameter cover height
2D	Two times Diameter cover height

Nomenclature

σ_H	= Circumferential stress
p	= Internal pressure
R	= Radius
t	= wall thickness
ε_L	= Longitudinal strain
E	= Young`s modulus
s_L	= Longitudinal stress
α	= Linear thermal expansion coefficient
θ	= Change in temperature
ν	= Poisson`s ratio = 0.3
S_0	= Effective axial force
H	= Residual lay tension
Δp_i	= Internal pressure difference compared to as laid.
A_i	= Internal area
υ	= Poisson`s Ratio
A_s	= Area of the steel
ΔT	= Temperature increase compared to temperature during installation
y	= height
x	= horizontal distance
H	= imperfection height
L	= imperfection length
q	= Total download (including resistance from cover if buried and own weight)
F	= Flexural rigidity
P	= Longitudinal compressive forced
R_m	= Mean radius between external and internal radius
q'	= Uplift resistance
γ	= Submerged weight of soil
H	= Height from top of pipe to seabed surface (top of cover)
D	= Total diameter including coating
f'	= Uplift coefficient determined experimentally
γ'	= Submerged weight of soil
ϕ	= Frictional angle
K	= Lateral earth pressure coefficient accounting for increased stress in vertical direction
N_c	= Theoretical bearing capacity coefficient

η = Empirical factor based on field tests
s_u = Undrained shear strength at centre of pipe
r = Roughness factor for pipe
$\bar{s}_u$ = Average undrained shear strength from centre of pipe to top of cover
γ_{UR} = Safety factor
$\sigma_{configuration}$ = Accuracy of surveys
$T(k_{BE})$ = Temperature at which failure occurs whit best estimate downward stiffness
$T_{failure}$ = Temperature at which failure occurs
p_{li} = Local incidental pressure
R_c = Sand and rock uplift resistance
γ_{UR} = Safety factor
k_{BE} = Best estimate downward stiffness
$T(k_{LB})$ = Temperature at which failure occur whit lower bound downward stiffness
k_{LB} = Lower bound downward stiffness
δ = Prop imperfection
T_{Rd} = Design resistance equivalent failure temperature
T_{Rd} = Design resistance equivalent failure temperature
H_{min}, = Minimum cover height
R_{min} = Minimum soil resistance
H_{spec} , = Specified cover height
R_{spec} = Specified soil resistance

For figure 4.5

y = height of arbitrary profile
x = horizontal distance
P = Longitudinal force
S = Shear force
q = External vertical force per unit length

Table of figures

List of tables

1. Introduction

In the offshore industry, submarine pipelines are used to transport hydrocarbons from a production facility to a receiving terminal. Pipelines can in some cases be buried under the seabed due to stability issues, risk of impact with fishing gear and due to other causes.

When production starts through a pipeline, internal temperature and pressure will rise. The temperature increase will lead to thermal expansion of the steel. A pipeline will be restrained variously along the routing due to soil friction, and the temperature rise will result in axial compressive forces in the pipe. As a response to the longitudinal compressive force interacting with local curvature of the pipe, global buckling may occur.

A pipeline can buckle downwards in a free span, sideways on the seabed or upwards for buried pipelines. Vertical buckling of a pipeline is called upheaval buckling, and the direction of the buckle is upwards because this is the way of least resistance. If a vertical buckle leads the pipe into exposure on the seabed, this is a severe problem. An expensive and time consuming operation is needed to re cover the pipe at this location. If the buckle damages the pipeline, this part must be replaced before re covering takes place.

2. Objectives

This thesis will deal with upheaval buckling of buried pipelines. Some theory behind the phenomenon of upheaval buckling is covered, and two types of experiments are carried out, where one is simulating an upheaval buckling occurrence in different soil conditions, and the other is a lifting experiment to detect the resistance in different soil materials. The purpose of this lifting experiment is to compare the resistance in different soil materials used as cover for buried pipelines. A 10 mm, a 22 mm and a 28 mm outside diameter Copper pipe will be buried in a test box with clay, gravel and sand as cover materials separately. Further the pipe will be lifted out of the mass by wires and a rotating reel. The forces needed to lift out the pipe will be measured by load cells, and a comparison of the forces will be performed for the different cover materials. Additional points with this experiment is to try to document the angle of the rupture lines in the cover materials, as well as finding a ratio between the resistance in the cover material, and the pipe diameter.

The upheaval buckling tests are performed with different cover materials and different cover heights. In order to make the pipe buckle, a hydraulic pump will push on the front end of the pipe, while the pipe is constrained at the counter end. The axial force from the pump will lead the pipe into compression. The pipe will have a slight vertical curvature initially to trigger the buckle upwards. The axial force will be increased continuously until the pipe has broken trough the surface of the cover material. A load cell will be attached to the hydraulic pump to measure the axial force. Strain gauges will be attached at certain positions of the pipe to monitor strain in the pipe. Further the vertical deflection of the pipe will be measured. Tests will be performed with various cover heights. As for the lifting experiments the materials used will be sand, gravel and clay. By the monitored strain at different locations the behavior of the pipe will be studied. The capabilities of the different soils to prevent the pipe from buckling will be decided by the axial force needed to make the pipe buckle. In addition a creep scenario simulating a pipeline going in and out of service will be performed. Two imperfection heights are also used for the experiments in clay, to find a relation between the imperfection height and axial force.

Analytical calculations of the experiments will be performed using the finite element method software ANSYS. The purpose for the analytical analysis is to compare the results with the derived test data gathered from the experiments.

3. Buried pipelines

3.1 Purpose of burying pipelines

When a pipeline routing is decided, considerations regarding outer activities that can interfere with the pipeline are made. For areas with frequent fishing, burying a pipeline will eliminate the risk of trawl gear interfering with the pipeline. There are also problems with ships anchoring near pipelines that can result in a pipeline being pulled out of position. A buried pipeline will also be protected from dropped objects. This is especially important near field installations with high activity due to modifications and maintenance. Pipelines with low submerged weight have challenges with stability due to buoyancy and currents. Burying the pipe will prevent pipe movements due to currents and buoyancy. The overlaid cover will isolate the pipe from the seawater. On the seabed the ambient temperature can be as low as -1.9 degrees in saltwater and low temperatures in the pipe may lead to hydrate formation. In addition burying of pipelines is common when pipeline crossings occur on a routing, or to prevent buckling on an uneven seabed. Figure 3.1 shows a typical cross section for a buried pipe.

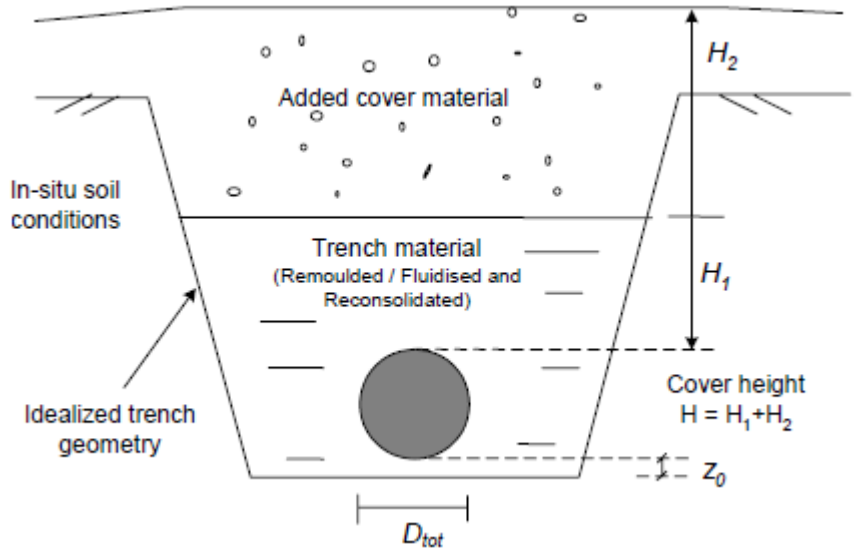

Figure 3.1 Cross section of buried pipeline [1]

3.2 Installation

The installation process of a buried pipeline includes several phases. The laying of a pipeline is similar to a conventional laying operation. The pipe can either be laid directly into a prepared trench, or be trenched after it has been laid on seabed. Before the pipe is lowered into a trench, it has to be filled with water to remain stable on the seabed. There are several vehicles available to trench the pipe. In areas with hard soil that is difficult to break, dumping of rock or gravel over the pipe can be applied. Rock dumping is also the most common way of burying pipelines, if only parts of the pipeline need to be buried. This can for example be over areas with uneven seabed, or over pipeline crossings. [3]

3.2.1 Jetting

A jetting system consists of a jetting vehicle and an assisting vehicle or barge. The jetting vehicle can typically be a ROV, remotely operated vehicle that receives power and signals through an umbilical from an assisting vessel. The vehicle flushes the seabed through jets with a high pressure fluid stream, eroding the seabed. Sand pumps are applied to move the spoil. The vehicle straddles the pipeline with one leg on each side and it is possible to perform several passes to reach a desired trench depth [3].

3.2.2 Mechanical cutting

A mechanical cutting machine has mounted equipment that can pick out the soil under the pipe. The machine is equipped with dredge pumps that suck the soil and ejects it to a suggested side. The machine can transport itself by wheels, and the orientation of the cutting blades can decide the angle of the slope sides of the trench [3].

3.3 Cover

Seabed soil, trenched soil or additional soil is used for covering pipelines. Additional soil can typically be rocks or gravel gathered from an onshore quarry. When rock dumping, cover material is dropped from a vessel through a steering pipe with acoustic profiling to minimize loss of rock. When trenching is performed, the spoil will lie as a pile alongside the trench. By use of a plow the spoil material can be moved into the trench to cover a pipeline. When using this method, water pockets appear in the material giving reduced strength at certain areas of the backfill. A jetting machine can also be capable to flush the spoil backwards alongside the trench. The soil will then be liquefied leaving a homogenous soil with remolded strength [1]. Different cover options are displayed in figure 3.2. At regions with hard seabed soil, rock-dumping can be applied. Trenching can also be performed without backfill to get a more even seabed.

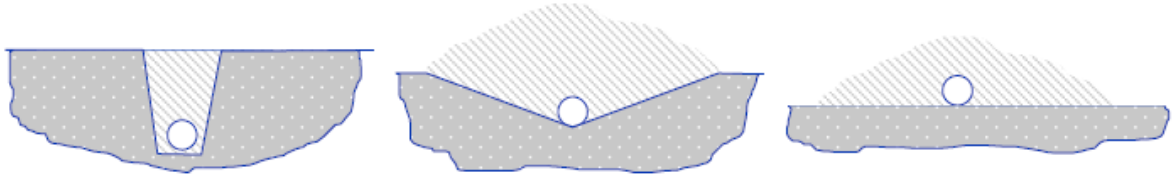

Figure 3.2 Schematic display of backfill options [2]

3.3.1 Cohesive soil

In this thesis, the clay used for experiments, falls under the category of cohesive soils. The properties of cohesive soils vary with water containment. The strength of cohesive soils is also affected by disturbance from external objects. This means that after a trenching operation on a seabed consisting of clay, the strength of the clay will be reduced. When using jetting tools to create a trench in a clayish seabed, the property of the clay is highly affected by the increased water containment due to water flushing. The shear strength of the clay will increase with time without external influence, until it reaches a constant level. If the trenching is performed by a plough, the water containment of the clay will not be sufficiently increased, but the shear strength of the clay may be reduced by the disturbance in the process. The shear

strength of the clay will generally regain, depending on the consolidation process, but the uplift resistance is not reliable shortly after a jetting process [1].

4. Upheaval Buckling Theory

4.1 General

Global buckling of a pipeline can be compared to a bar in compression or buckling of axially constrained railroad tracks at high temperatures. Before production starts trough a pipeline, the internal temperature is about the same as the ambient seawater temperature. When the pipeline is put into service the temperature and pressure in the pipe will increase. As a result of this, the pipe will expand. A constrained pipeline will not allow the expansion to occur which will result in axial compressive forces in the pipe wall. The pipeline will try to relieve the stresses by buckling. A buried pipeline will have sufficient resistance sideways provided by the soil. The pipe will buckle in the direction of least resistance which then will be upwards. For trenched pipelines the buckle will follow the side wall, while buried pipelines will buckle vertically. The red arrows on the cross section in figure 4.1, indicates the axial forces in the pipe caused by temperature and pressure expansion.

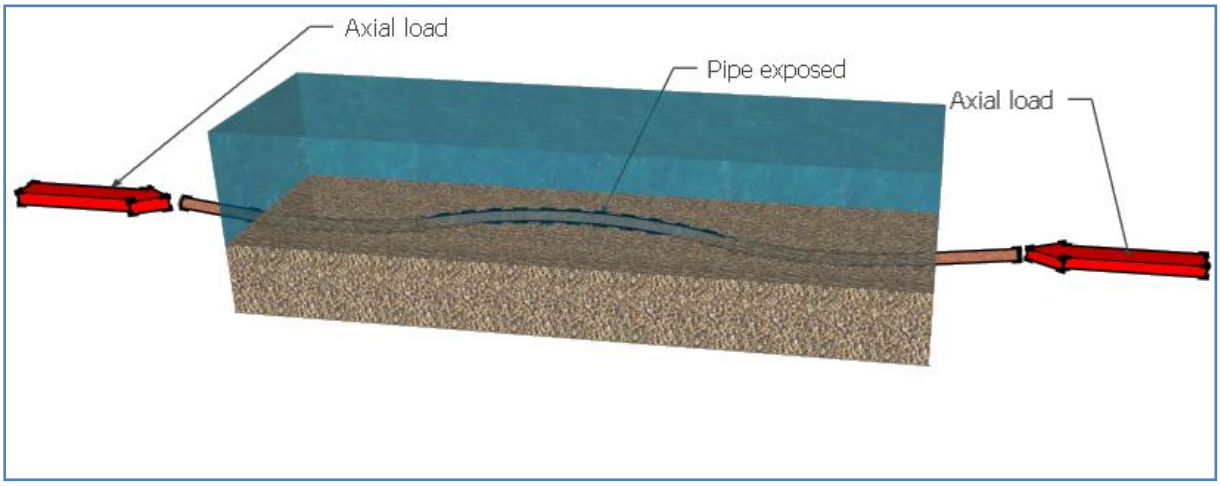

Figure 4.1 Buried pipe in compression

Typical candidates for global buckling are High Pressure and High Temperature (HP/HT) pipelines. Light pipelines with thin wall thicknesses may still be exposed to buckling at moderate temperature and pressure [1]. There are several failure modes for a pipe exposed to global buckling. Global buckling is a load response and not a failure mode alone, but global buckling may lead to failures such as fracture, fatigue, local buckling, bending moments and large plastic deformations. For pipelines lying exposed on the seabed, global buckling may be allowed as long as it is displacement controlled. This means that the pipeline integrity must be maintained in post buckling configurations, and that the displacement of the pipelines is within acceptable limits [2]. It shall not be able to interfere with surrounding structures or other pipelines. For buried pipelines, global buckling in the vertical plane shall be avoided [1]. If a buried pipeline is exposed to upheaval buckling and the pipeline breaks through the cover,

there are additional failure modes for such a scenario. The protection provided from the cover is lost, and if the curvature of the buckle leaves a gap between the pipe and seabed, a free span is formed. The pipeline may then be vulnerable to fatigue due to vortex induced vibrations at this region. If a buckle leads a pipeline into exposure on the seabed, the simplest solution would be to stabilize the pipeline at its new position. This can be done by covering the exposed part, for example by rock dumping. However if the integrity of the pipeline is reduced and the pipe wall is overstressed, this may lead to rupture. Then the damaged part will have to be replaced, before stabilizing it again [3].

4.2 Upheaval buckling failure modes

Failure modes for buried pipelines exposed on seabed due to upheaval buckling are:

- fracture
- fatigue
- local buckling
- plastic deformations
- bending moment and stress

Failures caused by pipe being exposed are;

- interference with fishing gear
- damage due to dropped objects
- damage due to anchoring
- temperature drop leading to hydrate formation in the pipe
- instability due to currents and buoyancy
- vortex induced vibrations
- fatigue

4.3 Driving force

4.3.1 Derivation of driving force

This derivation of the driving force for upheaval and lateral buckling is based on a thin walled tube idealization [3]. For situations with no external pressure circumferential stress, σ_H, is statically determined and given by equation 4.1;

$$\sigma_H = \frac{pR}{t} \tag{4.1}$$

where;

σ_H = Circumferential stress
p = Internal pressure
R = Radius
t = wall thickness

The longitudinal strain along the pipeline is given by the relationship between stress and strain for linear elastic isotropic material as in equation 4.2;

$$\varepsilon_L = \frac{1}{E}(-\nu\sigma_H + \sigma_L) + \alpha\theta \quad (4.2)$$

ε_L = Longitudinal strain
E = Young`s modulus
s_L = Longitudinal stress
α = Linear thermal expansion coefficient
θ = Change in temperature
ν = Poisson`s ratio = 0.3

The longitudinal stress σ_L is not statically determined. It depends on the level that the longitudinal movement is constrained. If there is no movement the longitudinal strain is equal to zero.

$$\varepsilon_L = 0 \quad (4.3)$$

The longitudinal stress is derived from equation 4.1, 4.2 and 4.3 and is given as equation 4.4:

$$\sigma_L = \frac{vpR}{t} - E\alpha\theta \quad (4.4)$$

The longitudinal stress occurs in the pipe wall. The cross section of a pipe wall is given as $2\pi Rt$. The longitudinal force in the pipe wall will then be;

$$2\pi Rt\sigma_H = 2\nu\pi R^2 p - 2\pi\, RtE\alpha\theta \quad (4.5)$$

An additional component of the longitudinal force is given by the pipe contents pressure. The cross section of the contents is πR^2. The longitudinal stress in the contents is –p if counting tension positive. The longitudinal force in the contents will therefore be;

$$-\pi R^2 p \quad (4.6)$$

By adding equations 4.5 and 4.6 we get an expression for the longitudinal force will be given as equation 4.7;

$$-(1-2\nu)\pi R^2 p - 2\pi\, RtE\alpha\theta \quad (4.7)$$

The first term of the equation involves the pressure, while the second term involves temperature. The pressure p and temperature θ are for most cases positive, which gives both terms a negative value and therefore compressive. As the two terms are independent this suggests that pressure alone can lead to upheaval buckling. This has been confirmed in laboratory experiments and by field experience. If an external pressure is present in the environment for which the pipeline is to be placed, p can be replaced by the difference in internal pressure p_i and external pressure p_e. A pipeline may have been through events before production start that has impact on the initial condition of the pipe. The tension introduced by laying and pressure testing should be accounted for.

4.3.2 Effective expansion force in DNV codes

The driving force for global buckling as introduced in equation 4.7 is given in the DNV codes, DNV-RP-F110 [1] and DNV-OS-F101 [4] as the effective axial force. The equation has been modified in the codes and is in the form of equation 4.8.

$$S_0 = H - \Delta p_i \cdot A_i(1 - 2 \cdot \upsilon) - A_s \cdot E \cdot \alpha \cdot \Delta T \tag{4.8}$$

where;

S_0 = Effective axial force
H = Residual lay tension
Δp_i = Internal pressure difference compared to as laid.
A_i = Internal area
υ = Poisson`s Ratio
A_s = Area of the steel
E = Young`s modulus
α = Thermal expansion coefficient
ΔT = Temperature increase compared to temperature during installation

Equation 4.8 for the effective axial force has here included a term H that involves the tension introduced by laying the pipe. The equation does not include the tension introduced by external pressure difference, which may be sufficient in deep waters. The tension from external pressure is introduced as the pipe is being laid and may be incorporated in the term for residual lay tension. The difference in internal pressure will not be affected by external pressure as the pipe goes into service, but the actual internal pressure in the pipeline will be lower if external pressure is subtracted.

The effective axial force in a pipe will vary in the longitudinal direction. For a pipe with free ends, the force will be larger in the central region of the pipe, while it will be zero in the ends. Expansion occurs from the virtual anchor points to the pipeline end. Between the virtual anchor points a pipeline with free ends is fully restrained. This means that there is no displacement of the pipe relative to the soil and fulfils equation 4.3 which says that no longitudinal strain occurs. [3].

The effective axial force in a pipeline with fixed ends will decrease slightly from the inlet point to the end. As the pipeline is restrained no relative movement with seabed will occur, and the effective axial force will be close to or at the level of fully constrained along the whole length. The slight reduction can be explained by temperature variation in the pipeline, due to cooling from the ambient seawater. While pipelines with free ends are more proposed to buckle in the region between the anchor points, a fixed pipeline may be equally exposed to global buckling during the whole routing. Figure 4.2 and figure 4.3 on the nest page describes the variation in the effective axial force.

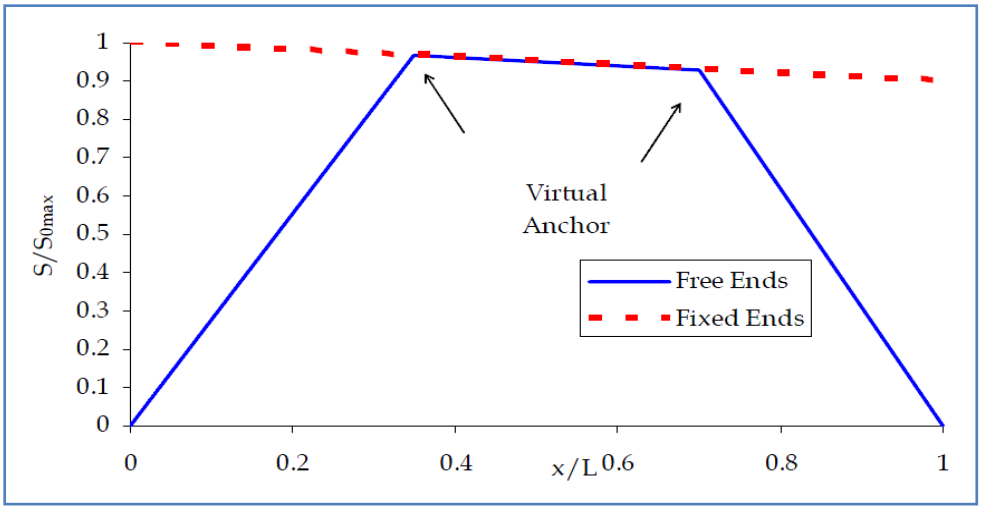

Figure 4.2 Effective axial force in pipe wall with free and fixed ends [7]

A short pipeline with free ends will not reach the level of fully constrained. A virtual anchor point will be formed near the center of the pipe, where the effective axial force will be at a maximum, but still below the level of fully constrained as shown in figure 5..

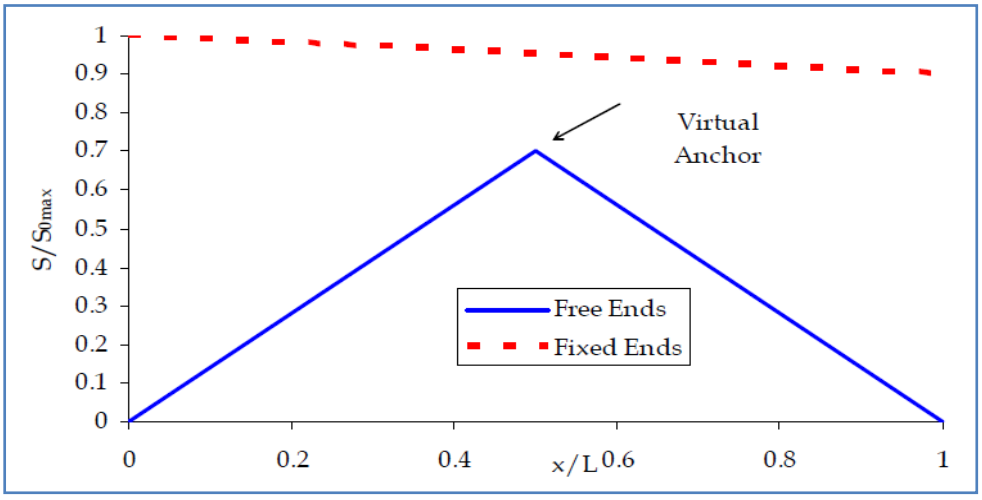

Figure 4.3 Effective axial force in a short straight pipeline [7]

The definition of short and long pipelines can be derived from figure 4.2 and figure 4.3. A short pipeline will not reach the level of the fully constrained axial force, while a long pipeline will develop the fully constrained axial force.

In practice, pipelines will normally be allowed to expand in the ends, by including a spool piece or an expansion loop between a pipeline and its connection points. This is to avoid the pipeline expansion causing high loads and damage to other structures like risers, subsea wells or to the pipeline it selves.

4.4 Strategies for analysis of upheaval buckling movements [3]

4.4.1 Strategy 1: Deriving universal design curve

The first strategy presented is further developed by Hobbs [6] from railway track buckling researches performed earlier by Martinet [7] and Kerr [8]. He considered how the conditions under which an initially straight pipeline could remain in equilibrium as a raised loop, when considering longitudinal movement towards the loop from both sides. A perfectly straight pipeline will according to structural mechanics terms have an infinite buckling force coupled with and infinite degree of imperfection sensitivity. The central feature of the problem is the imperfection of the seabed that the pipeline lays on. Further different profile imperfections where described by a height, length and a mathematically defined shape. Equation 4.9 describes a sinusoidal profile imperfection.

$$y = {}^{1}/_{2}\, H\left(1 - \cos\left({}^{2\pi x}/_{L}\right)\right) \quad 0 < x < L \tag{4.9}$$

where;

y = height
x = horizontal distance
H = imperfection height
L = imperfection length

Analysis determined the conditions where a pipeline can become unstable and lift away from the profile. This idea was developed in detail deriving a universal design curve, in terms of two parameters. A dimensionless download parameter Φ_q is given as equation 4.10;

$$\phi_q = \frac{qF}{HP^2} \tag{4.10}$$

where;

q = Total download (including resistance from cover if buried, and the pipe weight)
F = Flexural rigidity, see equation 4.12.
P = Longitudinal compressive forced

The second parameter derived was a dimensionless length given as equation 4.11;

$$\phi_L = L\sqrt{\frac{P}{F}} \tag{4.11}$$

The flexural rigidity is depending on the mean radius R, wall thickness t and Young`s modulus E and is given by.

$$F = \pi {R_m}^3 tE \tag{4.12}$$

where;

R_m = Mean radius between external and internal radius
t = Wall thickness

Figure 4.4 shoes the universal design curve for where a pipe can be unstable and lift away from its profile. It is described by the dimensionless download parameter in equation 4.10 and the dimensionless length parameter in equation 4.11.

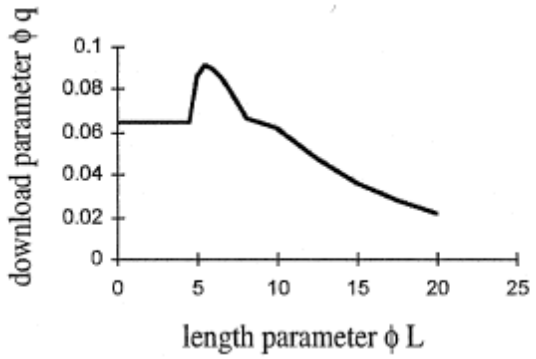

Figure 4.4 Universal design curve [4]

Limitations in this approach are that an elastic pipe is used, and that the idealization of imperfection shapes are rather simple compared to actual profiles can be complicated and hard to idealize.

4.4.2 Strategy 2: External force required to hold the pipe in position as production starts

This strategy looks on the possibilities to decide what external force is required to hold a pipe in position as production starts and the longitudinal force increases, if the initial profile of the pipe is known either by calculation or measuring.

The equations are derived from an arbitrary profile shown in figure 4.5.

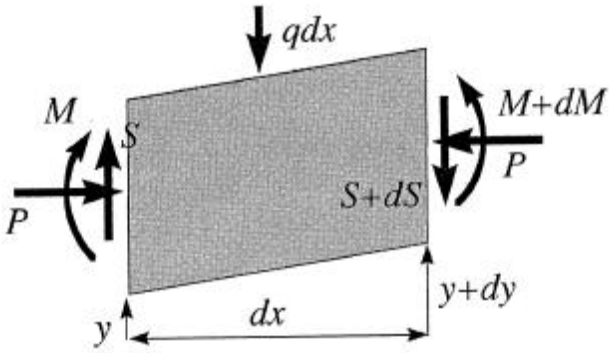

Figure 4.5 Element dx for deriving external force qdx

y = height of arbitrary profile
x = horizontal distance
P = Longitudinal force
S = Shear force
q = External vertical force per unit length
M = Bending moment

The shear force and moment can vary along the length. From vertical equilibrium of the element we get

$$q = -\frac{dS}{dx} \tag{4.13}$$

From the moment of equilibrium of the element we get

$$P\frac{dy}{dx} + \frac{dM}{dx} - S = 0 \tag{4.14}$$

From equation 4.12 and 4.13 we get the vertical force q

$$q = -P\frac{d^2y}{dx^2} - \frac{d^2M}{dx^2} \tag{4.15}$$

If the pipe remains elastic, the bending moment M is proportional to the curvature

$$M = F\frac{d^2y}{dx^2} \tag{4.16}$$

Where;

F = Flexural rigidity as given in equation 4.12.

From equation 4.15 and 4.16 we get

$$q = -P\frac{d^2y}{dx^2} - F\frac{d^4y}{dx^4} \tag{4.17}$$

In equations 4.17 and 4.15, the first term is a product of the curvature and the longitudinal force P. The curvature $\frac{d^2y}{dx^2}$ is negative where the pipe tends to push upwards, and requires a positive value of q to push it down. It is possible to determine the forces needed to hold the pipe in place from these two equations based on the pipeline profile. A more complex analysis is required to determine how the pipe moves and becomes unstable and jumps into a new position.

4.5 Measurements preventing upheaval buckling

The occurrence of an upheaval buckle is highly depending on the smoothness of the seabed profile. Suggestions of an imperfection height of 0,3 meter has been made as a design basis, but depending on the seabed soil, this is not rational [3]. Documentation of the seabed profile is essential and can be gathered from surveys performed by ROVs, divers or other available equipment. Choosing a routing that involves a smoother seabed and performing intervention by trenching the areas with peaks is a good option. A well documented seabed profile both before and after the pipe is laid, is important when designing acquired cover.

Reducing the driving force, equation 4.7, can be done in several ways. The highest contribution to the force is normally expected to come from the temperature term. This term involves the area of the steel, which can be modified by reducing the wall thickness t. The reduction of t will also affect the flexural rigidity F, equation 4.12. It has turned out that the improvement that comes from reducing the driving force more than outweighs the effect of reducing the flexural rigidity F [3]. However design strategies today have several reasons for optimized wall thickness design such as the rates for steel. The temperature can also be modified by decreasing the design temperature by coolers, heat exchangers or cooling loops that allow fluid to be cooled by heat transfer to the sea.

If the mentioned measurements are not enough to prevent upheaval buckling the pipeline must be buried. The cover options have previously been presented in chapter 3.3. There are different strategies to when it comes to covering a pipeline. A practical solution can be to cover the whole length, but this is not very economical. Covering at certain intervals can also be done. The most economical situation is to locate critical overbends, where an upheaval buckle might initiate, and apply cover at these locations. The operation of locating the areas that require cover includes a thoroughly performed survey operation, in order to find the locations later on when cover is to be applied.

4.5.1 Uplift resistance in non cohesive soils

The uplift resistance shall be sufficient to avoid the pipe to buckle vertically. For pipelines buried in non cohesive soils the uplift resistance can often be calculated as equation 4.18 [3].

$$q' = \gamma HD(1 + f\frac{H}{D}) \tag{4.18}$$

where;

q' = Uplift resistance
γ = Submerged weight of soil
H = Height from top of pipe to seabed surface (top of cover)
D = Total diameter including coating
f = Uplift coefficient determined experimentally

Figure 4.6 displays a cross section of a buried pipe with defined geometrical parameters used in equations for uplift resistance.

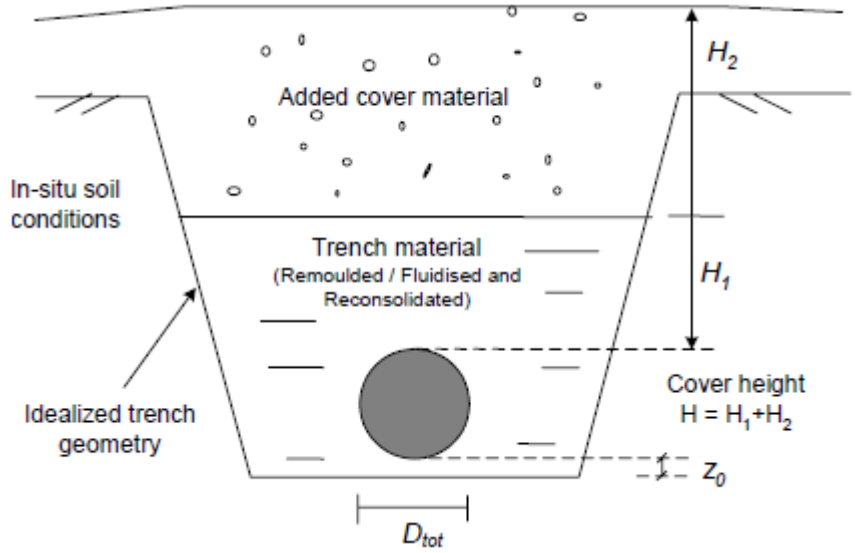

Figure 4.6 Dimensions for pipe cover [1]

DNV codes [1] suggest a formula to calculate the uplift resistance including shear and weight.

$$R = \gamma' \cdot H \cdot D^2 \left(\frac{1}{2} - \frac{\pi}{8}\right) + f(H + \frac{D}{2})^2 \tag{4.19}$$

where;

γ' = Submerged weight of soil
ϕ = Friction angle
f = $K \cdot \tan(\phi) \cdot \gamma'$
K = Lateral earth pressure coefficient accounting for increased stress in vertical direction

4.5.2 Uplift resistance in cohesive soils

4.5.2.1 Local failure mode

When it comes to uplift resistance in clay, two failure modes are given [1]. Local failure mode, see figure 4.7, is when the soil above the pipe displaces around and below the pipe as the pipe moves upwards.

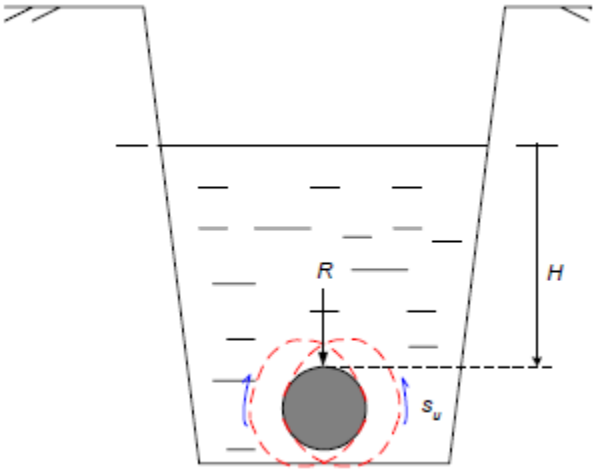

Figure 4.7 Uplift resistance in clay – local failure mode

In local failure mode the uplift resistance can be calculated as equation 4.20;

$$R = N_c \cdot \eta \cdot s_u \cdot D \tag{4.20}$$

where;

N_c = Theoretical bearing capacity coefficient (See equation 4.21)
η = Empirical factor based on field tests
s_u = Undrained shear strength at centre of pipe

For shallow water the bearing capacity coefficient is given as

$$(N_c)_{shallow} = 2\pi\left[1 + {}^1/_3 \cdot arctan\left(\frac{H+{}^D/_2}{D}\right)(1+r)\right] \tag{4.21}$$

where;

r = Roughness factor for pipe

4.5.2.2 Global failure mode

In global failure mode the soil will displace upwards when the soil moves upwards. Figure 4.8 shows that the direction of the soil failure.

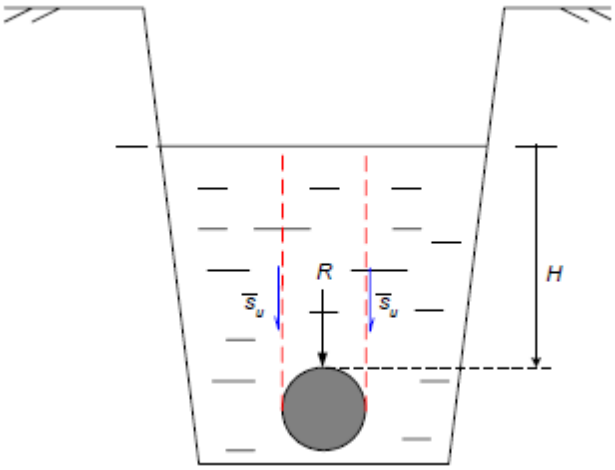

Figure 4.8 Uplift resistance in clay – global failure mode

In global failure mode the uplift resistance can be calculated as equation 4.22;

$$R = \gamma' \cdot H \cdot D\left(\frac{1}{2} - \frac{\pi}{8}\right) + 2 \cdot \bar{s}_u (H + \frac{D}{2})^2 \quad (4.22)$$

$\bar{s}_u$ = Average undrained shear strength from centre of pipe to top of cover

4.6 Brief look at upheaval buckling design according to Det Norske Veritas

On the subject of global buckling of high pressure high temperature pipelines Det Norske Veritas, DNV, has developed the recommended practice DNV-RP-F110, Global Buckling of Submarine Pipelines – Structural Design due to High Temperature/High Pressure [1]. The RP gives criteria to avoid upheaval buckling from occurring, by designing sufficient cover providing enough resistance for pipelines to remain in place. Upheaval buckling may be acceptable if the integrity of the pipe is maintained in post buckling condition, but the RP gives no procedures in performing integrity check for pipelines at this state. Therefore upheaval buckling is considered as an ultimate limit state, ULS, in the recommended practice. An upheaval buckle is a violation to the design premise and thus safety factors must be in coordination with an annual probability of occurrence at $Pf < 10^{-4}$/year. This is for Safety Medium Class according to the DNV Offshore Standard DNV-OS-F101, submarine pipeline standard [4].

The structural design flow for in place design is given as figure 4.9.

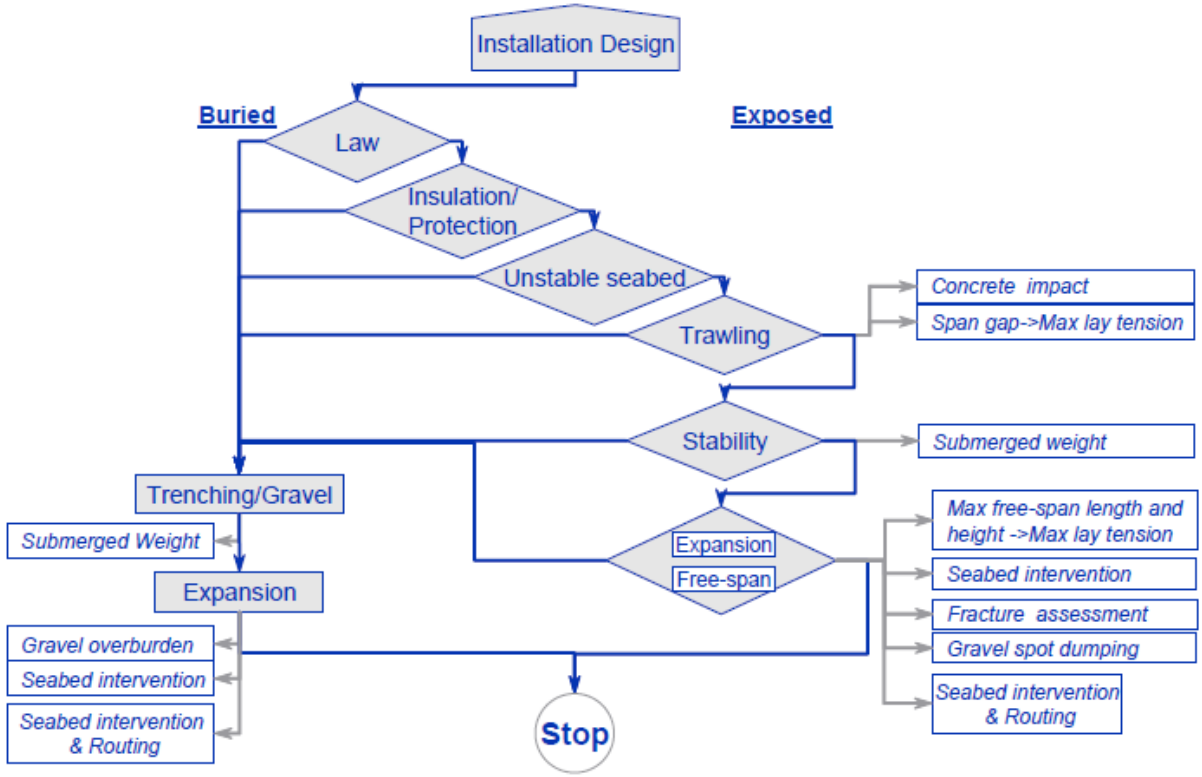

Figure 4.9 Structural design flow chart [1]

The design process includes four steps. The two first steps are specific cover design and minimum cover design. The first step is pre installed phase, and the second is as installed phase. The two steps are based on the same criteria, but with assumed or measured configuration. Before applying complex analysis, common practice is to calculate a tentative overburden. When the pipeline configuration is documented by survey, analysis of the measured pipeline will give necessary uplift resistance. The specific cover height, H_{spec}, will

vary with the curvature of the pipe, pressure and temperature. The downward stiffness may also be taken into account, when the uplift resistance is high.

Because of the uncertainties in surveys a minimum cover resistance shall be determined by running analysis with a prop shape imperfection depending on the level of accuracy of the surveys.

The design process for buried pipelines is organized in the following steps:
1) Specific cover design
    - Initial configuration
    - Soil resistance modeling
    - Upheaval buckling design criterion
2) Minimum cover design
3) Specification of cover
4) Pipe integrity check.

The design is mainly based on the design temperature. The design temperature is normally given by a client and a pipeline engineering company has normally no option to modify the given design temperature. The design approach is based on designing a sufficient cover by performing analysis, for the given design temperature. A further description of the steps in the design process follows.

4.6.1 Step 1: Specific cover design

This step determines the required cover on buried pipeline based on actual measured imperfections by surveys. The required cover determined from this step is given as $H_{spec.}$

Figure 4.10 illustrates the design principles for deriving the design resistance equivalent failure temperature, T_{Rd}. E[R] is the expected uplift resistance which is represented by a lower bound characteristic value R_c in the load response model. The lower bound uplift resistance is further reduced by the safety factor γ_{UR}, which is depending on the accuracy of the configuration survey.

$$\gamma_{UR} = 0.85 + 3 \cdot \sigma configuration\ [m^{-1}] \quad \text{for non cohesive soil} \quad (4.23)$$

$$\gamma_{UR} = 1.1 + 3 \cdot \sigma configuration\ [m^{-1}] \quad \text{for cohesive soil} \quad (4.24)$$

Where;

γ_{UR} = Safety factor
$\sigma_{configuration}$ = Accuracy of surveys

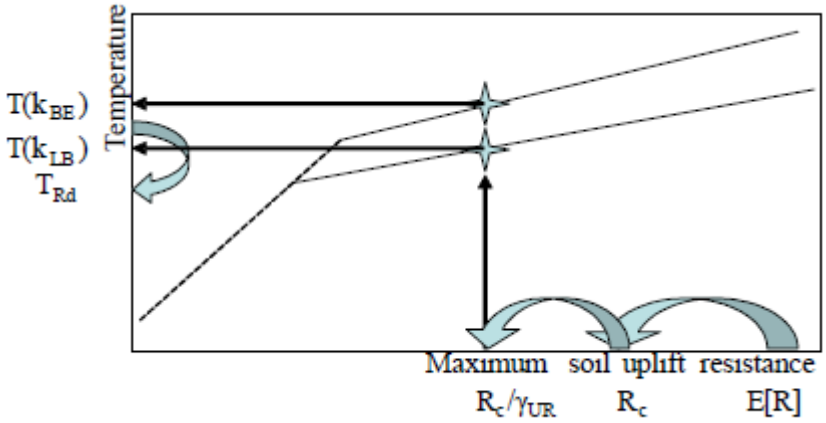

Figure 4.10 Deriving design resistance equivalent failure temperature, T_{Rd} [1]

The procedure is performed including two downward stiffness conditions whereas one is the best estimate, k_{BE}, and the other is lower bound, k_{LB}. The lower bound stiffness differs from the best estimate by including the safety factor γ_{UR}. When the best estimate is used all loads are applied, and the temperature is increased until failure occurs at $T(k_{BE})$. This is also performed using the lower bound stiffness until failure occurs at $T(k_{LB})$. Based on the difference between the best estimate and lower bound failures, it is possible to decide the direction which the pipeline fails. The equations for best estimate and lower bound failure temperature are given in equations 4.24 and 4.25 on the next page;

$$T(k_{BE}) = T_{failure}\ (p_{li}, \frac{R_c}{\gamma_{UR}}, k_{BE}) \quad (4.25)$$

where;

$T(k_{BE})$ = Temperature at which failure occur whit best estimate downward stiffness
$T_{failure}$ = Temperature at which failure occur
p_{li} = Local incidental pressure
R_c = Sand and rock uplift resistance
γ_{UR} = Safety factor
k_{BE} = Best estimate downward stiffness

$$T(k_{LB}) = T_{failure}\ (p_{li}, \frac{R_c}{\gamma_{UR}}, k_{LB}) \quad (4.26)$$

Where;

$T(k_{LB})$= Temperature at which failure occur whit lower bound downward stiffness
k_{LB} = Lower bound downward stiffness

If $T(k_{LB})$ is close to $T(k_{BE})$ – The pipeline will fail upwards implying that its limited by the uplift resistance and located on the dashed line in figure 4.10.

If $T(k_{LB})$ is different from $T(k_{BE})$ – The initial soil failure is downward eventually causing the pipeline upward penetration. This implies that it is limited by downward stiffness conditions and is located on the solid lines to the left in figure 4.10.

The temperature at which the soil fails and upheaval buckling occurs, $T_{Rd,}$ is calculated as;

$$T_{Rd} = \frac{3 \cdot T(k_{LB}) - T(k_{BE})}{2} \quad (4.27)$$

Where;

T_{Rd} = Design resistance equivalent failure temperature

The equation for calculating the design load temperature includes an axial effective load factor of γ_{UF}.

$$T_{Sd} = T_d \cdot \gamma_{UF} + \frac{[\Delta p_i \cdot A_i \cdot (1-2\cdot\upsilon) - H]}{A_s \cdot E \cdot \alpha} \cdot (\gamma_{UF} - 1) \quad (4.28)$$

Where;

T_{Sd} = Design load equivalent temperature

γ_{UF} = Axial effective load factor; $\gamma_{UF} = \begin{cases} 1.00 & for\ normal\ safety\ class \\ 1.15 & for\ medium\ safety\ class \\ 1.30 & for\ hihg\ safety\ class \end{cases}$

Δp_i = Internal pressure difference compared to as laid

A_i = Internal area of pipe

ν = Poisson`s ratio

H = Residual lay tension

A_s = Area of steel

E = Young`s modulus

α = Thermal expansion coefficient

The design load equivalent temperature shall be lower than the design resistance equivalent failure temperature.

$T_{Sd} < T_{Rd}$

If the criterion is not fulfilled, the cover or the configuration must be modified and the analysis must be performed again.

This step will give a specific cover height for sand and rock, H_{spec} , or specific soil resistance for clay, R_{spec}.

4.6.2 Step 2: Minimum cover design

The minimum cover design shall be derived using a prop shape imperfection. This allows for undetected imperfections due to accuracy of survey equipment to be accounted for in analysis. What separates the minimum cover design from the specific cover design is that the uplift resistance / cover height is determined from the prop shape imperfection, δ_f, meaning that the pipeline is resting on an imperfection. This can be analyzed in a finite element model by lowering the pipe onto a single contact point, with the distance δ_f above the seabed. The height of the prop shape, δ_f, shall be put equal to one standard deviation of the accuracy from the surveys, previously defined as $\sigma_{configuration}$. See equation xx.

$$\delta_{f=max\,(\sigma_{configuration}\ \ |0.025m)} \quad (4.29)$$

The safety factor related to upward soil resistance, $\gamma_{UR,}$ is here reduced by setting the $\sigma_{configuration}$ as zero.

γ_{UR} = 0.85 + ~~$3\cdot \sigma configuration$~~ [$m^{-1}$] for non cohesive soil (4.30)

γ_{UR} = 1.1+ ~~$3\cdot \sigma configuration$~~ [$m^{-1}$] for cohesive soil (4.31)

Besides this the principle of running the analysis follows the same pattern as for the specific cover design, and we end up with a minimum cover height, H_{min}, for sand and rock, or minimum soil resistance, R_{min} for clay

4.6.3 Step 3: Specification of cover

If granular mass like sand or rock is used for cover, the resulting cover height shall be taken from step one or two as the maximum of the specific or minimum cover height.

$$H(Kp) \geq Max[H_{spec}\ (Kp), H_{min}\ (Kp)] \tag{4.32}$$

Kp = Kilometer post

The resulting cover resistance for clay shall be taken as the maximum of the specific soil resistance, R_{spec} and the minimum soil resistance, R_{min}.

$$R(Kp) \geq Max[R_{spec}\ (Kp)\ R_{min}\ (Kp)] \tag{4.33}$$

When constructing the cover an additional margin may be added to account for uncertainties. At least two surveys shall be performed after the cover is in place. Calculating the average of the surveys can be applied, to get the general cover resistance / cover height. The cover heights derived from the surveys shall independently be verified by the procedures in step 1.

$$\bar{H}(Kp) = \frac{1}{n}[H_1(Kp) + H_2(Kp) + \cdots + H_n] \tag{4.34}$$

$$\bar{R}(Kp) = \frac{1}{n}[R_1(Kp) + R_2(Kp) + \cdots + R_n] \tag{4.35}$$

Depending on the number of surveys the safety factors can be reduced. The T_{Rd} however remains the same for each survey.

$$\gamma UR = 0.85 + \frac{3 \cdot \sigma configuration}{\sqrt{n}}\ [m^{-1}] \quad \text{for non cohesive soil} \tag{4.36}$$

$$\gamma UR = 1.1 + \frac{3 \cdot \sigma configuration}{\sqrt{n}}\ [m^{-1}] \quad \text{for cohesive soils} \tag{4.37}$$

The minimum cover height can be calculated for an imperfection height of;

$$\delta f = (\frac{\sigma_{configuration}}{\sqrt{n}}) \tag{4.38}$$

The final cover resistance / cover height for n surveys is taken as the maximum of the specific and the minimum cover height.

$$H(Kp) \geq Max[\bar{H}\ (Kp), H_{min}\ (Kp)] \tag{4.39}$$

$$R(Kp) \geq Max[\bar{R}(Kp)\ R_{min}\ (Kp)] \tag{4.40}$$

4.6.4 Step 4: Pipe integrity check

The recommend practice has been based on risk principles and limit state methodology with the offshore standard, DNV-OS-F101 [. The most governing integrity checks for a buried pipeline are given in table 4-1.

Table 4-1 Governing pipe integrity check [1]

Table 8-1 Required and Normally most governing pipe integrity check								
	Pressure Cont.	*Local buckling*		*Axial*	*Ratcheting*	*Fatigue*	*Trawl interf.*	*Free span*
		Load Controlled	Displacement Controlled					
Reference	DNV-OS-F101	DNV-OS-F101	DNV-OS-F101	Eq. (65)	DNV-OS-F101	DNV-OS-F101	DNV-RP-F111	DNV-RP-F105
Buried pipe	X		X	X	X	X	-	-

5. Experiment

5.1.1 Pipe

The pipe used for this experiment is a 10 mm outside diameter copper pipe. A further description of the actual pipe follows.

5.1.2 Material properties for Copper pipe

Tensile strength, σ_t:	min 310 N/mm^2
Yield strength, σ_y:	min 280 N/mm^2
Young`s Modulus, E:	1.2E11 N/m^2
Density, ρ:	8.94 kg/dm^3
Poissons`s ratio, ν:	0.3
Coefficient of Linear Thermal Expansion, α:	17E-6

5.1.3 Geometric parameters

Outer diameter, OD:	10 mm
Inner diameter, ID:	8 mm
Wall thickness, T:	1 mm
Second moment of area cross-section, I:	2.89E-10 m^4
Steel area, A_s:	2.83E-5 m^2
Length of pipe, l:	6 m
Total weight of 6 meter pipe, w:	1.517 kg

5.1.4 Hydraulic cylinder and jack

A hydraulic cylinder is used to apply compression forces in the pipe. The pipe is fixed in one end while the hydraulic cylinder gives an axial force on the other end. The cylinder is an Enerpac RC-1014 with specifications given in table 5-1. The jack is used to achieve pressure in the cylinder and thus displace the piston rod. Figure 5.1 on the next page shows the hydraulic cylinder and jack.

Table 5-1: Enerpac RC 1014 specifications

Cylinder Capacity	Stroke	Cylinder effective area	Oil Capacity	Collapesed Height	Weight
10 tonnes	356 mm	14,5 cm^2	516 cm^3	450 mm	8,2 kg

Figure 5.1 Enerpac hydraulic cylinder and jack

5.2 Measuring equipment

5.2.1 Loadcell

A loadcell is mounted at the end of the piston rod of the hydraulic pump. The loadcell used in the experiments is a HBM U2A delivered by Hottinger Baldwin Messtechnik. The purpose of the load cell is to measure the axial force applied to the pipe by the hydraulic pump. It is mounted by a 15 pin socket to a Spider 8 data acquisition device that is further presented in section 5.2.3. The model used can measure loads up to 200 kg. The same model will also be used for the lifting tests. Figure 5.2 shows the loadcell mounted on the hydraulic cylinder.

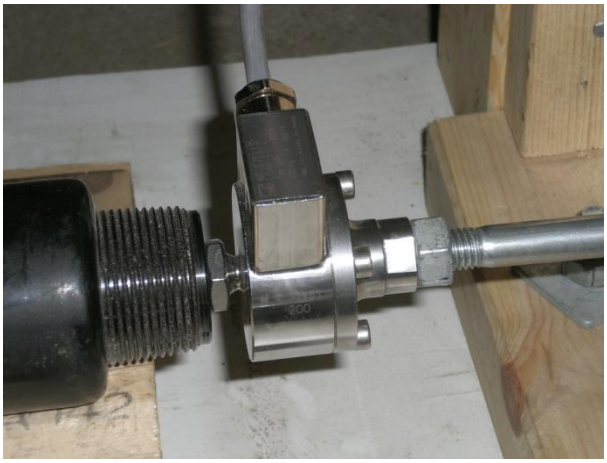

Figure 5.2 Load cell mounted on the end of the piston rod of the hydraulic pump.

5.2.2 Strain gauges

Strain gauges are mounted on the pipe at specific location in order to measure the strain in the pipe. In the upheaval buckling experiment two types are used. One type is meant for measuring axial strain. This type is a single directional strain gauge. The other type is for measuring of torsion moment. The mounting of the strain gauges is a critical operation hence to getting good measuring results on the experiments.

When using single directional strain gauges, two strain gauges are required. This is because of temperature effects. One strain gauge will be active, while the other one will function as a

dummy. The dummy will be mounted on a piece of pipe with same configurations as the actual pipe, but without loading. The dummy will ensure that strain caused by thermal expansion during experiments is left out while measuring. The active strain gauge will be mounted on the actual pipe for experiments. There are three wires connected to the strain gouges that further must be mounted to a 15 pin socket. The wires have to be connected at specific pinholes on the socket depending on the function of the strain gauge. Figure 5.3 shows how to mount the different wires from the strain gouges to the 15 pin socket for active and passive single directional strain gauges. Figure 5.4 shows the strain gauges mounted on the dummy pipe and the pipe for experiment.

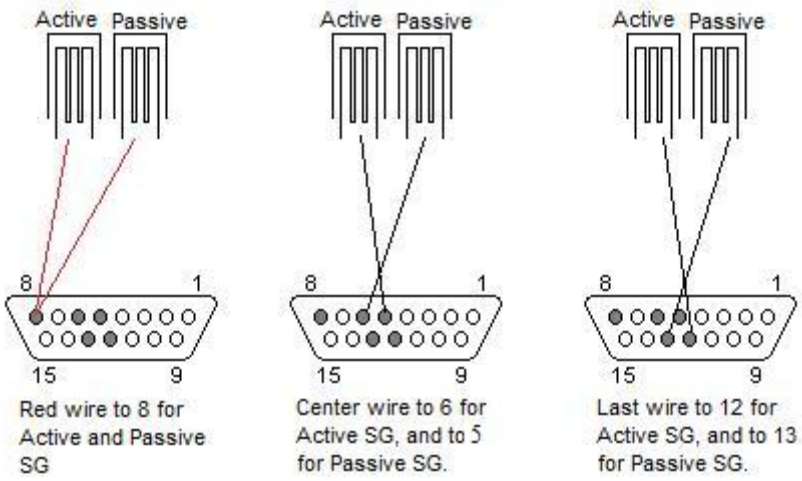

Figure 5.3 Schematic guide for mounting of SG wires to 15 pin socket for single directional strain gauges.

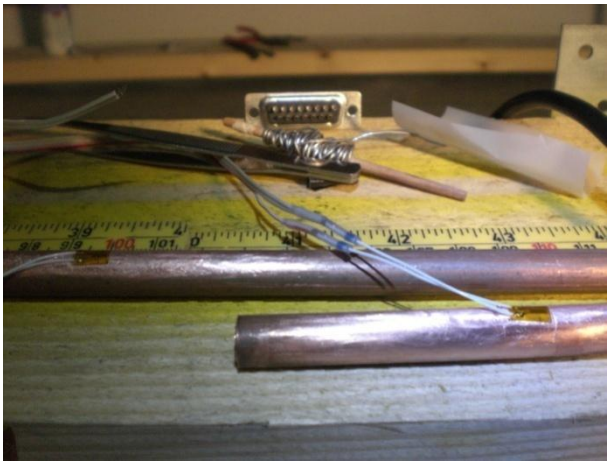

Figure 5.4 Strain gauges mounted on dummy and the pipe used for experiment, 15 pin socket in the back.

The strain gauges used for measuring torsion does not require a dummy strain gauge, but is still capable of neglecting temperature effects, because a dummy function incorporated in the strain gauge. However the mounting of the wires is different and requires two loops as shown in figure 5.5 on the next page. It is possible to control the sign of the measured strain according to which direction the pipe twists, by the mounting of the wires.

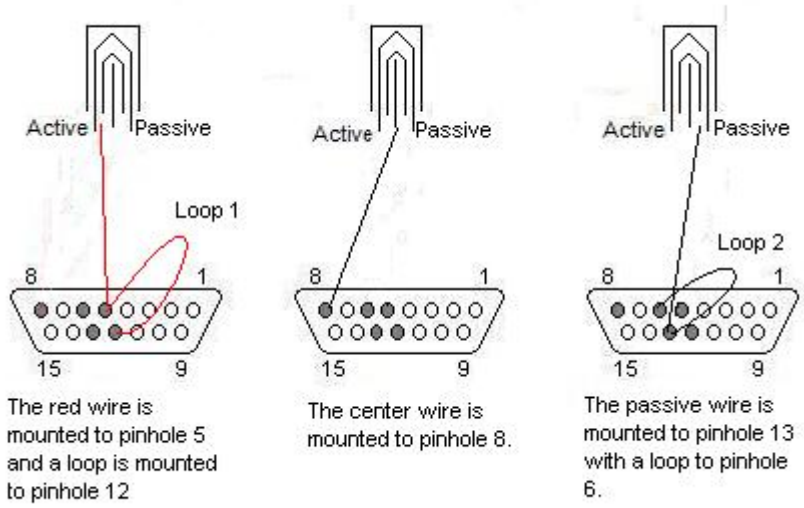

Figure 5.5 Schematic view of mounting for torsion strain gauges.

5.2.3 Spider 8

Spider 8 is a PC based data acquisition devise. After the wires from the strain gauges are mounted to the 15 pin socket, the socket is ready to be mounted to the Spider 8. The data collected from the strain gauges goes via the Spider 8 to a PC. There are six ports available for strain gauges and two additional ports for distance measurers or other devices. Figure 5.6 shows a picture of the Spider 8.

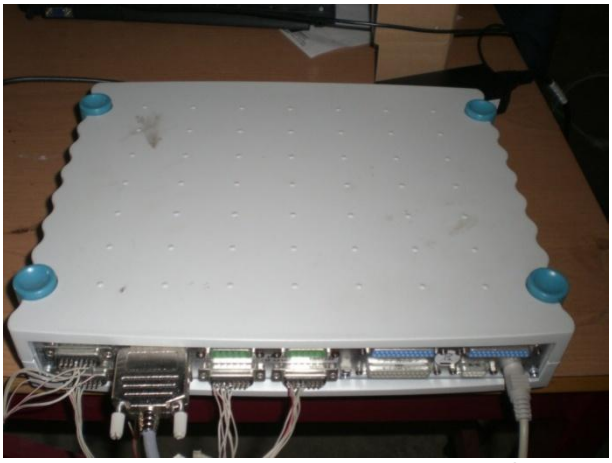

Figure 5.6 Spider 8 data acquisition amplifier

5.2.4 PC with Catman software

Catman is a software acquisitioning application that logs and displays measurements received from the spider 8 in wanted time intervals. Each port on the spider 8 can be displayed in the software. Setups can be configured by needs for individual experiments, and easily be stored and retrieved.

5.2.5 Geonor H60 hand-held vane tester

The H60 hand-held vane tester shown is figure 5.7 is used to measure the undrained shear strength of clay. The conditions in the clay will vary with evaporation, consolidation or external interaction. It is therefore important to measure the undrained shear strength of clay frequently.

Figure 5.7 Geonor H-60 hand-held vane tester

5.2.6 Speedy Moisture Tester

The moisture tester was used to detect the water containment in sand during the period that the sand experiments performed. This was because variation of the water containment in sand has impact on the weight. Using this method for moisture documentation is very practical for in situ measurements, and gives actual results in a short amount of time. The kit contains a balance scale with a cup for portioning the correct amount of sand into the moisture tester. In addition to the sand Calcium Carbide is added as a regent. The Speedy body is then shaken to get a chemical reaction, where the moisture forms Acetylene gas. The Speedy body has an integrated Bourdon tube gauge on the bottom that measures the pressure difference. It is scaled for direct reading of the water containment. Figure 5.8 shows the Speedy Moisture Tester kit.

Figure 5.8 Speedy moisture tester

5.2.7 Balance scale and cylinder

To detect the density of the different masses, a scale weight and a cylinder has been used. The weight of the mass is first decided. Then the cylinder is filled to the top with distilled water at 20 degrees Celsius. When the weight of the water alone is decided, the cylinder is filled with the actual mass and water to the top. Stirring is performed to leak out any air pockets in the mass. The formula for calculating the density is given in equation (5.1);

$$\rho_m = \frac{m_s}{m_w - (m_{s,w} - m_{s)}} \tag{5.1}$$

where;

ρ_m = Density where the subscript notes the soil type
m_s = Weight of the soil
m_w = Weight of water
$m_{s,w}$ = Weight of cylinder with mass and water

5.2.8 Metric measure

A metric ruler is used to measure the vertical deflection of the pipe from the prop imperfection to the maximum height after axial force has been applied. The metric measurer is mounted on the wall of the test rig as seen on figure 5.9.

Figure 5.9 Pipe exposed after experiment and metric measurer to detect the vertical deflection.

5.2.9 Reel

A manual reel is used to lift the pipes out of the masses. The intended purpose for the specific reel is to land small boats on to trailers, and the capacity is well within the limits for the lifting tests. Figure 5.10 shows the reel used in the experiments.

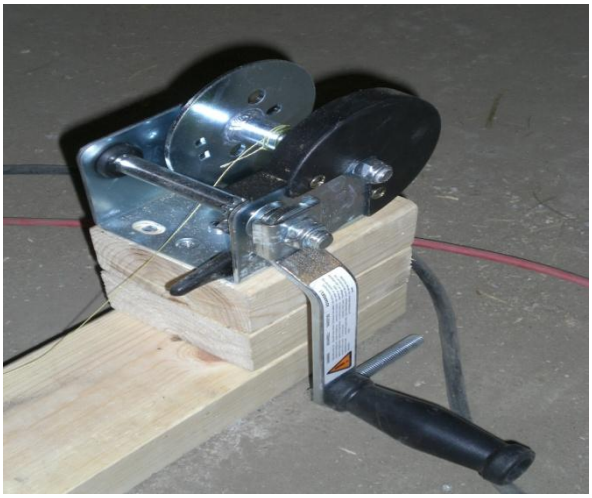

Figure 5.10 Reel used to lift the pipe

5.3 Experiment description

5.3.1 Lifting test

The pipes will be buried in clay, gravel and sand respectively at specific cover heights. Load cells will be mounted on the wires to measure the forces needed to lift the pipe out of the mass. The task of the lifting experiment is to detect the resistance in the different masses, and to find a ration between the resistance and outside diameter of the pipe. Additional pipes have been tested for this cause. Pipes with outside a diameter of 22mm and 28mm have been lifted in addition to the 10mm pipe.

Figure 5.11 shows the lifting system. In the back the reel showed in figure 5.10 is mounted. The test rig is the same as for the upheaval buckling test rig, but only the back part of the cabinet is used. The wire used is a fishing line, with a capacity of 22 kg. The reason for choosing the fishing line for the lifting purpose is because it has very little flexibility. Applying as much stiffness as possible in the system is an important factor in getting good results.

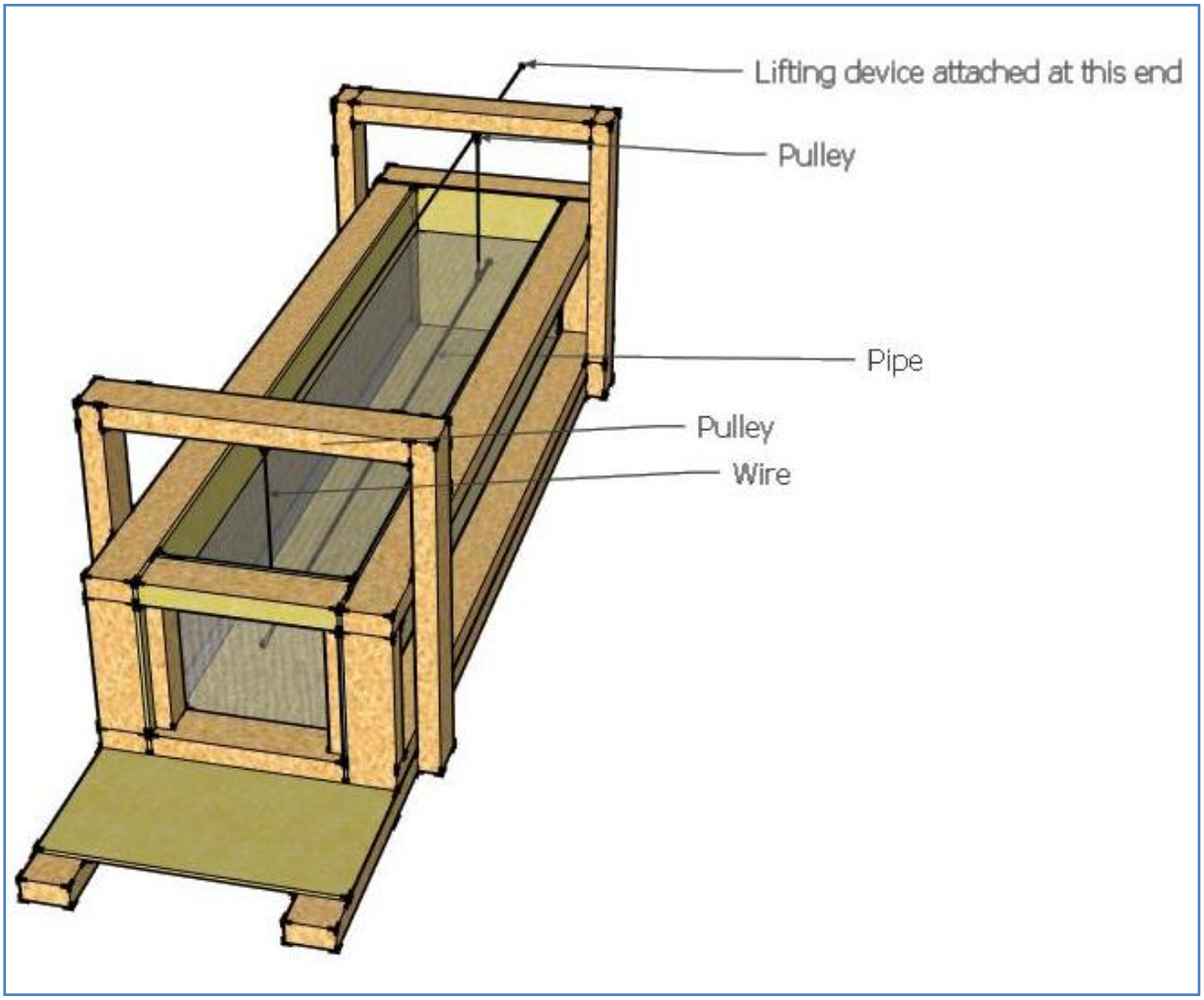

Figure 5.11 The lifting test rig

The lifting system was found to be too light for the larger diameter pipes and heavier masses as sand and clay. The solution was to tie with four lines increasing the capacity utterly. Figure 5.12 shows a schematic build up of the lifting system, and the positioning of the loadcells. A total of four pulleys were used. Because of the positioning of the loadcells the friction in the pulleys has no effect on the measurements, as the measuring points were between the pipe and the first pulleys.

As the purpose of the experiments was to detect a relation between the resistance provided by the different soil types and the diameter, the self weight of the pipes was excluded from the experiments. This was done simply by zero balancing the loadcells in the Catman software when the pipe was hanging by wires in free air. This means that the results only show the resistance in the different masses without the effect of the pipes own weight.

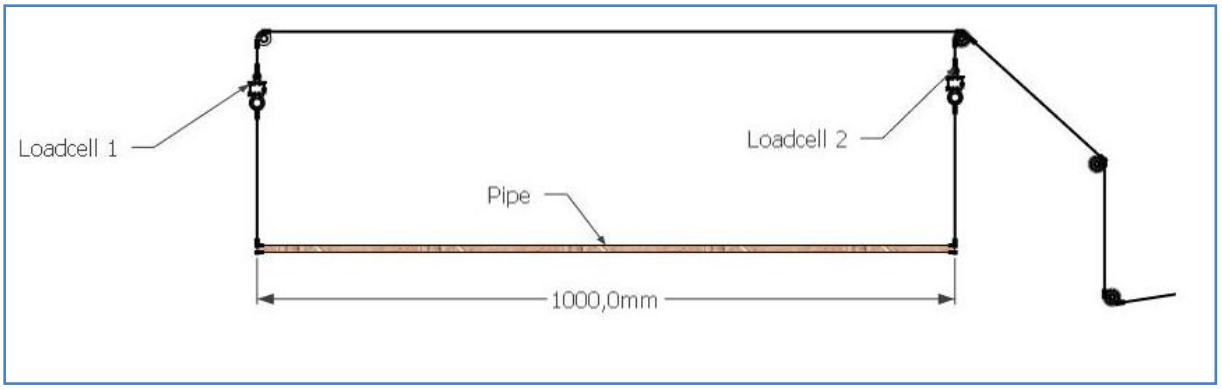

Figure 5.12 Edge cross section of lifting system

The experiments were carried out such that the height of the cover was in relation with the diameter for each pipe. There were performed at least three tests with the except for the 2D experiments in gravel and clay where only one test was run. Table 5-2 shows the cover heights that were tested for the pipes individually.

Table 5-2 Different cover heights for the lifting experiments

Pipe	Cover		
OD	1D	2D	Unit
10	10	20	[mm]
22	22	44	[mm]
28	28	56	[mm]

How to get the force required to lift the pipe per meter is shown in figure 5.13. As the length of the pipes used for the lifting experiments were 1 meter and two lifting points were used, it only involved a small calculation of adding the forces and dividing it by 1 meter.

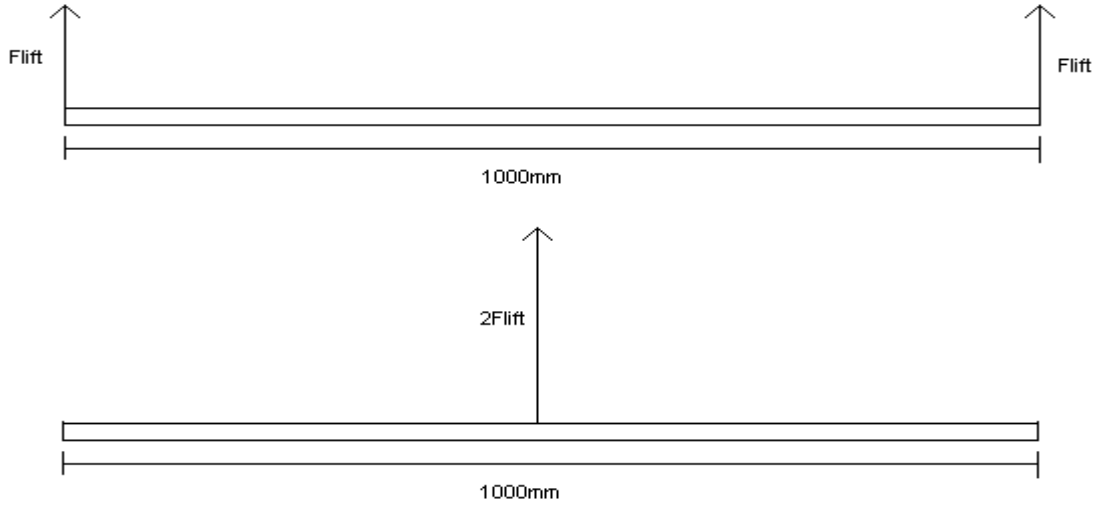

Figure 5.13 Deriving of lifting force per meter

5.3.2 Upheaval buckling test

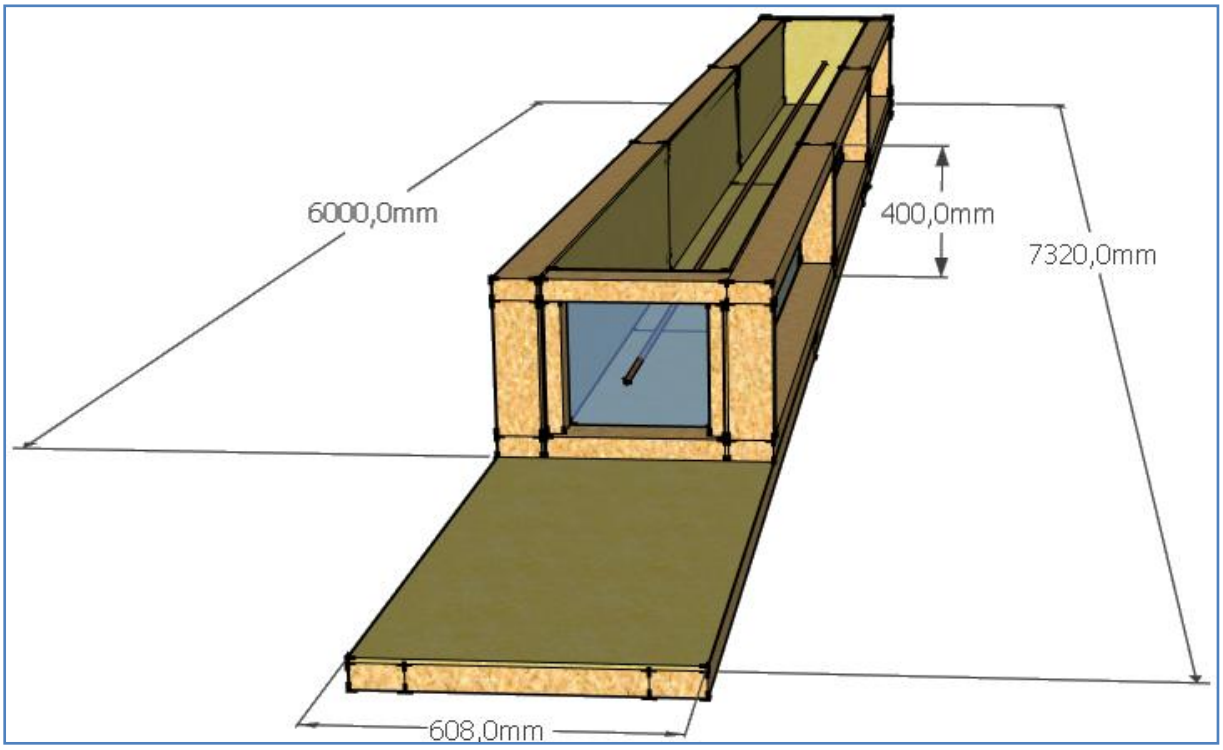

Figure 5.14 Upheaval buckling test rig.

5.3.2.1 Upheaval buckling tests description

Figure 5.14 shows a drawing of the test rig with dimensions. The experiments were carried out as a scenario for upheaval buckling of a fully constrained pipeline. The pipe was fixed axially at the back, while the hydraulic pump applies a force at the front. As the force was applied, the pipe got a displacement axially at the front, while no movement occurred axially at the back. The pipe was then in compression. In realistic situations the compression forces is caused by expansion due to pressure and temperature increases, and friction in the underneath soil and cover preventing the expansion. Heating a pipe that is fixed axially in both ends could be done, but applying the hydraulic pump was found to be a more practical way to get the pipe in compression.

A prop imperfection is applied at the center of the pipe longitudinally. The imperfection has been fixed for the tests in sand and gravel, but for the tests with clay two different imperfection heights were used. The height of the imperfection was decided based on the behavior of the pipe with different imperfections tested. A small imperfection will give a small vertical component of the axial force from the pipe above the imperfection. To get the pipe to buckle a larger axial force is then required. For small imperfection heights the buckle will occur as a snap. A prop imperfection of 33mm was found suitable for the experiments as the pipe then moved at a more controllable speed as the buckling occurred. However, for the experiments in clay an 18mm imperfection was also used. The prop imperfection was a simple structure including a pipe mounted between two pieces of wood. It was not fixed to the bottom of the test box, since it has been moved in and out during changing of the different

masses, and such that the imperfection height could be varied. The prop imperfection can be seen under the pipe in figure 5.15.

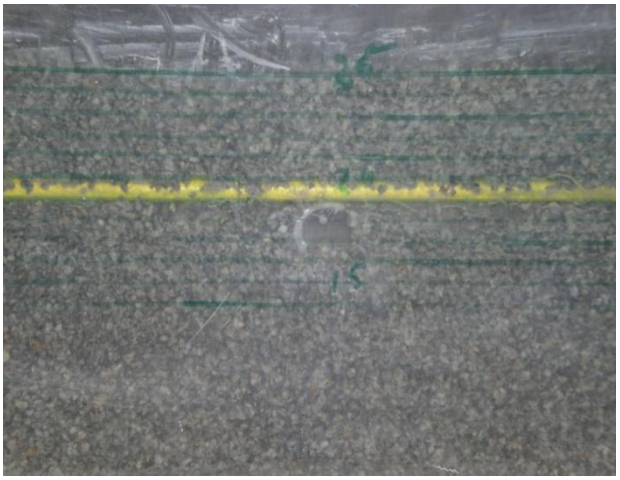

Figure 5.15 Edge cross section of pipe and gravel showing the prop imperfection

Some experiments were also performed as a scenario for trenched pipelines without cover. These tests were performed in sand and gravel. One test was run while the pipe was half buried with cover on the sides to provide lateral resistance, while there was no cover on the top of the pipe. The other test included forming of a trench in the mass material, where there was no backfill or cover of any kind. The two scenarios are referred to as half buried and trenched in the results.

When a pipe starts to buckle vertically in granular soils, soil may fill in the gap caused by the pipe moving upwards. If a pipeline goes in and out of service, it might be possible that it stabilizes at a higher location as production stops, because of soil filling in the gaps. This phenomenon is referred to as creep. The clay has the ability to deform plastic, and because of this a creep scenario was simulated in the test cabinet. This was done by adding and releasing axial force to the pipe in several steps, while investigating the strains after the force had been released. This creep scenario was only performed with clay.

5.3.2.2 Orientation of measuring points

The XY notation is used for the torsion strain gauges. These strain gauges have been mounted near the center of the pipe. The reason for locating them at the center is because if twisting of the pipe was to occur, it would be expected to occur in the center region where the pipe will break through the cover. The torsion strain gauges were mounted within short distance. This was done in order to secure good measurements, as they are expected to show somewhat the same values.

In the experiments, three main measuring points for single directional strain gauges have been used on the pipes. Figure 5.16 on the next page shows how the strain gauges are mounted on the Copper pipe. The notation LY is used for single directional strain gauges monitoring axial strain. These strain gauges where mounted at the top of the pipe at locations 1 meter, 3 meter

and 5 meter, respectively. The reason for the chosen locations for the LY strain gauges is that the largest differences in the curvature during the experiments were expected at these locations. The variations in the strain can either be caused by tension or compression. An increase of the curvature radius will give larger strains, while a decrease of the curvature radius will give reduced strains. The strain gauges located at 1 meter and 5 meter will show negative strain, because they are mounted on the compression side of the curvature.

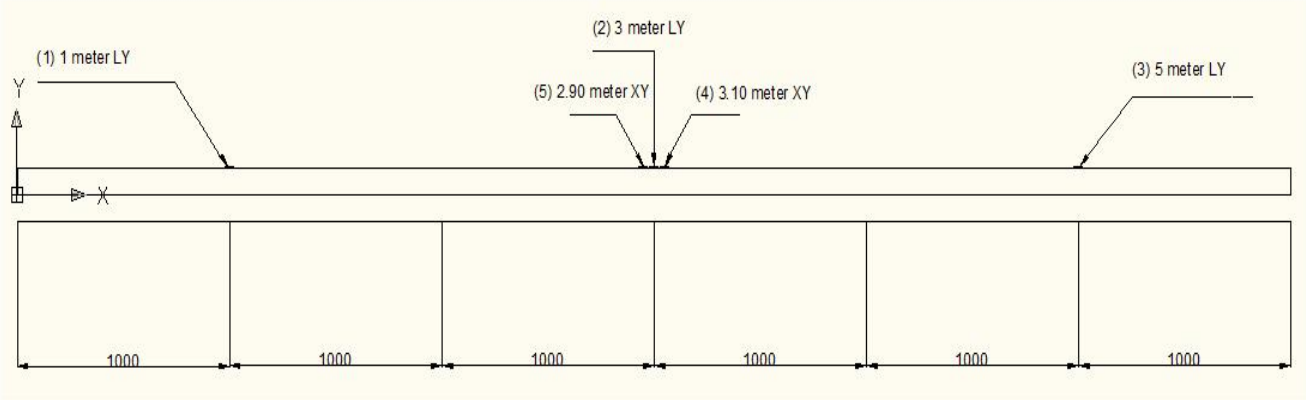

Figure 5.16 Positions where strain gauges are mounted on the pipe used for clay, sand and gravel

Figure 5.17 shows the tendency of the curvature variation of the pipe during the experiments as the force is applied. Initially there is an overbend above the imperfection, while there are sagbends on the sides. The best way to get the pipe to have a similar initial curvature before each test was to remove the mass under the pipe after each experiment, such that it was in contact with the imperfection, forming two spans towards the ends. When the pipe was in this position, filling the gaps beneath the pipe was performed, before adding cover on top. This way the pipe had more or less the same initial strains before the load was put on. The measured strain is not the actual strain that is acting in the pipe, but the strain that has occurred from when the pipe was in the initial position until it had been exposed to loading and lifted of the imperfection. If the actual strain was to be measured, the pipe would have to be laid on a flat surface, before zero balancing the strain gauges between each experiment. This would have taken a lot of time, as moving the pipe had to be performed by two persons to avoid plastic deformation of the pipe. Instead the pipe was zero balanced while laid in the initial position after the cover has been applied.

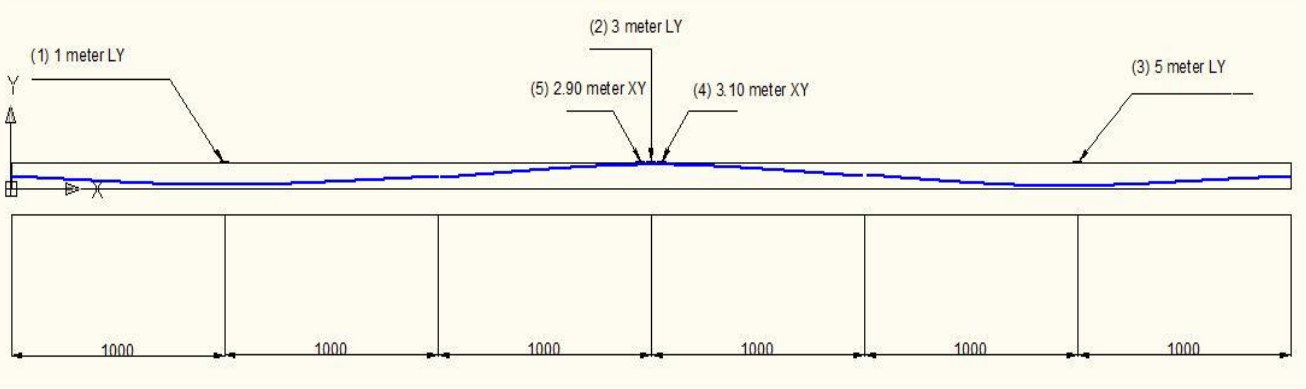

Figure 5.17 The blue line indicates the curvature of the pipe during the experiments

During the upheaval buckling experiments in clay, two pipes ended up being plastically deformed. Some of the experiments where run with a back up pipe that only had single directional strain gauges mounted. The strain gauges on this pipe were mounted as shown in figure 5.18.

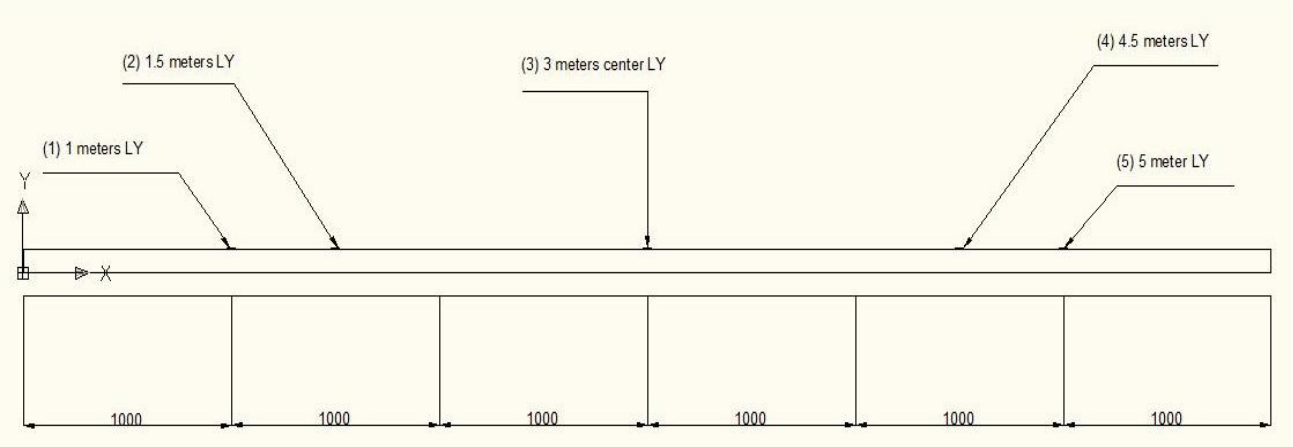

Figure 5.18 Strain gauge configurations for the backup pipe

In addition to the data collected from the strain gauges, the load cell mounted on the hydraulic cylinder monitored the axial force acting on the pipe. Post buckling the exposed length of the pipe, and the vertical displacement of the pipe above the imperfection, was also measured. The exposed length of the pipe, is the length of the pipe which has broken through the cover, and creating a span above the surface of the cover. The red line of figure 5.19 indicates the exposed length of the pipe. It was measured using a metric ruler.

Figure 5.19 Pipe exposed post buckling

When simulating the experiments in ANSYS, the gravitational loads from the cover are distributed along the pipe as an even load. To achieve an even load along the whole pipe in the experiments, this included forming an equal cover height for the whole pipe. As the pipe was laying over an imperfection, forming a cover providing an even load was difficult and time consuming. Some experiments were carried out with a cover following the pipes initial curvature, while most of the experiments were carried out forming a cover with an even surface as this was found more practical. This would however mean that the pipe had an

uneven vertical load distribution provided by the overlaid soil, and the results from these experiments could not be directly comparable with the ANSYS results. Figure 5.20 describes the different load distributions. Forming an even cover in the horizontal plane gives an unevenly distributed load.

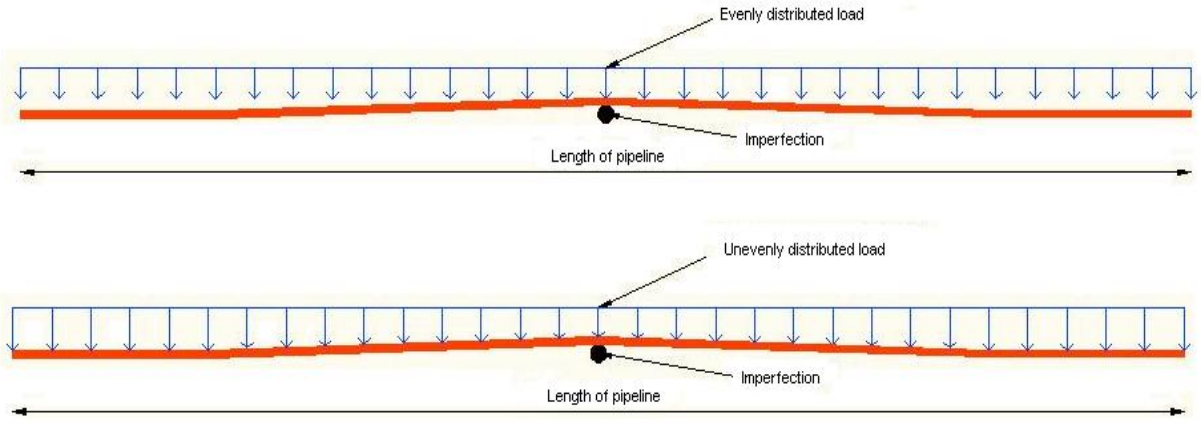

Figure 5.20 Load distribution from overlaid soil

Table 5-3 shows the test matrix for gravel. The measures gathered from the experiments are noted with a cross.

Table 5-3 Test matrix for gravel

Test matrix – gravel						
		Experiment				
Measured	Location	No cover	Trenched	Gravel 10mm	Gravel 20mm	Gravel 40mm
Load [kg]	Front	X	X	X	X	X
Strain [µm/m]	1m LY	X	X	X	X	X
	3m LY	X	X	X	X	X
	5m LY	X	X	X	X	X
	3.10m XY	X	X	X	X	X
	2.90m XY	X	X	X	X	X
	1.5m LY	-	-	-	-	-
	4.5m LY	-	-	-	-	-
Geometry	Exposed lenght	-	-	X	X	X
	Vertical disp.	-	-	X	X	X

Table 5-4 shows the test matrix for experiments with sand as cover. The only difference from the test matrix for gravel is the measured exposed length for the trench experiment.

Table 5-4 Test matrix for sand

Test matrix – sand						
		Experiment				
Measured	Location	No cover	Trenched	Sand 10mm	Sand 20mm	Sand 40mm
Load [kg]	Front	X	X	X	X	X
Strain [µm/m]	1m LY	X	X	X	X	X
	3m LY	X	X	X	X	X
	5m LY	X	X	X	X	X
	3.10m XY	X	X	X	X	X
	2.90m XY	X	X	X	X	X
	1.5m LY	-	-	-	-	-
	4.5m LY	-	-	-	-	-
Geometry	Exposed lenght	-	X	X	X	X
	Vertical disp.	-	-	X	X	X

Table 5-5 shows the test matrix for clay. Exposed lengths and vertical displacements where not measured for clay as they were difficult to observe and measure. Some tests were performed with the backup pipe with single directional strain gauges along the whole pipe.

Table 5-5 Test matrix for clay

Test matrix – clay						
		Experiment				
Measured	Location	No cover	Trenched	Clay 10mm	Clay 20mm	Clay 40mm
Load [kg]	Front	-	-	X	X	X
Strain [µm/m]	1m LY	-	-	X	X	X
	3m LY	-	-	X	X	X
	5m LY	-	-	X	X	X
	3.10m XY	-	-	X	X	X
	2.90m XY	-	-	X	X	X
	1.5m LY	-	-	X	X	X
	4.5m LY	-	-	X	X	X
Geometry	Exposed lenght	-	-	-	-	-
	Vertical disp.	-	-	-	-	-

5.4 Soil data

5.4.1 Gravel

The gravel used is shingle that normally is strewed on icy roads to ad friction. After some consideration the decision fell on shingle from Velde Pukk, as the grain size of this product was found suitable for the experiments. The general grain size of the shingle is 2 – 5 mm, but screen tests are performed for more precise data, see figure 18. The shear strength of the mass is detected by the shear vane tester just before the experiments are initiated. The density of the gravel was derived from the method described in *chapter 5.2.7*, and was found to be 2,25 kg/ dm^3, see table 5-3. The density distribution curve for the shingle is presented in figure 5.21.

Table 5-6 Density calculation for gravel

Density of gravel		
Weight of gravel	300,00	[g]
Weight of water	2224,60	[g]
Weight of gravel and water	2391,30	[g]
Density of gravel ρ_{gravel}	**2,251**	**[kg/dm^3]**

From figure 5.21 we can see that the shingle mainly consisted of grains larger than 2mm, but there are some finer grains in between.

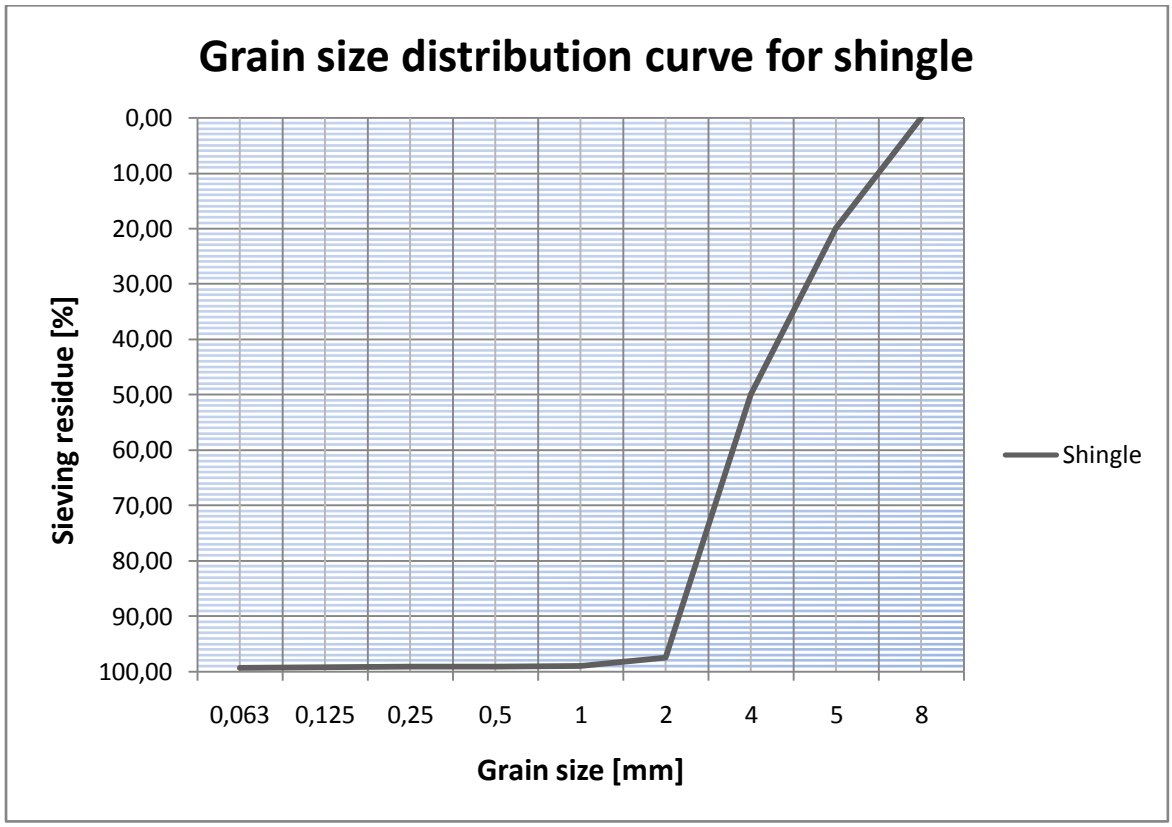

Figure 5.21 Grain size distribution curve for gravel.

5.4.2 Sand used in experiments

For the upheaval buckling experiments in sand, molding sand was used. The test cabinet was filled sand only. This sand is especially used as an aggregate in concrete mixtures and has general grain size from 0 – 6 mm. To deal with the uncertainty of water evaporating from the sand, water containment was checked using a Speedy Moisture Tester regularly at certain depths. The sand could also be compressed to some level, and this might also have impact on the results. For each experiment the sand was compressed as equally as practically possible by hands. At this level the weight of the sand is approximately 1,6 kg/dm^3. The density of the sand was detected as described in *chapter 5.2.7*, and was found to be 2,65 kg/dm^3, see table 5-5.

Table 5-7 Density calculation for sand

Density of sand		
Weight of sand	300,00	[g]
Weight of water	2224,60	[g]
Weight of sand and water	2411,20	[g]
Density of sand ρ_{sand}	**2,646**	**[kg/dm^3]**

Figure 5.22 shows the grain size distribution curve for sand. The sand contained some larger grains, but most of the sand grains had a diameter below 2mm.

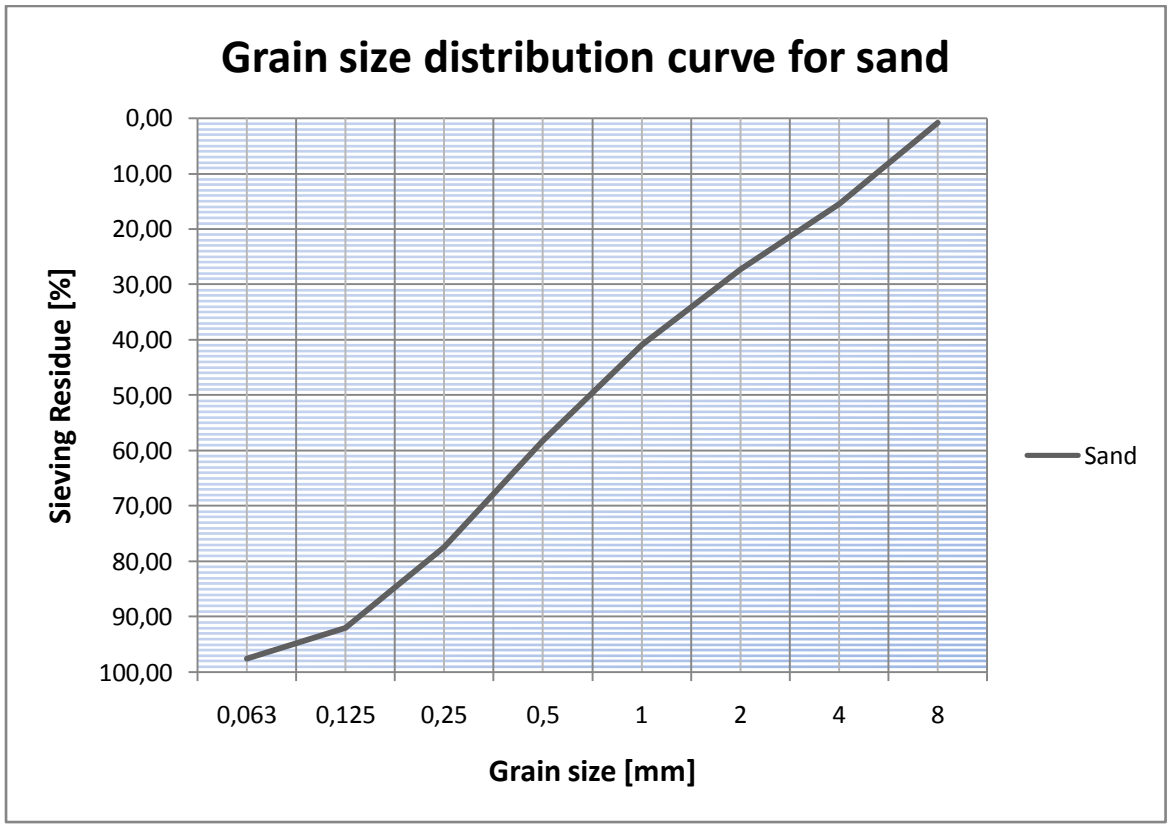

Figure 5.22 Grain size distribution curve for sand.

5.4.3 Clay used in experiments

The clay that has been used in this thesis has previously been used by Ingar Stava in experiments for his master thesis, Design of Arctic Pipelines in Areas Subjected to Ice Ridge Gouging, in the spring of 2007 [11]. The clay was stored under a tarpaulin outside the concrete lab at the University of Stavanger, after he was finished with his experiments. To get the clay in a homogeneous condition it was run in a cement mixer and a sufficient amount of water was added. It was chosen to fill a layer of shingle in the bottom of the test cabinet, before adding the clay. This was done because getting the clay in a suitable condition, consumed a lot more time than expected. The layer of clay started at least 3 cm below the pipe in the front and back end. The reason for this was to prevent that the shingle layer at the bottom form having a large influence on the pipe movements during experiments.

The density of clay varies with water containment. During the test period the water containment in the clay varied due to evaporation. Because of this there was not put any effort in deriving the actual density. Stava measured the dry density in the same clay to be 1309 kg/m^3 [11].

The undrained shear strength of the clay, s_u, was measured using the Geonor H-60 vane tester. The measures should preferably have been performed in the cover above the pipe. The pipe was not buried deep enough for the vane tester to measure the shear strength in that area. Because of this, measures were performed around the central region of the pipe, as it was expected upward movements of the pipe in this region. The undrained shear strength is also affected by disturbance. The clay was moved around and formed to achieve the different cover heights, especially in the region above the pipe. Because of this the measures from the vane tester may not be reliable.

The grain size distribution curve for the clay used in this thesis is the left curve shown in figure 5.23.

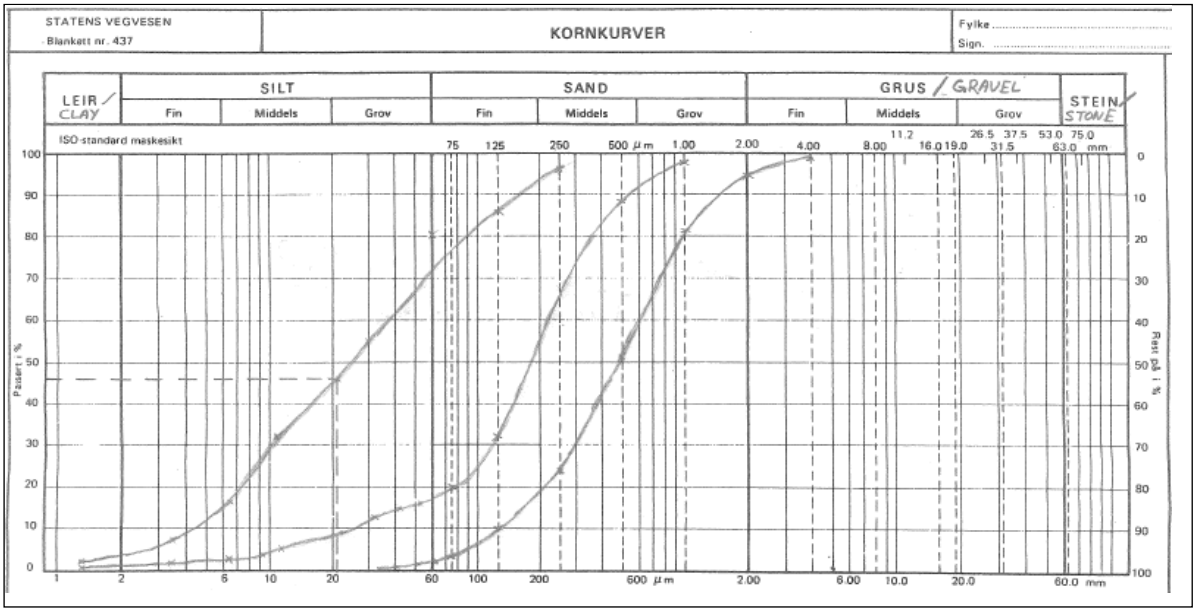

Figure 5.23 Grain size distribution curve for clay [11]

6. Finite element method – analysis

In this thesis the practical experiments have also been simulated using Pipeline Simulator, developed by IKM Ocean Design. The Pipe Simulator is a program based on the general purpose finite element package ANSYS. ANSYS is a large scale general purpose computer program used to solve several classes of engineering problems. The program is fully validated and used within several engineering areas including pipeline and risers analysis. The method used in the program is the matrix displacement of analysis based upon finite element idealization. It uses the wave front direct solution method for the system of linear equations developed from the matrix displacement method.

There are two ways of working with the ANSYS program. One way is to use the Graphics user interface, GUI, which has a graphical layout as conventional Windows programs. It displays a main menu tree where you can navigate through the different modules to run analysis, and a graphic window for displaying optional parts of the model. The other way is to write codes in command files that can be read into the program. When using codes it is possible to prepare scripts for a certain problem, such that input values like geometry and material properties can be changed for solving similar problems with different material properties or geometry. The Pipe Simulator is an example of a pre programmed script.

There are three phases to go through when working with ANSYS.

6.1 Preprocessing

The first phase is the preprocessing. In this phase the problem is defined by means of geometry and material properties. Geometry can be created manually or read in from for example computer aided design programs, CAD, or digital terrain models, DTM, based on surveys. The geometry is meshed into suitable sized elements, which are given an element type based on a degree of freedom set and material properties inputs suitable for the analysis. Data that is required for the calculation of the element matrix that cannot be determined from the node location or the given material properties are input as “real constants”. For pipe elements typically real constants can be inner diameter, outer diameter and thickness. Element types, material properties and real constants are normally defined before creating the geometry.

6.2 Solution

In this phase loads are applied. There are six categories of loads which are DOF constraints, forces, surface loads, body loads, inertia loads and coupled field loads. The loads can either be applied on the solid model, keypoints, lines, and areas or on the finite element model, nodes and elements. It is possible to specify different load steps, where different loads can be applied and solved. When all loads and constraints are applied and loadstep configurations are set, the solution calculations can be run.

6.3 Post processing

In post processing the desired results from the solutions can be gathered. From the solutions there can be obtained contour displays, deformed shapes, and tabular listings for each loadstep.

7. Results

The results presented in this chapter is further discussed and analyzed in chapter 8.

7.1. Results from lifting tests

7.1.1 Results from lifting tests in gravel

The lifting tests in gravel with one diameter cover height, 1D, and two times diameter cover height, 2D, were performed with different water containment in the gravel. For the 2D cover tests the gravel had a larger weight as the gravel had been stored outside in between the tests. The water containment was larger for the 2D tests, and explains the high increase in resistance from 1D to 2D. It was also difficult to get an even cover on top of the pipes because of the grain size of the gravel, especially for the 10mm pipe. However several tests were performed and averaged. Figure 7.1 shows the increase in uplift resistance for the different cover heights when gravel was used as cover.

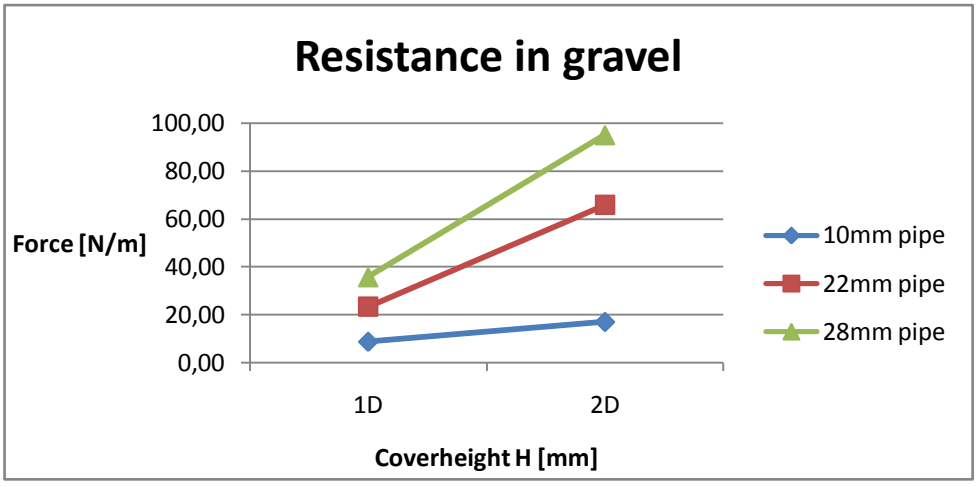

Figure 7.1 Resistance in gravel

Extensive data derived from the lifting test in gravel is shown in table 7-1.

Table 7-1 Resistance in gravel

Resistance in gravel								
Diameter [mm]	Cover [mm]		Resistance[N/m]		R/D Ratio 1	R/D Ratio 2	H/D Ratio	
OD	1D	2D	1D	2D	1D	2D	1D	2D
10.00	10.00	20.00	8.68	16.96	0.87	1.70	1.00	2.00
22.00	22.00	44.00	23.32	65.68	1.06	2.99	1.00	2.00
28.00	28.00	56.00	35.71	95.04	1.28	3.39	1.00	2.00

7.1.2 Results from lifting in sand

The variation in water containment during the sand test period was detected by the Speedy Moisture Tester and results are shown in table A-3 in the appendix. The measurements of sand containment were performed before experiment sessions were initiated. This meant that the sand had been lying undisturbed with the upper layer exposed to air for some time. Generally the water percentage was lower at the top surface of the sand. During preparation of the experiments, the sand was moved around and mixed such that sand with more wetness lower in the sand was on top. This way it was not expected that the water containment has had any sufficient impact on the results. In addition the results show a quite low water percentage in the sand.

When comparing the results from sand and gravel this shows that lifting the pipes buried in sand required higher tensional forces than for the pipes buried in gravel. The sand provided higher resistance than gravel, see figure 7.2.

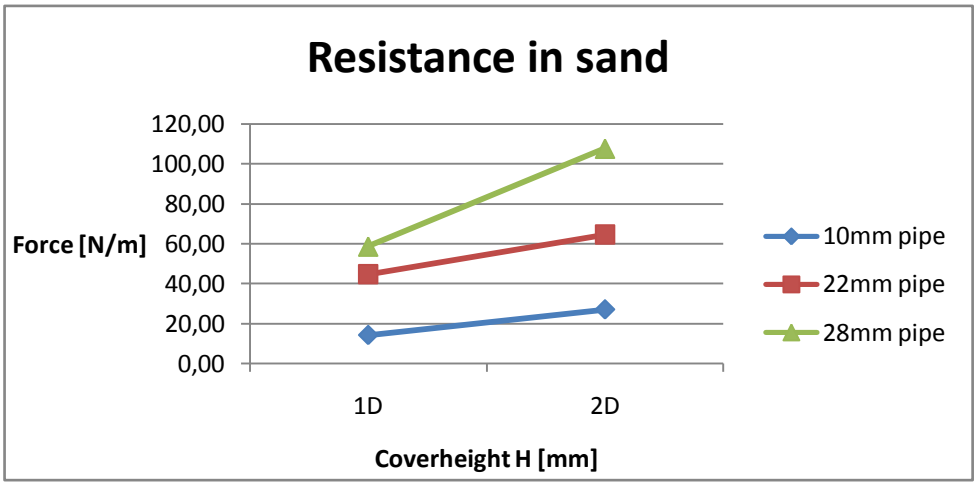

Figure 7.2 Resistance in sand

Extensive data for the lifting tests in sand are given in table 7-2.

Table 7-2 Resistance in sand

Resistance in sand								
Diameter [mm]	Cover [mm]		Resistance[N/m]		R/D Ratio 1	R/D Ratio 2	H/D Ratio	
OD	1D	2D	1D	2D	1D	2D	1D	2D
10.00	10.00	20.00	14.14	27.03	1.41	2.70	1.00	2.00
22.00	22.00	44.00	44.62	64.55	2.03	2.93	1.00	2.00
28.00	28.00	56.00	58.47	107.54	2.09	3.84	1.00	2.00

7.1.3 Results from lifting in clay

The clay used in these tests provided higher resistance than expected. As previously mentioned the strength of the clay is depending on water containment and disturbance among other. The tests were performed frequent, leaving little time for any significant consolidation to take place after adding the clay on top of the pipe. The average of the measured undrained shear strength $\overline{s}_u$ between the experiments was 11.5 kPa.

The results from tests with various cover height shows clearly that the resistance in clay is less depending on the cover height. The suction forces in the clay surrounding the pipe, has a higher impact on the resistance then the gravitational contribution caused by the weight of the soil. Figure 7.3 shows how the uplift force increases when the cover height is doubled. The results indicate that the resistance increases more with larger cover heights for larger diameter pipes.

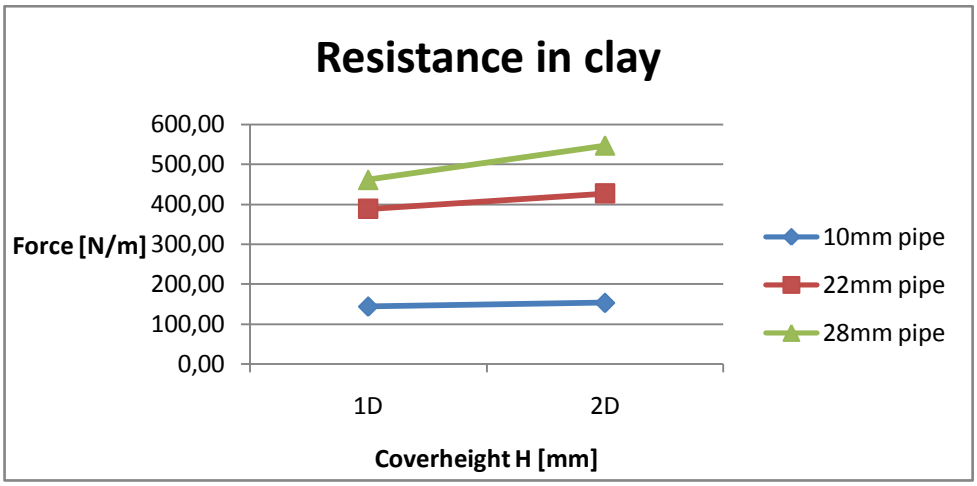

Figure 7.3 Resistance in clay

Extensive data from derived from the lifting tests in clay are shown in table 7-3.

Table 7-3 Resistance in clay

Resistance in clay								
Diameter [mm]	Cover [mm]		Resistance [N/m]		R/D Ratio 1	R/D Ratio 2	H/D Ratio	
OD	1D	2D	1D	2D	1D	2D	1D	2D
10.00	10.00	20.00	143.94	153.16	14.39	15.32	1.00	2.00
22.00	22.00	44.00	388.32	426.85	17.65	19.40	1.00	2.00
28.00	28.00	56.00	461.20	547.05	16.47	19.54	1.00	2.00

7.1.4 Ratio between diameter and resistance

Figures 7.4 to 7.6 show the ratios between resistance and the diameter for each pipe with the tested soils.

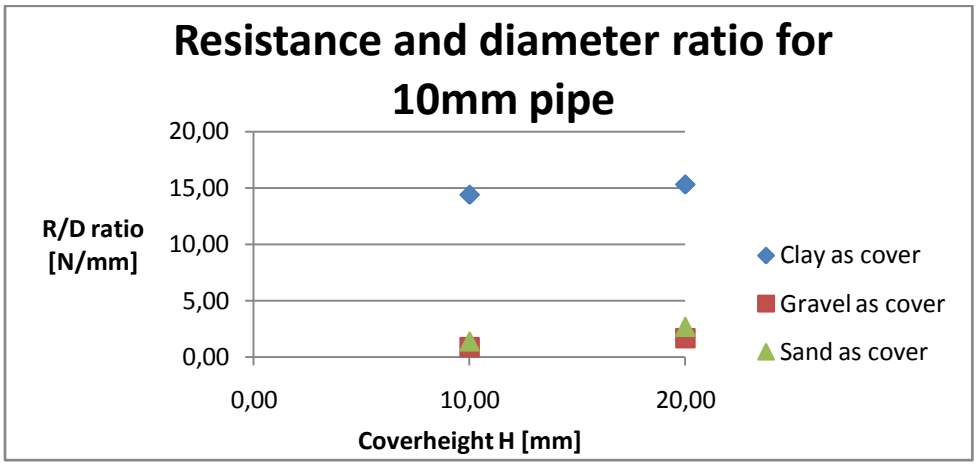

Figure 7.4 Resistance for 10mm pipe

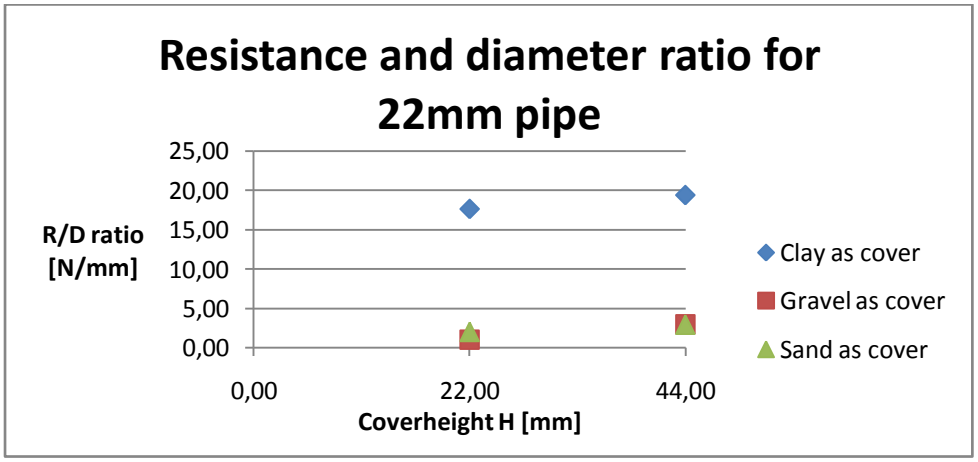

Figure 7.5 Resistance for 22mm pipe

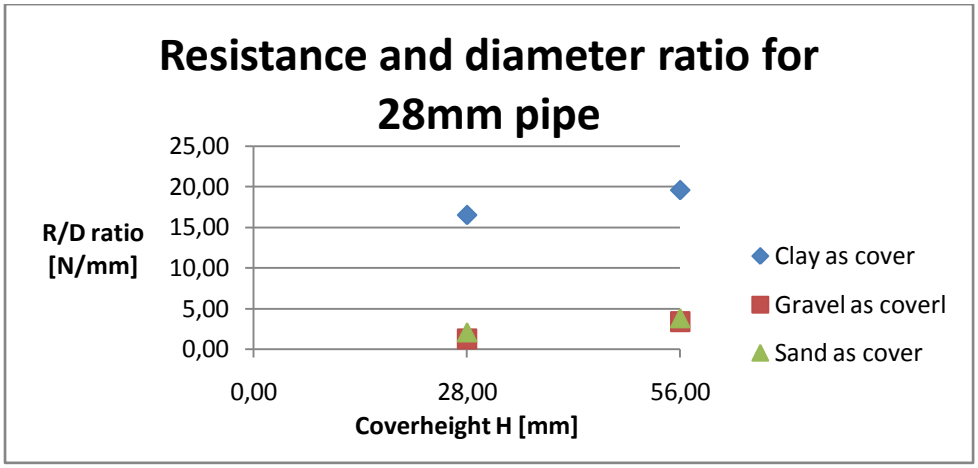

Figure 7.6 Resistance for 28mm pipe

7.2 Results from upheaval buckling tests

7.2.1 General behavior of pipe in experiments

Based on the experiments performed in this thesis, it is possible to detect a general behavior of a small scale pipe exposed to an axial force buried over an imperfection. Figure 7.7 shows the results from a random experiment performed for this thesis. The maximum axial force varies for different cover height scenarios.

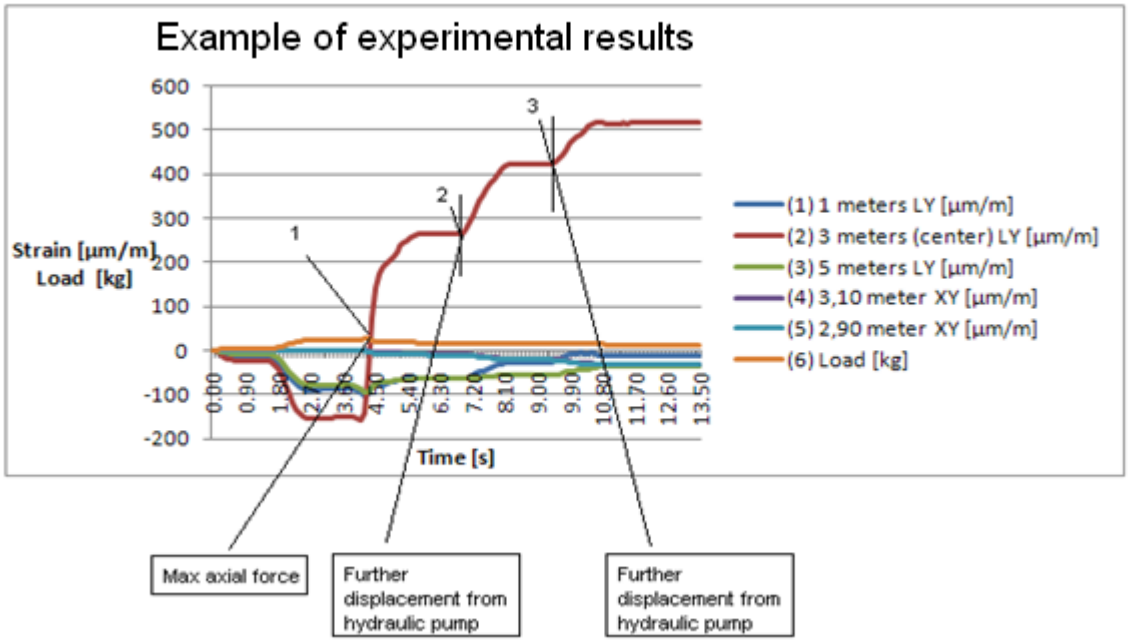

Figure 7.7 Results from a random experiment

The red curve in figure 7.7 shows the strain variation at the center of the pipe during increased displacements of the hydraulic pump, while the orange curve shows the axial force. Before the maximum force is reached, the difference in the strain at the center is negative. Because the imperfection supporting the pipe at the center allows no downward displacement of the pipe, this indicates that the curvature of the pipe has a smaller slope than before the force was applied, and that the pipe has started to displace vertically on both sides of the imperfection. The green and dark blue curves are showing increased negative values until this stage, indicating a steeper slope in the pipe curvatures pointing downwards. This also corresponds with a vertical displacement of the pipe on both sides of the imperfection as shown in figure 7.8 on the next page. The pipe movements can be explained by the soil failing downwards initially allowing the pipe do displace downwards in the sagbends. While the pipe displaces downwards in the sagbends, it moves slightly upwards on both sides of the imperfection.

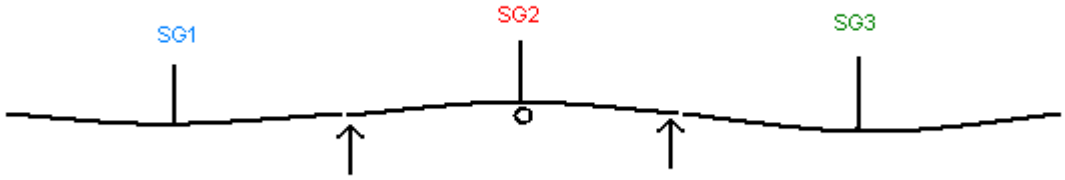

Figure 7.8 Curvature variation post until max force

When the maximum axial force is reached, noted as (1) in figure 7.7, the strain at the center of the pipe increases significantly while the force is reduced. The pipe has lifted of the imperfection and vertical deflection has occurred. Any further displacement applied on the hydraulic pump will not result in a higher force, but in a larger vertical deflection of the pipe above the imperfection. This is corresponding with existing theory, and proves that displacement controlled buckling by laying a pipe with horizontal curvatures, may be an option to reduce an effective axial force caused by thermal expansion. The curvature in figure 7.9 shows the movement after the maximum axial force is reached. The slope of the pipe curvature above the imperfection gets steeper, while the curvature of the sagbends straightens more out. This indicates that the whole central region of the pipe deflects vertically, but more significantly over the imperfection.

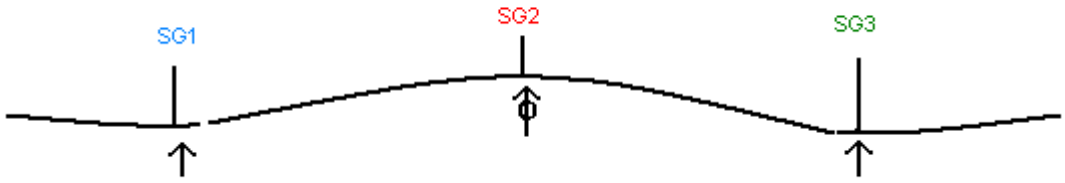

Figure 7.9 Curvature variation post max force

As the hydraulic pump is operated manually by jacking, the axial force / displacement is applied in steps. In figure 7.7, the additional steps post buckling are noted as (2) and (3). For each step the force is actually further reduced but the strain increases. This can be better seen when plotting load and strain on individual axis as in figure 7.10 on the next page.

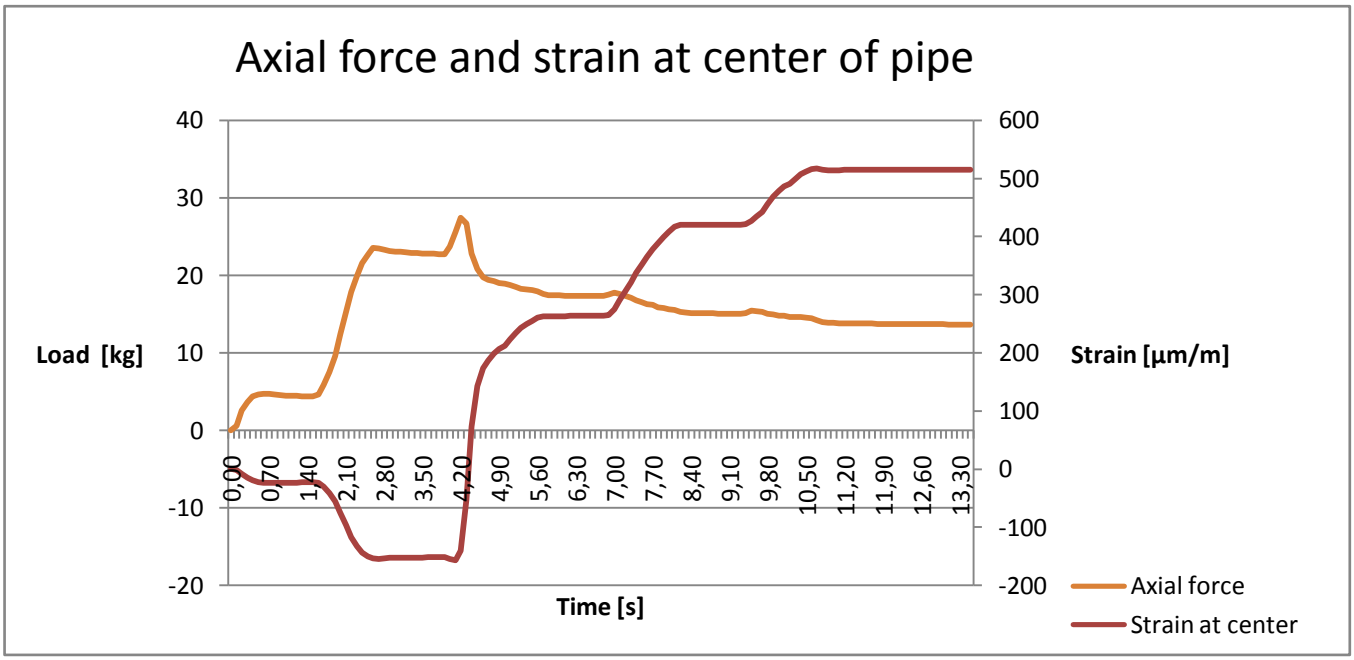

Figure 7.10 Load versus strain

For each step with further displacement on the pump, the axial force peaks and the strain in

7.2.2 Results from buckling experiments without cover

The purpose of these tests was mainly to demonstrate the behavior of a trenched pipeline exposed to buckling. The general behavior of a pipe exposed to buckling is to follow the way of least resistance, which in general will be up one of the walls on the sides. Failure will occur if the pipe buckles such that it is exposed over one of the wall edges. Figure 7.11 shows the pipe post buckling in the sand experiment. The length of the curvature at this specific experiment, which was performed as a pipeline trenched in sand, was 313 cm.

Figure 7.11 Buckling of trenched pipe

As the tests were carried out for demonstration purposes, there was not put any effort into getting similar geometry on the trenches in the different soil types. The strains and axial force was monitored and the measured results can be seen in tables 7-4 and 7-5. The results from the trenched scenarios in gravel and sand are still comparable.

Table 7-4 Results from no cover experiments

Sideways resistance						
Soiltype	**Gravel**					
Direction	LY			XY		AXIAL
Location	SG1 [µm/m]	SG2[µm/m]	SG3 [µm/m]	SG4 [µm/m]	SG5 [µm/m]	Load [kg]
Max	48	44	49	0	0	12.71
Min	-80	-125	-132	-92	-78	-0.04
Mass	**Sand**					
Location	SG1 [µm/m]	SG2[µm/m]	SG3 [µm/m]	SG4 [µm/m]	SG5 [µm/m]	Load [kg]
Max	2	0	0	1	1	11.35
Min	-106	-130	-127	-74	-77	0.00

Table 7-5 Results from trench experiments

Trenched						
Mass	Gravel					
Direction	LY			XY		AXIAL
Location	SG1 [µm/m]	SG2[µm/m]	SG3 [µm/m]	SG4 [µm/m]	SG5 [µm/m]	Load [kg]
Max	12	-1	9	1	1	11.45
Min	-85	-121	-101	-77	-81	0.06
Mass	Sand					
Location	SG1 [µm/m]	SG2[µm/m]	SG3 [µm/m]	SG4 [µm/m]	SG5 [µm/m]	Load [kg]
Max	-1	23	0	0	1	11.49
Min	-89	-122	-96	-68	-68	0.09

7.2.3 Max axial force in upheaval buckling experiments

The axial force has been measured for each experiment, except for two experiments in clay. The first test in clay led to plastic deformations in the pipe. This was not detected and several tests were run with the pipe in this condition. It is uncertain if the pipe broke through the cover because the maximum axial force was reached, or if it broke through because of the plastic deformations. When the plastic deformations were discovered, the pipe was replaced with a backup pipe. This pipe also ended up with plastic deformations, but it never broke through the cover. It is not unlikely that the maximum axial force would be higher if the pipes had not experienced plastic deformations. For the 10mm cover height in clay, the pipe did not break through the cover and thus the maximum axial force was not reached. This was planned to avoid plastic deformations in the pipe.

Figure 7.12 shows a summary of the axial forces for the different cover heights and soil types. For the scenarios where several tests have been performed, the average force from the different tests has been calculated.

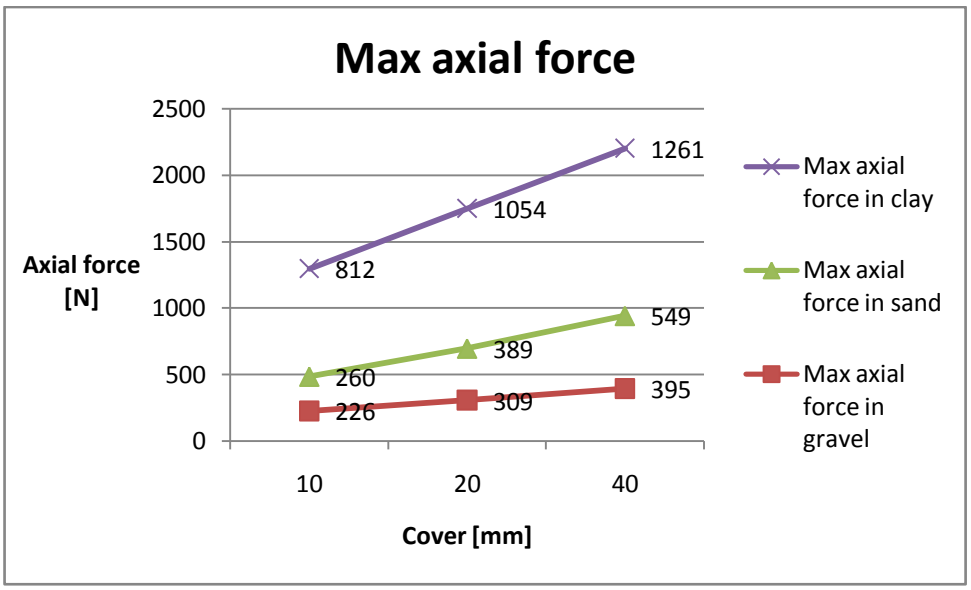

Figure 7.12 Max axial force in upheaval buckling experiments

The axial force needed to make the pipe buckle through the cover, corresponds with the previous results from the lifting test. Sand provides more resistance than gravel, and the clay has a significant higher resistance than the other soil types. Because of the experienced plastic deformations with the clay tests, it is likely that the maximum axial in clay could be higher.

7.2.4 Length of exposed pipe and vertical deflection

The exposed lengths and vertical deformations varied for each test. Even for the scenarios where several tests were performed, it was difficult to get similar results. This is mainly because the hydraulic jack was operated manually, and the displacement of the pump was difficult to control. The strain at the center of the pipe is also highly dependent on the vertical deflection and length of exposed pipe, and thus the maximum strain also varied. For the tests in clay vertical deflections and exposed lengths were not measured. An example of exposed length is shown in figure 5.19. Figures 7.13 to 7.19 show the length of the exposed part of the pipe, and the vertical deflection after buckling has occurred. The actual curvatures can be derived by subtracting the cover height from the vertical deflection. This has not been performed in these figures because the vertical deflections are also compared.

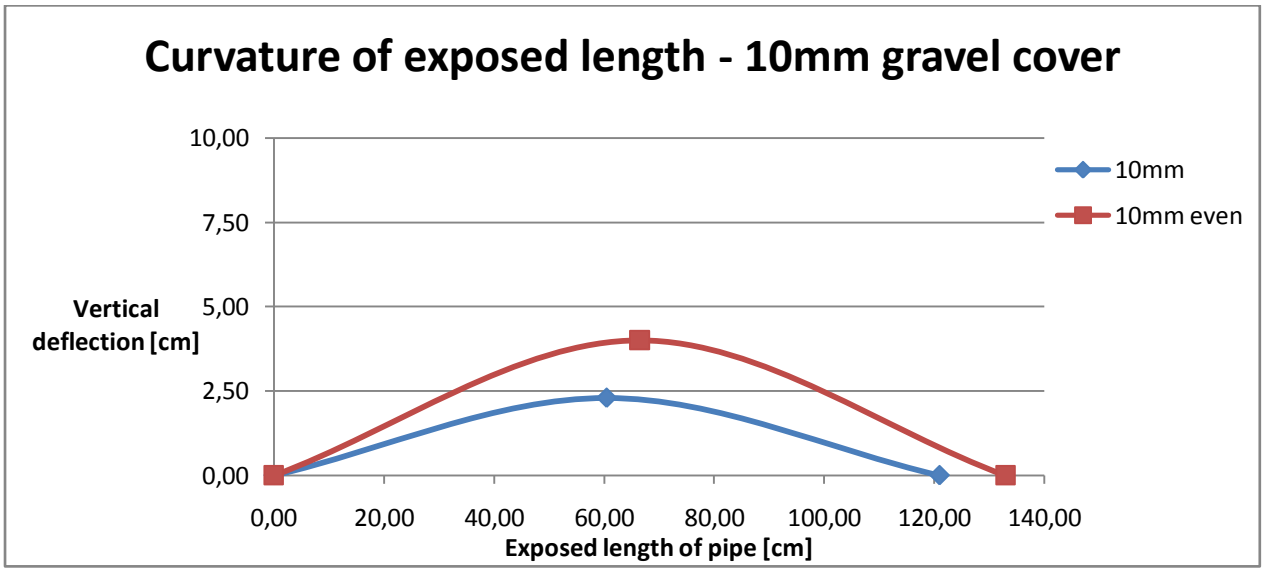

Figure 7.13 Curvature of exposed length - 10mm gravel cover

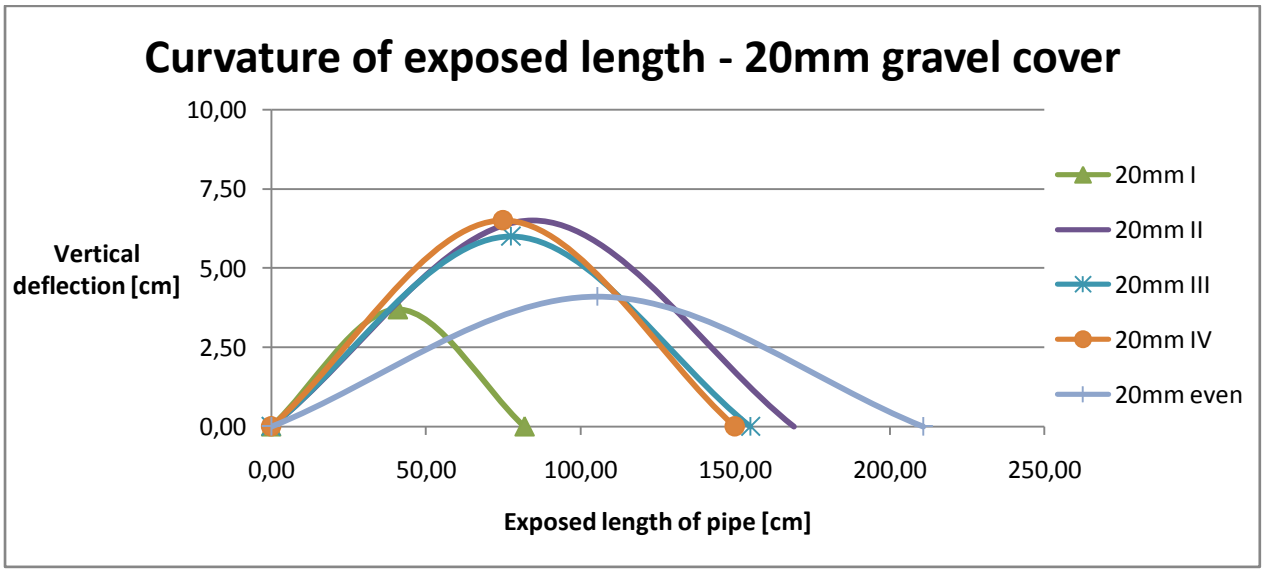

Figure 7.14 Curvature of exposed length - 20mm gravel cover

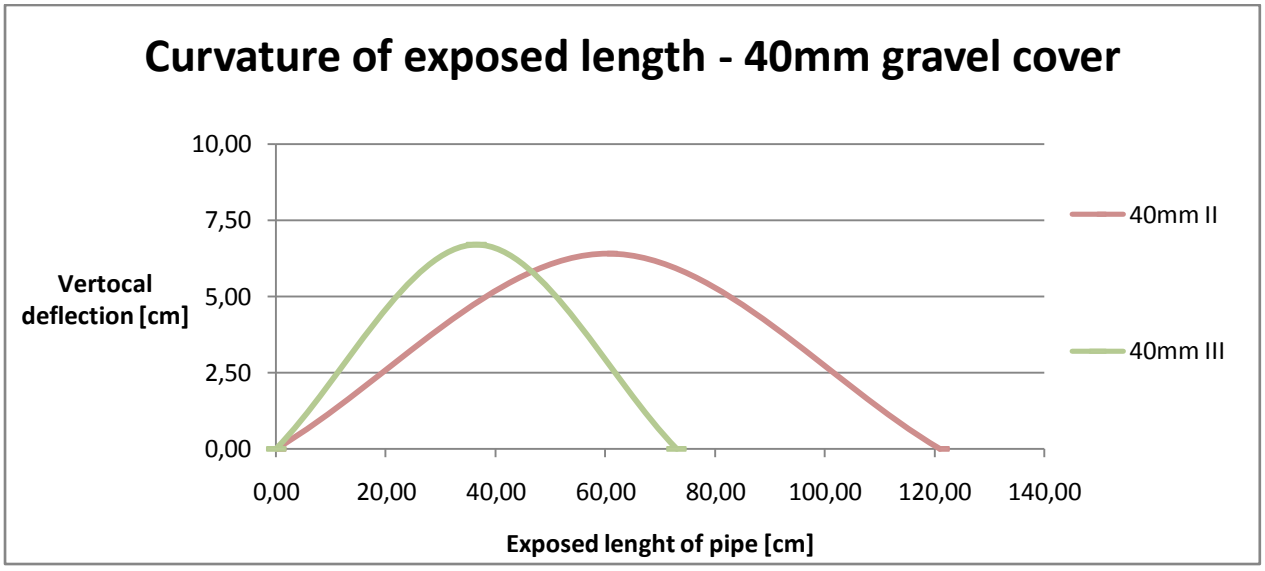

Figure 7.15 **Curvature of exposed pipe - 40mm gravel cover**

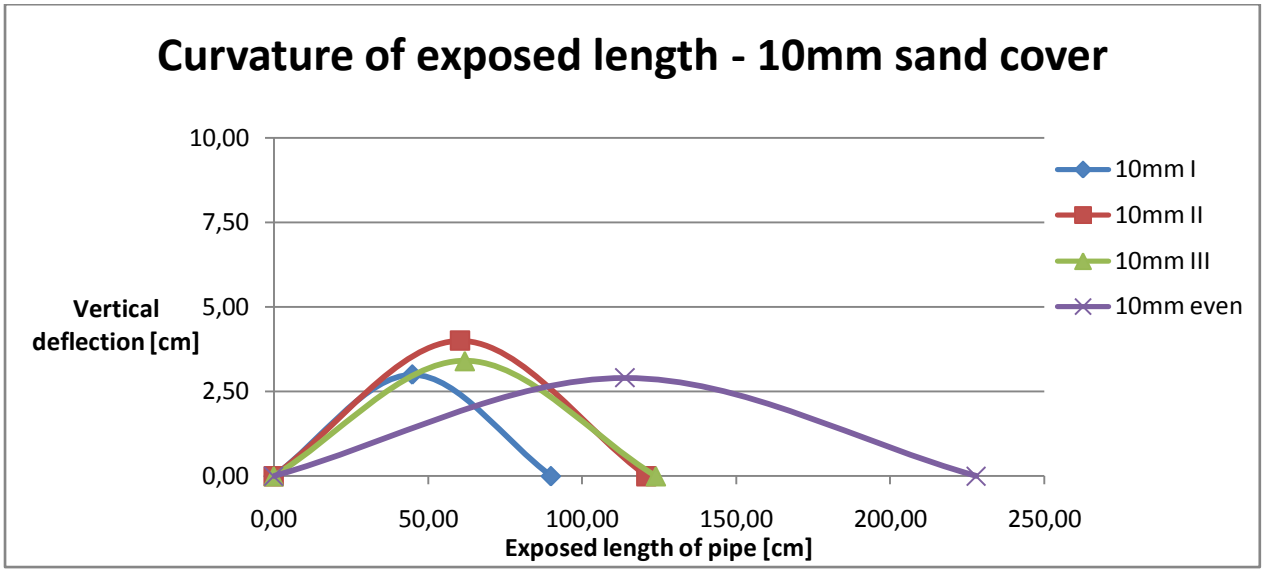

Figure 7.16 **Curvature of exposed length - 10mm sand cover**

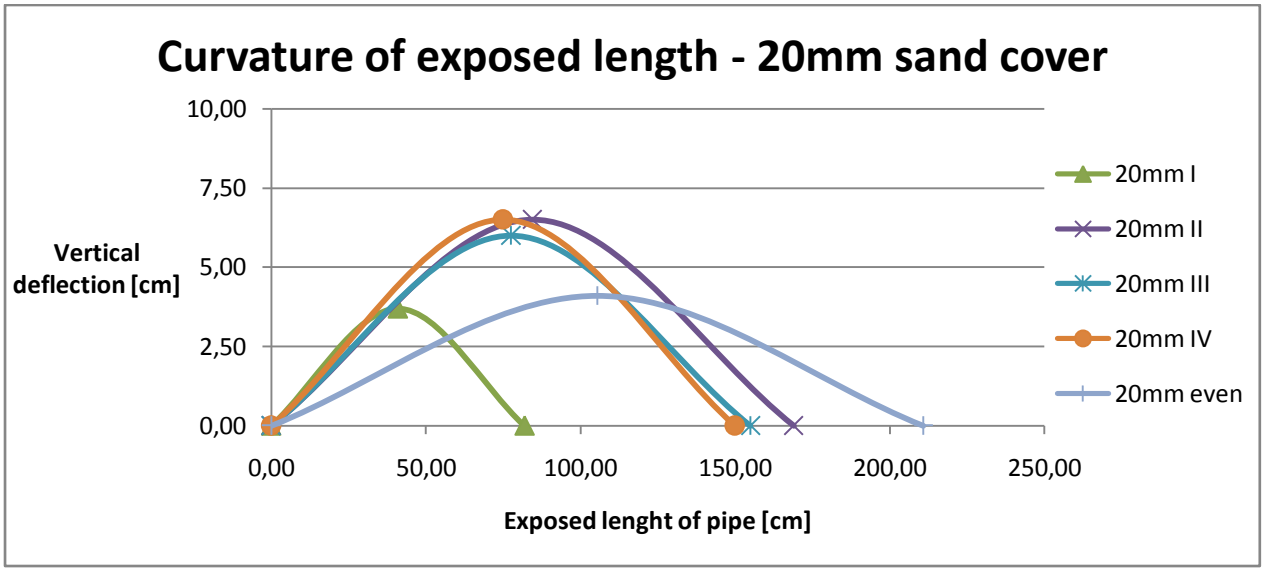

Figure 7.17 **Curvature of exposed length - 20mm sand cover**

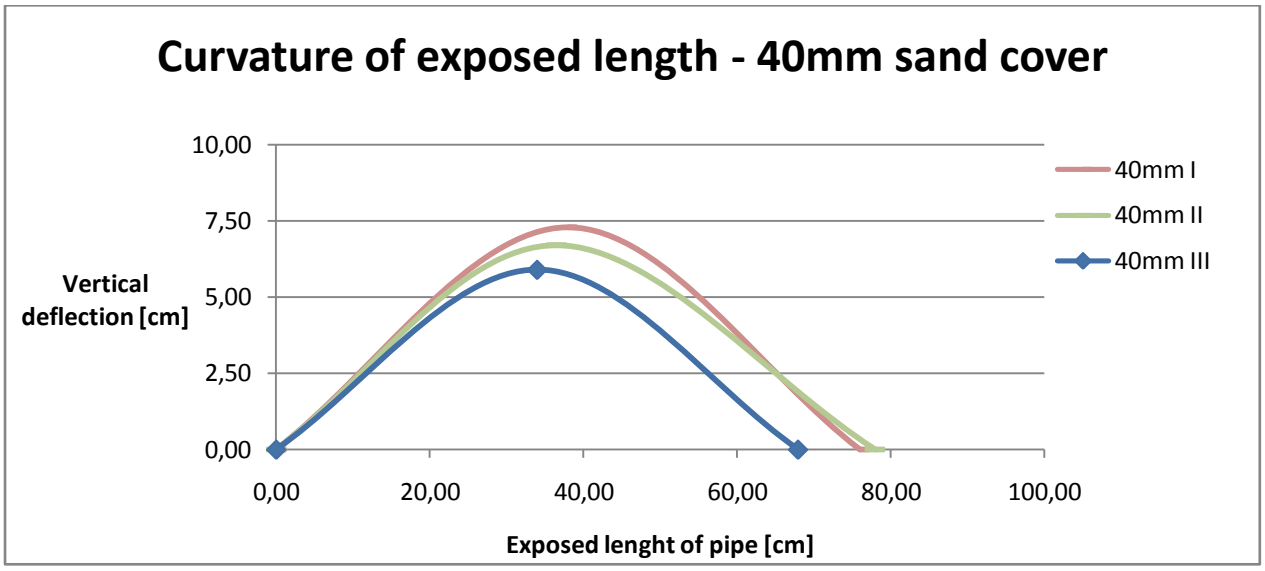

Figure 7.18 **Curvature of exposed length - 40mm sand cover**

In general the exposed length is longer with smaller cover heights. This is caused by the pipe needing a smaller vertical deflection to break through the cover. At larger cover heights the pipe will need a larger vertical deflection to break through the cover. In addition the resistance provided by the increased cover height tends to hold the pipe down on the sides of the imperfection.

7.2.5 Strain in pipe with various cover heights

As previously mentioned, the strain is measured from the initial position until post buckling. The strains are zero balanced in the initial position such that any strain in this position is neglected from the measures, and only the differences are measured. As the curvature in the sagbends is pointing downwards, and the strains are measured on the compression side of the pipe, the strains are given with a negative value. The minimum strains for the sagbends will therefore be presented. For the overbend the maximum strain is presented, as a curvature pointing upwards will gives positive values for strains. Figure 7.19 shows the locations where the axial strain is measured, and where the pipe curvature forms sagbends and overbend indicated by the red lines. The axial force is applied in positive x direction on the figure.

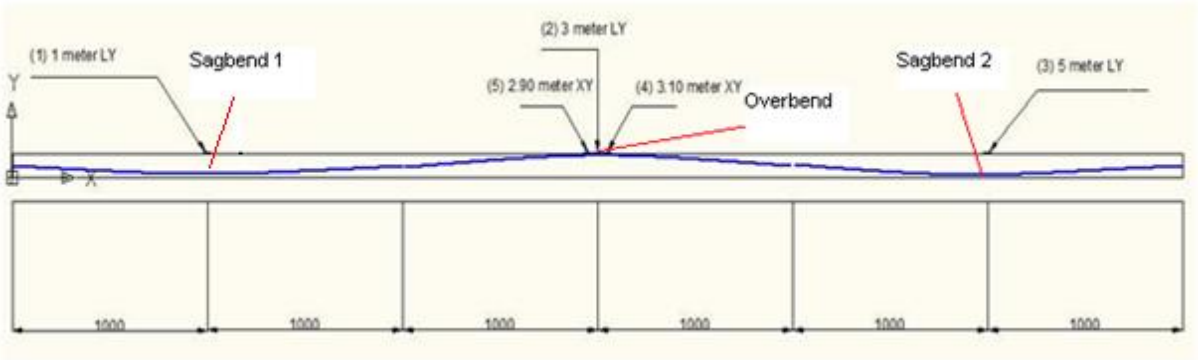

Figure 7.19 Curvature of pipe – red lines indicating sagbend and overbend positions.

Figure 7.20 shows the measured strain at the center of the pipe for experiments carried out with the different cover heights and in the different soil types. Some experiments with the same cover height and in the same soil ended up with quite different strains. To calculate an average of measured strains is not suitable. Because of this, if experiments resulted in various strains, the test with results in the middle range is presented.

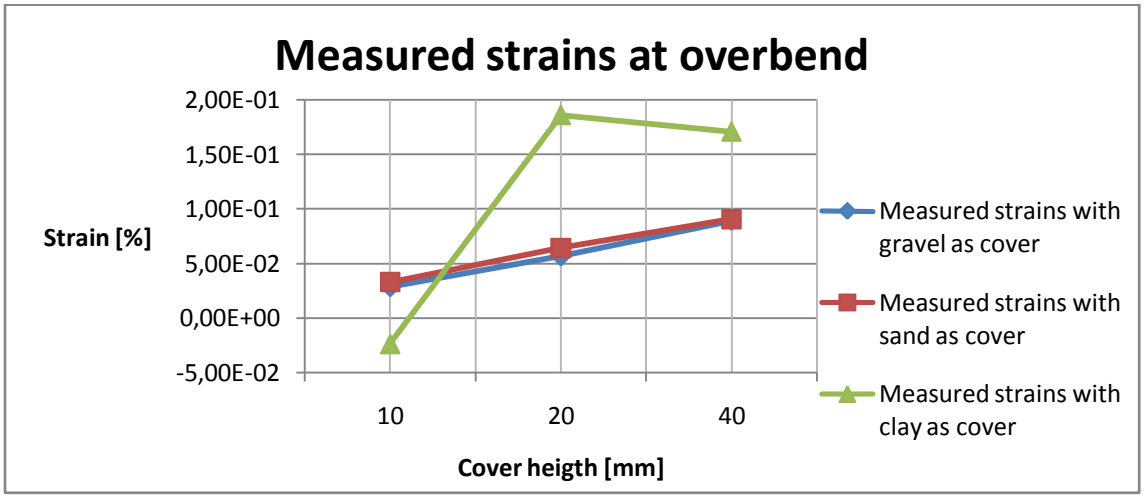

Figure 7.20 Measured strains at overbend

There was no significant difference in strain when the pipe was buried in sand or gravel. Still the pipe buckled at higher axial forces when covered with sand. When clay was used as cover, the strain in the pipe was much higher than when covered with the other two soils. The exposed length was not measured, as it was difficult to see if or where the pipe had broken through the cover. The strains still indicate a much steeper curvature that could be caused by the pipe being allowed to buckle downwards in the sagbends.

Note that for the 10mm cover height with clay, the pipe was exposed to an axial force that did not lead to upheaval buckling to avoid plastic deformations of the pipe.

Figures 7.21 to 7.22 show the minimum strain in the sagbends. The strain in the sagbends indicates that a pipe buried in clay is allowed a significant larger deflection downwards, compared to a pipe buried in sand or gravel. The failure of the soil has briefly been described in chapter 4.4.1. It is depending on the relation between downward and upward stiffness of the soil. In clay the pipe is able to deform utterly downwards compared to sand and gravel, and this can explain the steeper curvature of the pipe upwards from the imperfection.

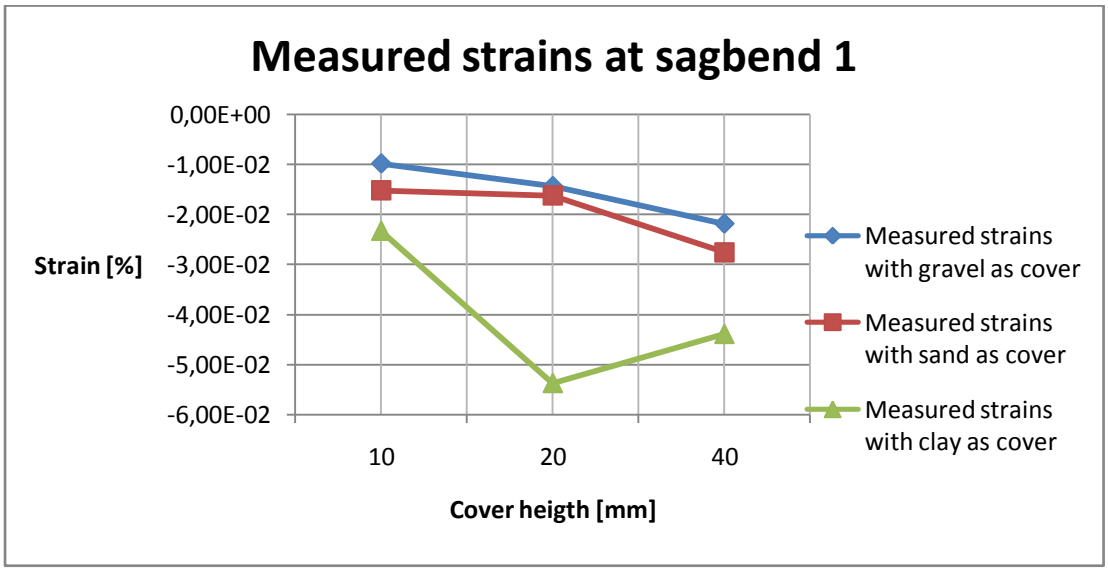

Figure 7.21 Measured strains at sagbend 1

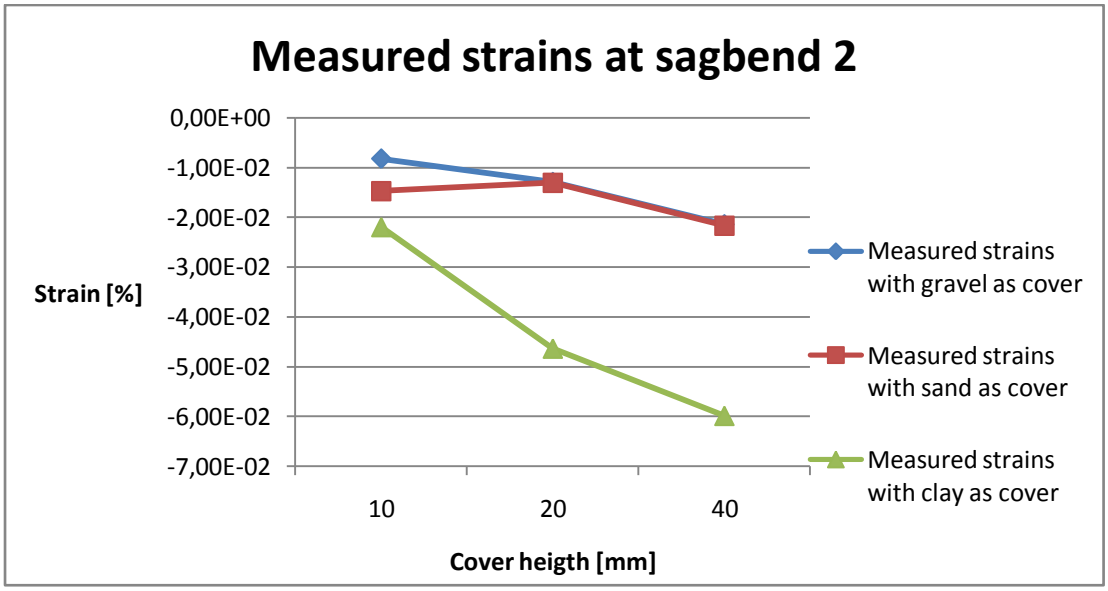

Figure 7.22 Measured strains at sagbend 2

7.2.6 Creep tests in clay

The creep tests were performed with the backup pipe with only single directional strain gauges. The tests were performed by applying force in a series, to simulate the pipe going in and out of service. In between each force build up the force was released to zero. Figure 7.23 shows the measured strain for each force build in steps. The results are showing that the pipe practically has the same initial position after being exposed to an axial force of at least 600 N.

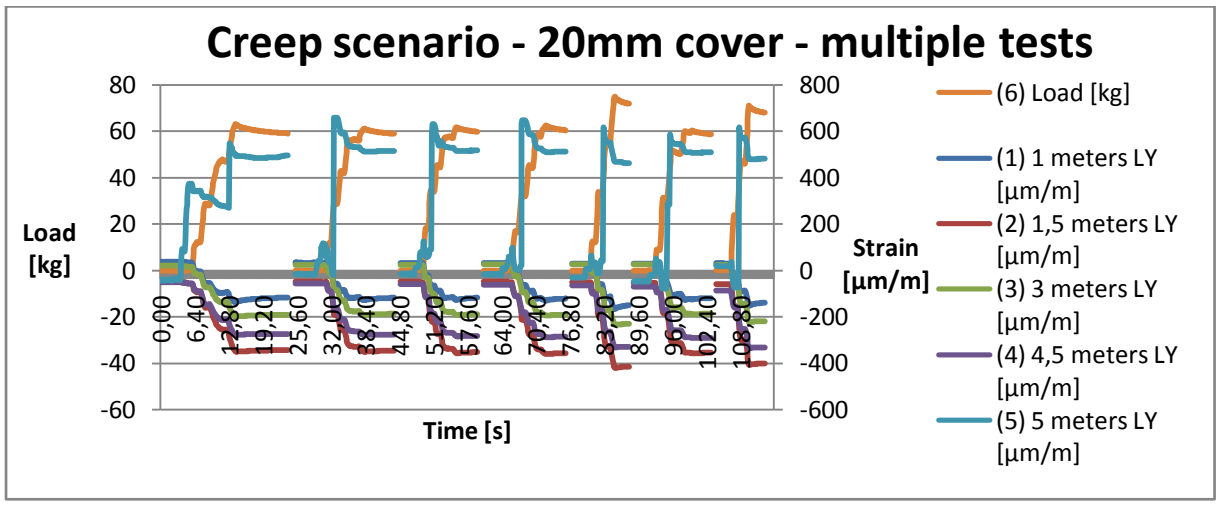

Figure 7.23 Creep scenario experiment measures

Figure 7.24 shows the measured strain from the strain gauges before and after loading. There is very small difference in the strain after the load has been released, and this suggests that the pipe has returned to its initial curvature after the force is released. The high result on the strain gauge 5, SG5, was found to be caused by plastic deformations in the pipe near the strain gauge. This should however not have any effects on the result of this test.

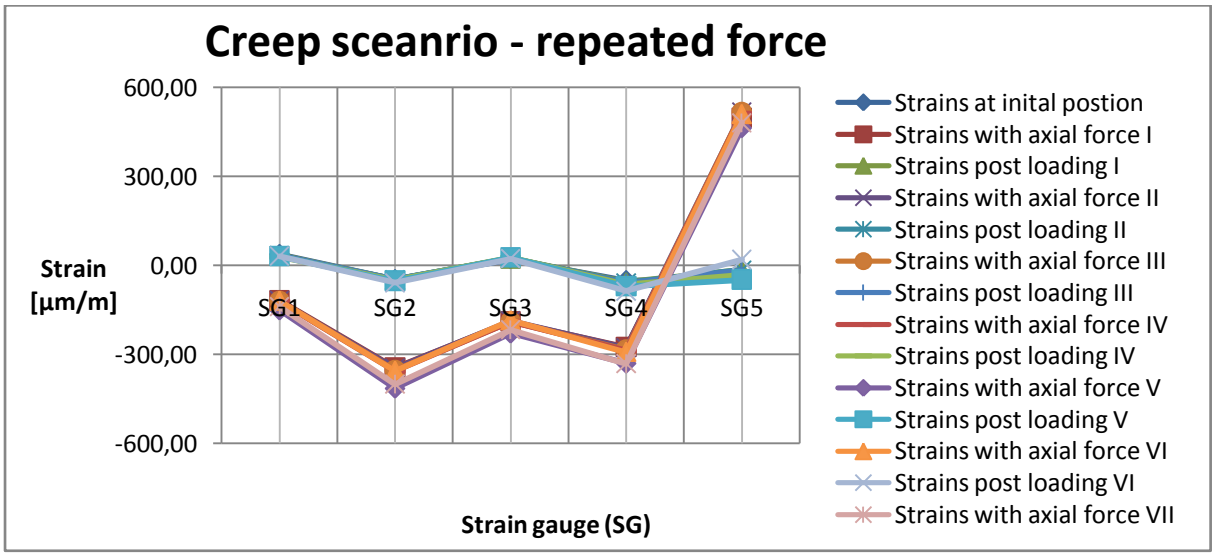

Figure 7.24 Measured strain pre and post loading in creep test

7.2.7 Various imperfections with clay as cover

Figures 7.25 to 7.27 show a comparison of the strains with different imperfections at the overbend and the sagbends. The intended purpose of these tests was to compare the maximum axial force. To avoid getting plastic deformations on another pipe, the axial force was not build up to a maximum making the pipe buckle through the cover. The figures also show the effect an increased cover height has on the strains.

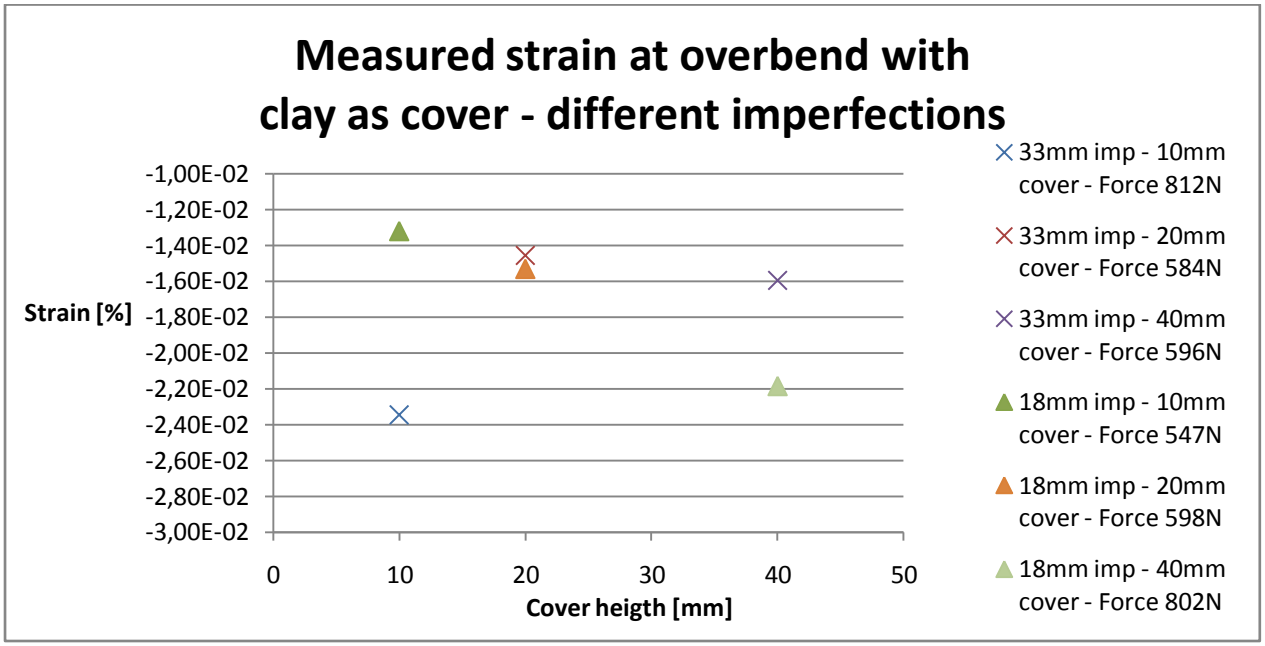

Figure 7.25 Measured strains at overbend with 33mm and 18mm imperfections

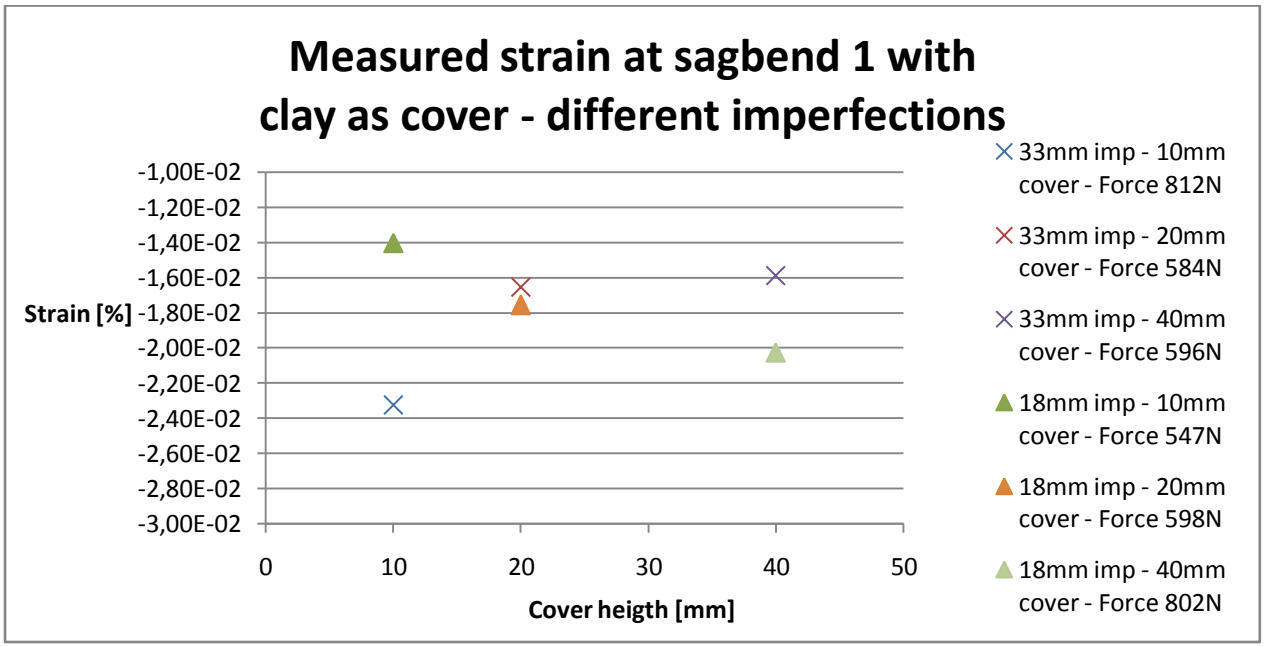

Figure 7.26 Measured strains at sagbend 1 with 33mm and 18mm imperfections

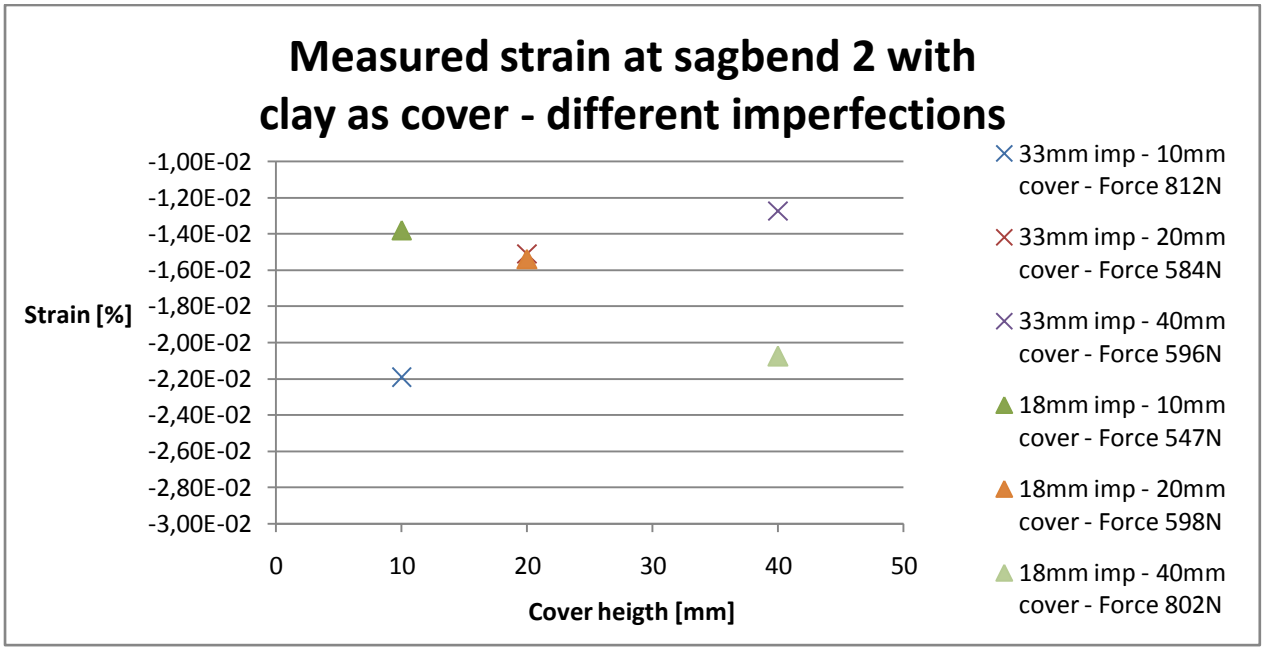

Figure 7.27 Measured strains at sagbend 2 with 33mm and 18mm imperfections

7.3 Comparison of experimental - and analytical results

This chapter shows a comparison of the strains from the finite element method analysis and the monitored strains from the strain gauges in the experiments. The axial forces added in the ANSYS model were in the same range as the measured maximum axial forces from the experiments. The ANSYS based Pipe Simulator gave an envelope of axial strains where minimum and maximum axial strains where given through the whole pipe. In the experiments the strain variation from the initial position until buckling occurred was monitored at 1 meter, 3 meters and 5 meters, respectively. The strains at these locations were derived from the ANSYS results for comparison.

Results in ANSYS were given for individual loadsteps. One loadstep was empty condition where no axial force was added. Further loadsteps included an increase in the axial force. As the strain gauges measured the strain difference from the initial position to post buckling, the ANSYS strains for empty condition was subtracted from further loadsteps to get the difference in strains. The analytical results from ANSYS are given for two loadsteps whereas one has an equal axial force to the experiment for comparison.

As the resistance from the cover is added as an evenly distributed load in ANSYS, the experiments with an even cover height were used for comparison if applicable. Figures 7.28 to 7.39 on the following pages present the analytical calculated strains from ANSYS and the experiments at certain cover depths. The strains from the experiments are noted with a cross.

7.3.1 ANSYS results from upheaval buckling tests in gravel

The comparison of strains with gravel as cover shows that the experiments gave larger strains at the overbend. However for the 10mm cover, an increase of only 3 N in ANSYS gave a dramatic increase in strains. For the 40mm cover much larger strains occurred in the experiment.

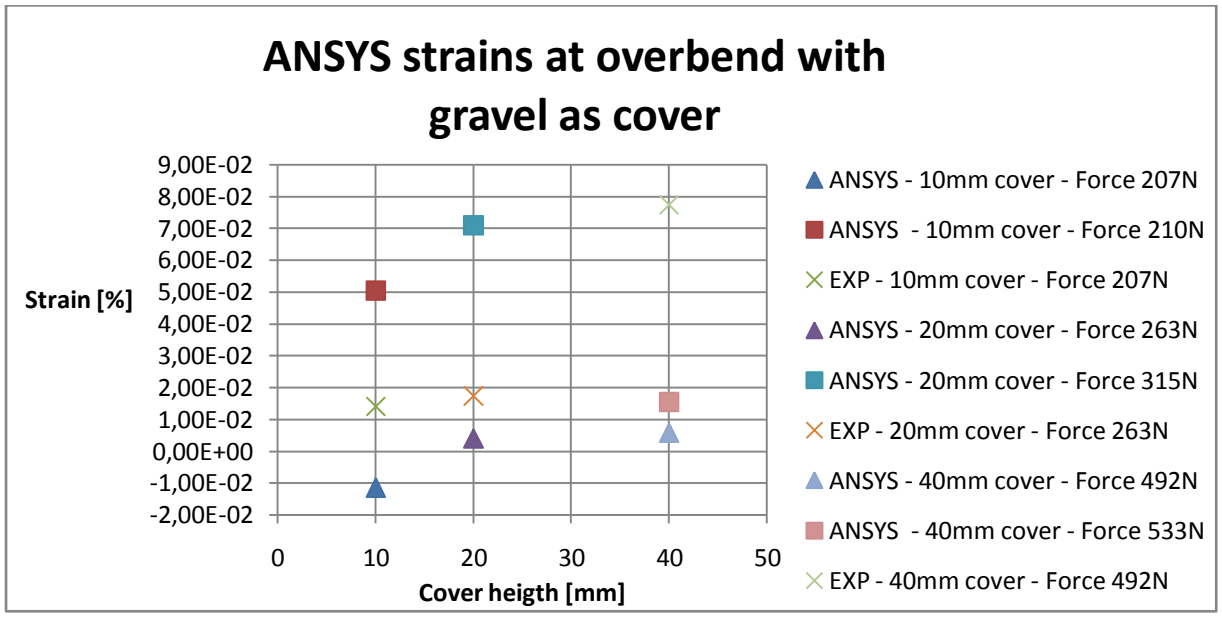

Figure 7.28 **Axial strain comparison for pipe covered with gravel at overbend**

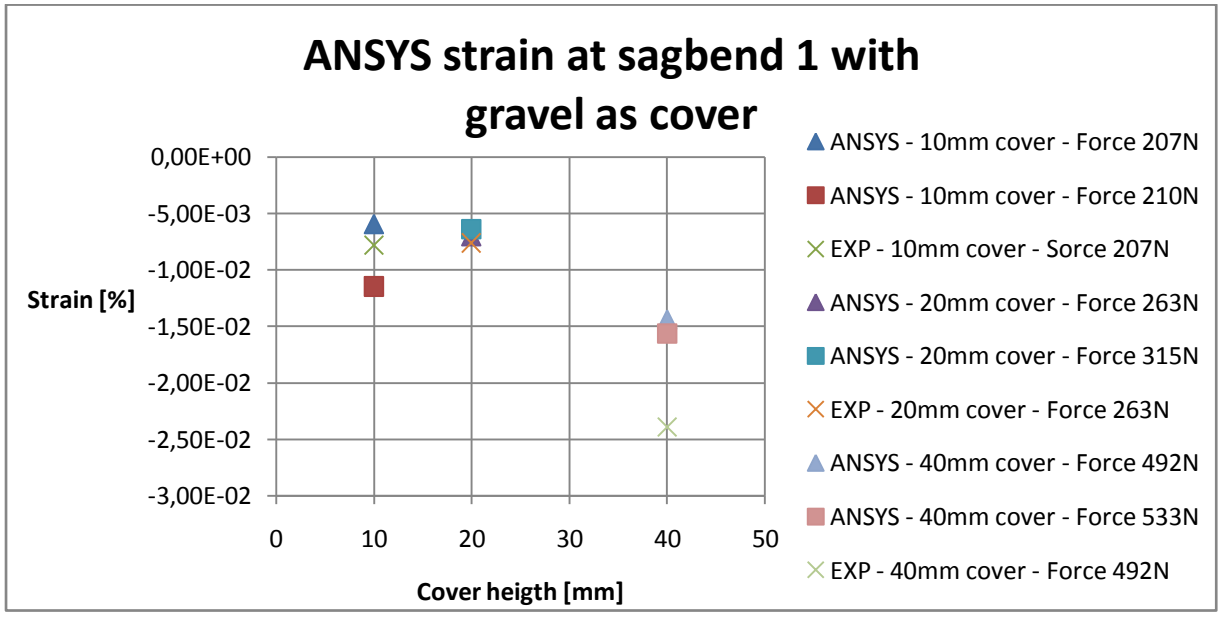

Figure 7.29 **Axial strain comparison for pipe covered with gravel at sagbend 1**

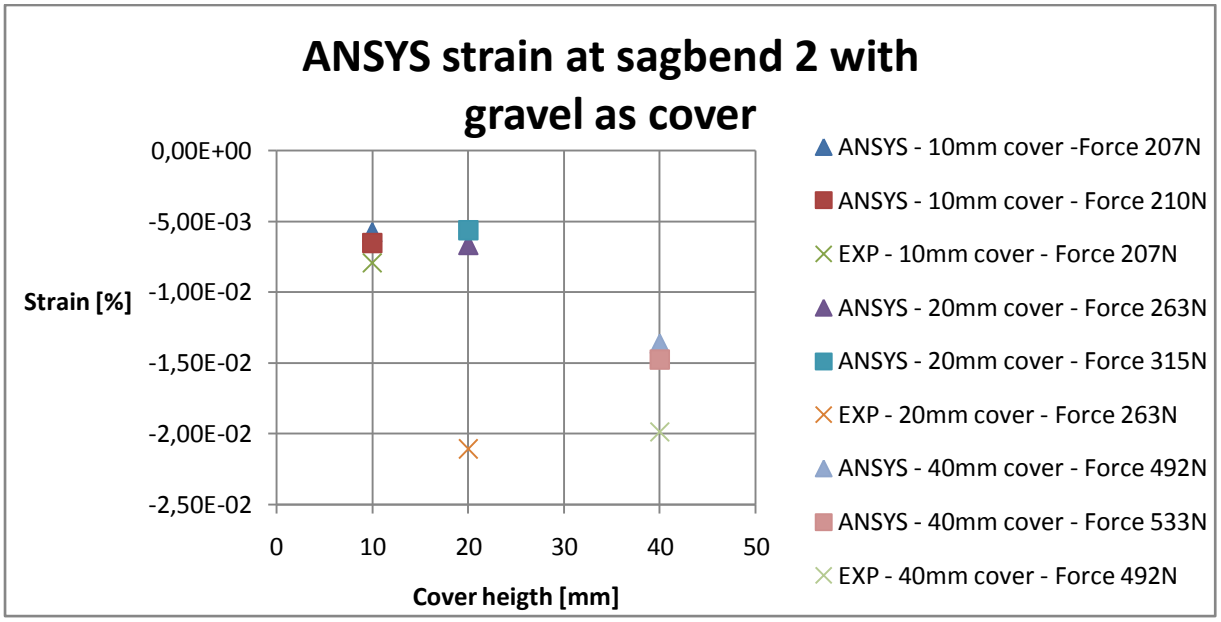

Figure 7.30 **Axial strain comparison for pipe covered with gravel at sagbend 2**

7.3.2 ANSYS results from upheaval buckling in sand

The comparison of strains when sand was applied as cover gave more comparable results. With 10mm cover there is a dramatic increase in the strain with an increase of 12 N in ANSYS.

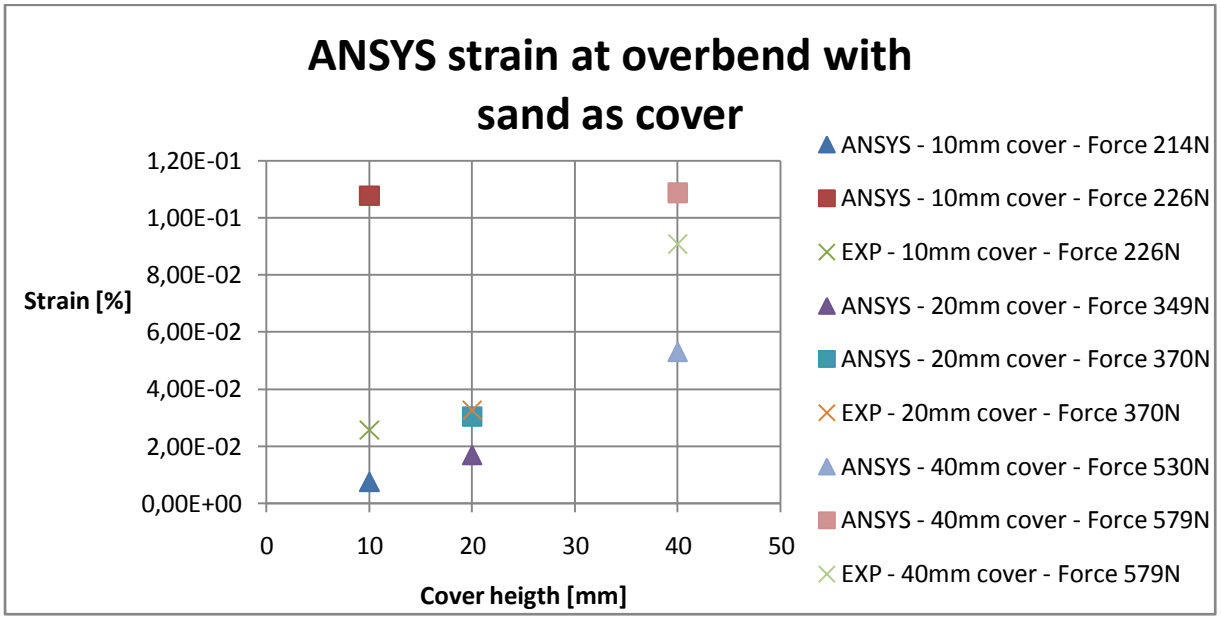

Figure 7.31 **Axial strain comparison for pipe covered with sand at overbend**

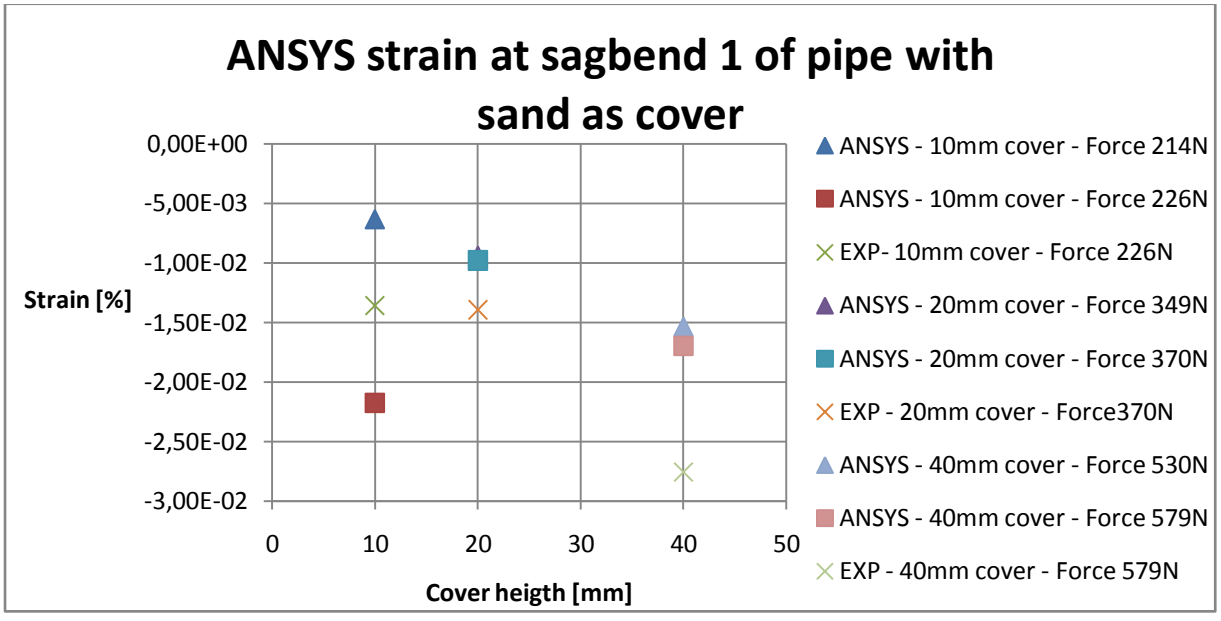

Figure 7.32 **Axial strain comparison for pipe covered with sand at sagbend 1**

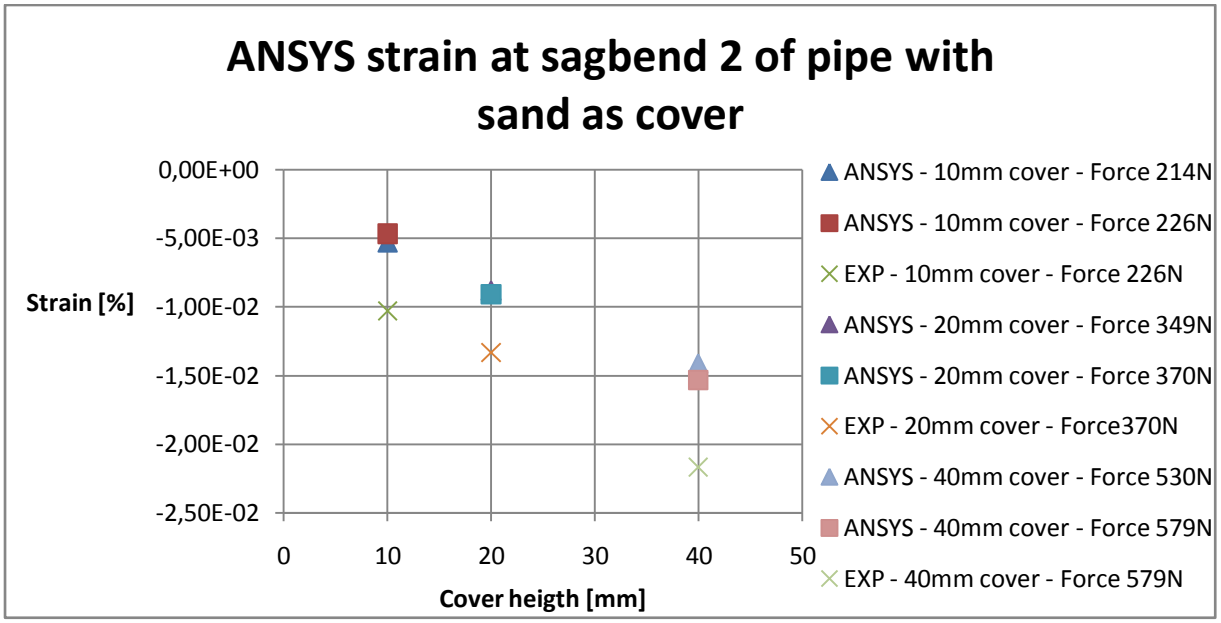

Figure 7.33 **Axial strain comparison for pipe covered sand at sagbend 2**

7.3.3 ANSYS results from upheaval buckling in clay – 33mm imperfection

The experiments in clay have turned out to be best suited for comparison with the analytical results derived from ANSYS. The reason for this is because the axial forces in the compared experiments did not lead to upheaval buckling. The soil was still failing downwards when the maximum axial force was reached, and the analytically derived strains suggest that the same failure direction appears in ANSYS for the given axial forces.

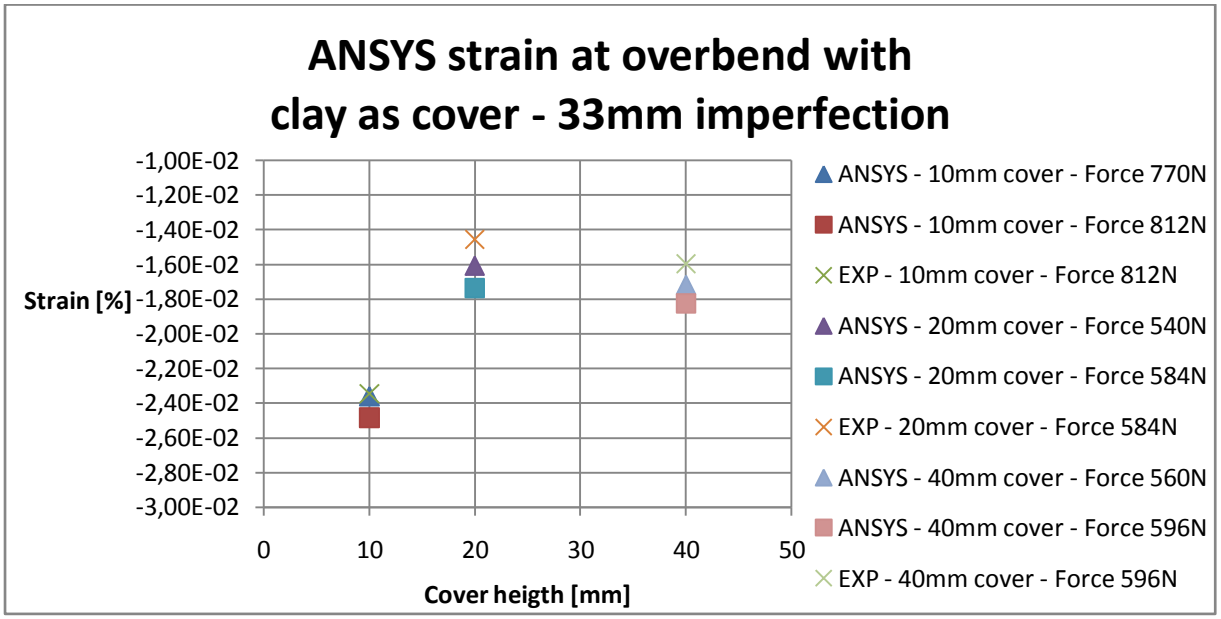

Figure 7.34 Axial strain comparison for pipe covered with clay at overbend – 33mm imperfection

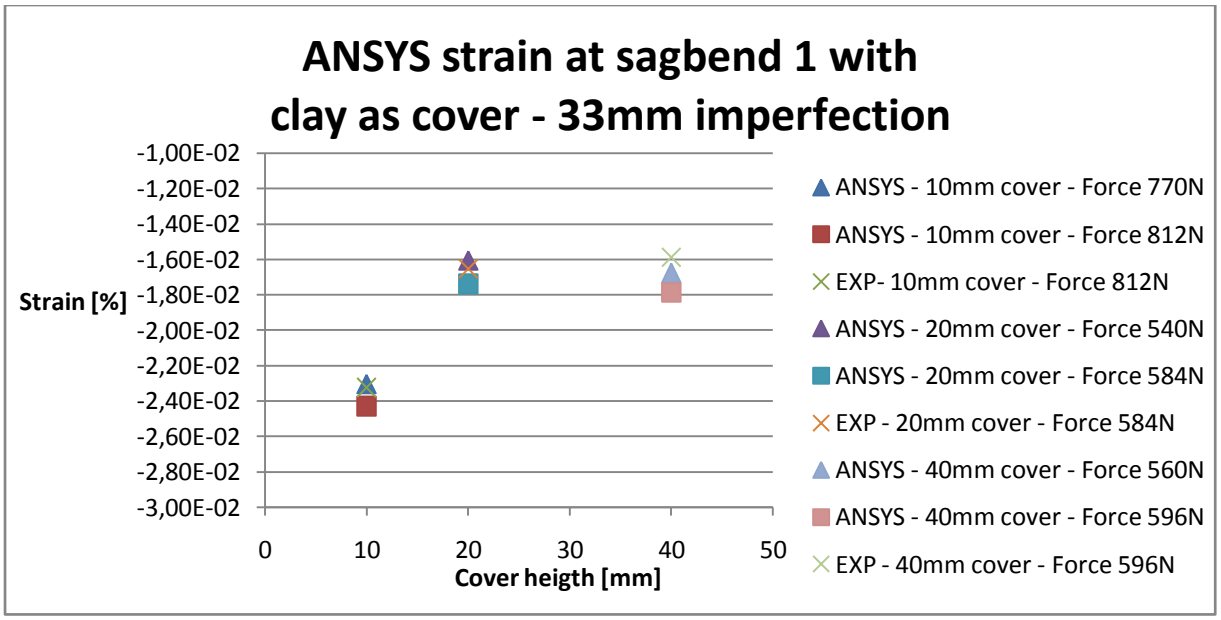

Figure 7.35 Axial strain comparison for pipe covered with clay at sagbend 1 - 33mm imperfection

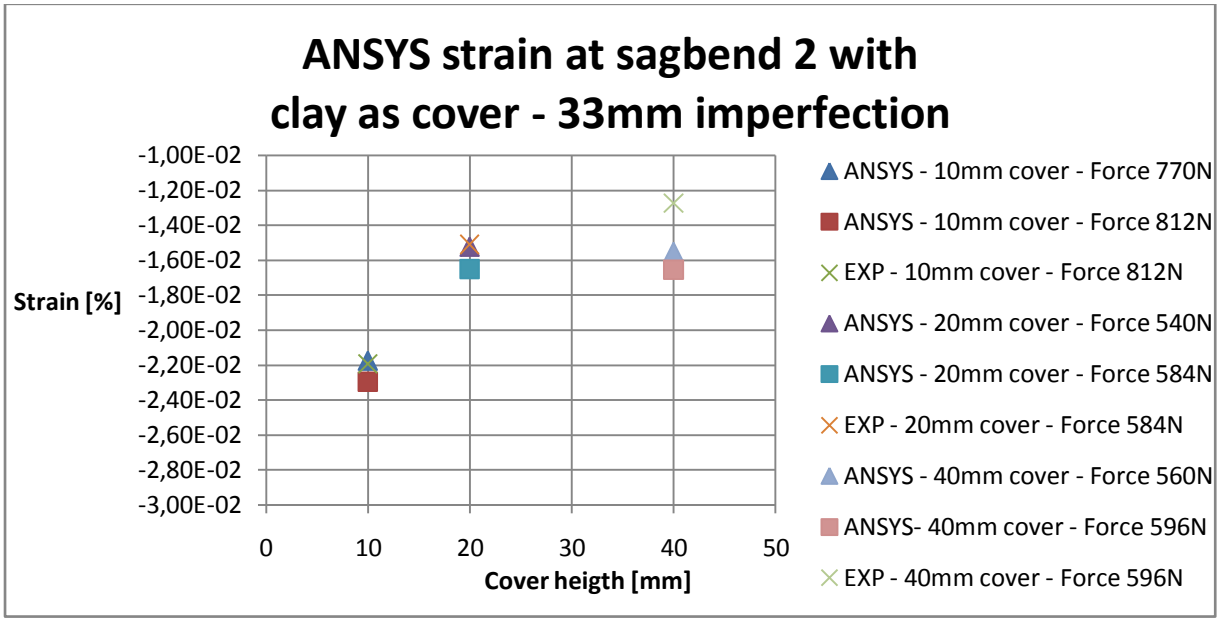

Figure 7.36 Axial strain comparison for pipe covered with clay at sagbend 2 – 33mm imperfection

7.3.4 ANSYS results from upheaval buckling in clay – 18mm imperfection

The reason for using a smaller imperfection was originally to detect a relation between the required maximum axial force and the imperfection size. As the resistance in clay was much higher than expected, it was difficult to make the pipe buckle such that it broke through the cover.

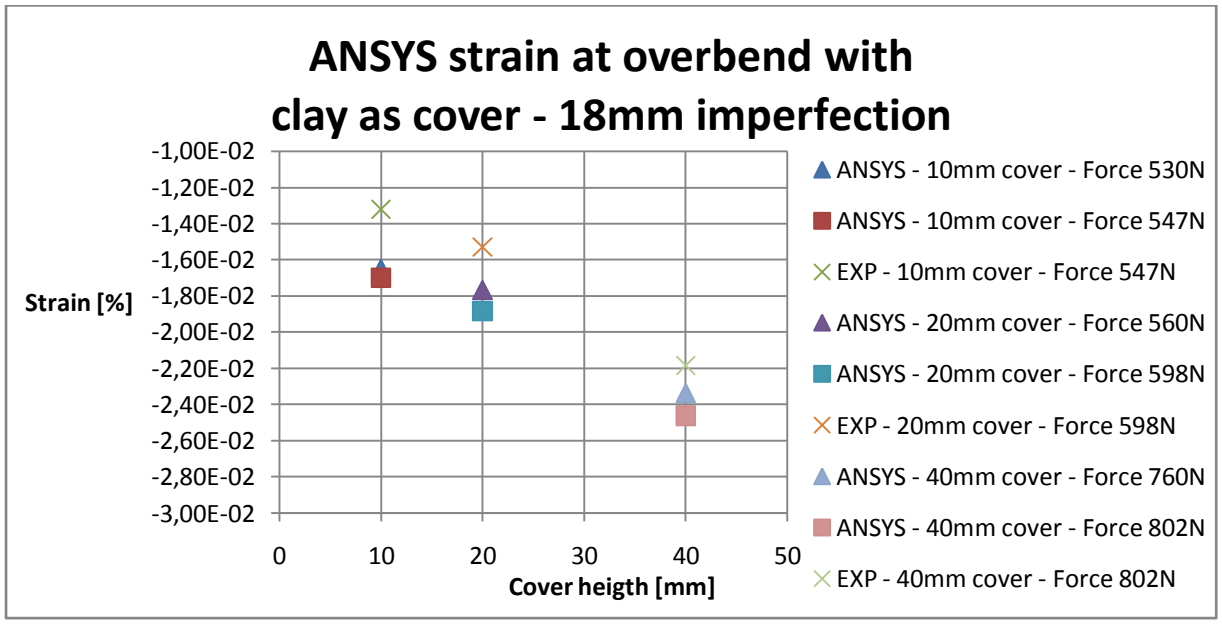

Figure 7.37 **Axial strain comparison for pipe covered clay at overbend – 18mm imperfection**

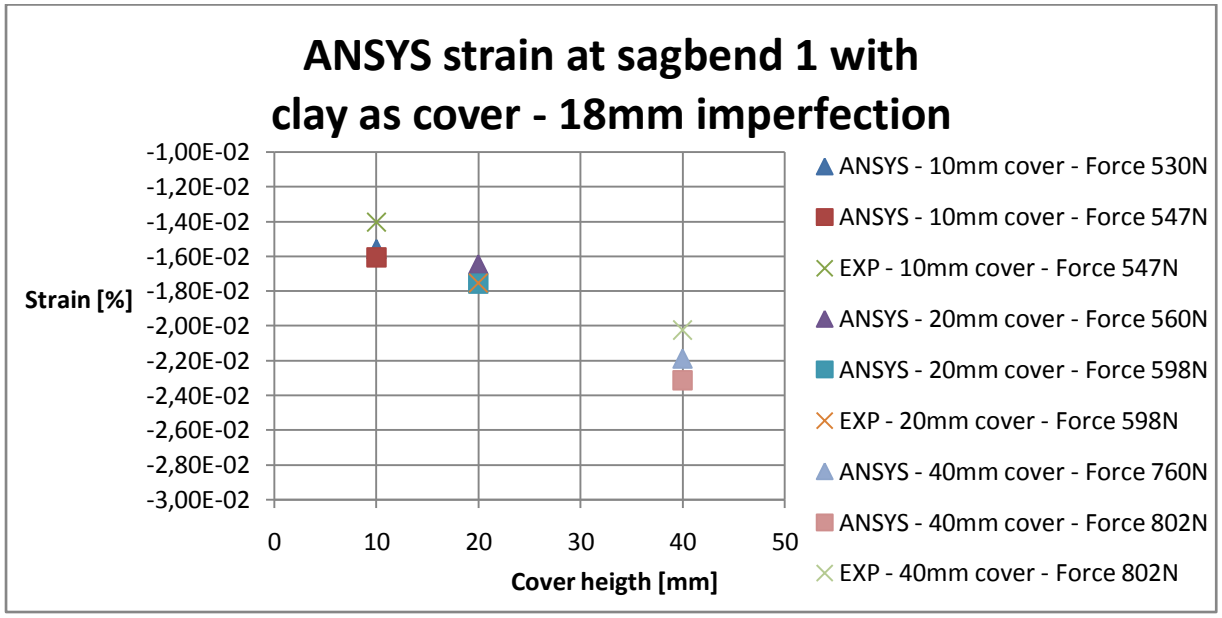

Figure 7.38 **Axial strain comparison for pipe covered with clay at sagbend 1 – 18mm imperfection**

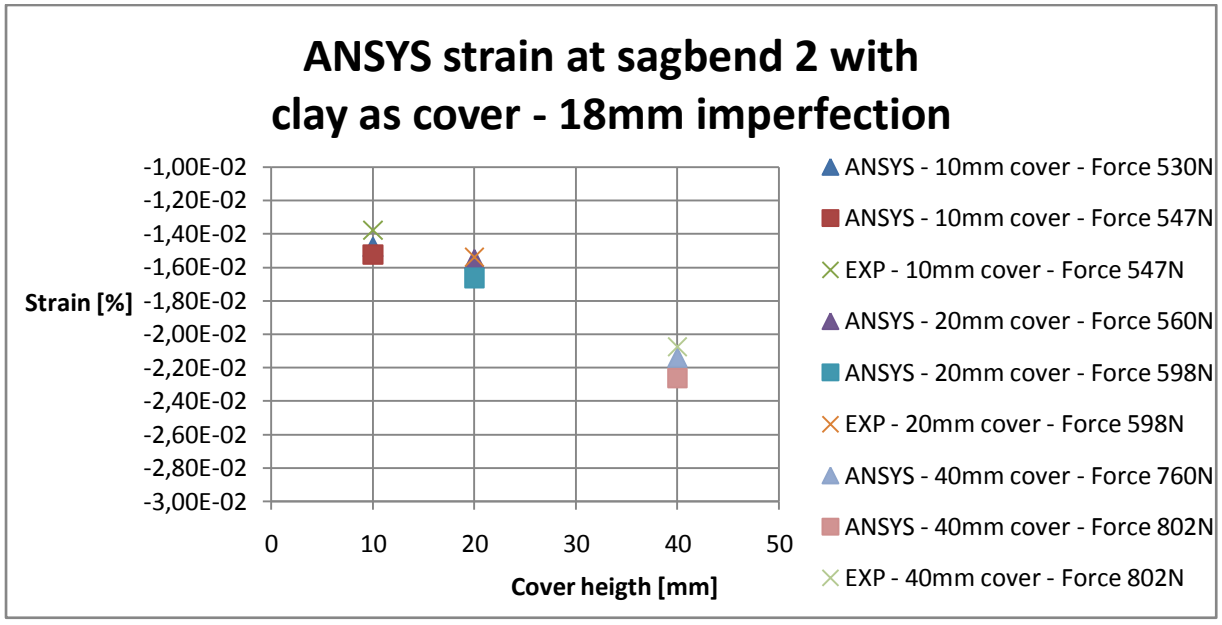

Figure 7.39 Axial strain comparison for pipe covered with clay at sagbend 2 – 18mm imperfection

8. Analysis of results

8.1 Lifting experiment

The results have shown that the sand used in the experiments provides a larger resistance than gravel, when a pipe tries to lift out of the soil. The upheaval buckling experiments has proved just the same, as a pipe needed higher axial forces to break through the cover. The experiments in clay showed some interesting results. The experiments have clearly shown that the clay provided a significant higher resistance than the granular soil types. In addition increasing the cover height did not have a very large impact on the resistance.

When the cover was doubled, the 10mm diameter pipe gave near a doubled value of resistance, when it was buried in granular soils. Figure 8.1 shows the cross section of the pipe when buried, and the soil column above the pipe limited by the pipe diameter. Since the height of the cover was measured from the top of the pipe, doubling the cover height did not double the actual mass column above the pipe. For the larger diameter pipes, the contribution of the additional mass is larger. This implies that the resistance contribution from the weight of the soil column, should give less than a doubled increase in the resistance when the cover height is doubled.

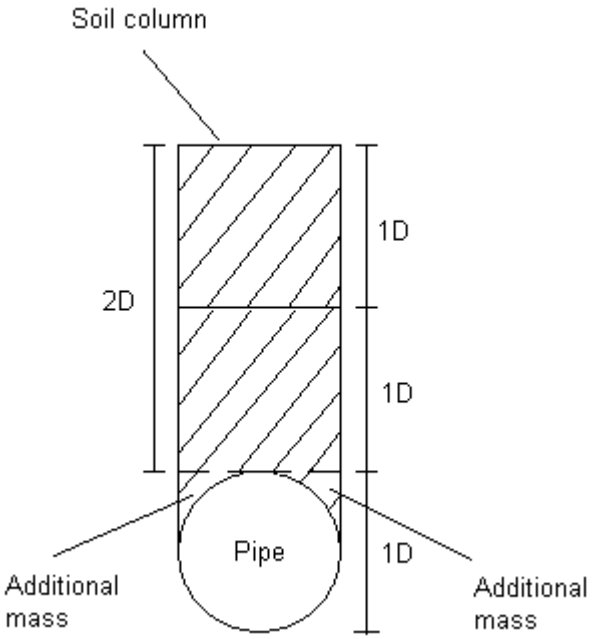

Figure 8.1 Cross section of buried pipe and soil column

When considering the resistance contribution from the mass weight, the relation between the resistance - and diameter ratios, should give an increased value with increasing diameter, as the additional mass contribution, see figure 8.1, is larger with larger diameter pipes. However the results do not show such an increase whit the tests performed with larger diameter pipes. The frictional resistance contribution is limited by the surface of the soil column interfacing with the surrounding soil. The frictional contribution to the resistance is not analyzed for the

results, but it is probable that it should follow the same pattern as for the weight contribution, as a doubled cover height does not double the height of the soil column. Based on these considerations the results derived from the experiments are uncertain, as they do not show results in accordance with the considerations. Table 8.1 shows the calculated relation between the derived resistance and diameter ratio, R/D ratio.

Table 8-1 Relation between R/D ratios with increased diameter

(R/D Ratio 1) / (R/D Ratio 2)			
OD	Gravel	Sand	Clay
10mm	0.51	0.52	0.94
22mm	0.36	0.69	0.91
28mm	0.38	0.54	0.84

8.2 Upheaval buckling experiment

The upheaval buckling experiments was the main task for this thesis. The measurements performed during these experiments, has given some interesting results.

8.2.1 Upheaval buckling results in gravel

All the experiments in gravel with the various cover heights led the pipe into an upheaval buckle that broke through the cover. In general the strains indicated a slight failure in the soil below the pipe, before the soil failed upwards above the imperfection. The exposed length of the pipe and the vertical deflection above the imperfection varied clearly with the cover height. The gravel used in these experiments had the least capability to prevent upheaval buckling from occurring.

8.2.2 Upheaval buckling results in sand

The experiments with the pipe buried in sand, showed a similar pipe behavior compared to when the pipe was buried in gravel. All the measures except for the axial load where in somewhat in the same range. As a larger axial force was needed to make the pipe buckle through the cover, the sand proved to be more applicable to prevent the pipe from buckling.

8.2.3 Upheaval buckling results in clay

Performing the upheaval buckling tests in clay, turn out to be a great challenge. Several pipes ended up being plastically deformed. The experiments gave a vertical deflection above the imperfection that was smaller or in the same range as the previous experiments with granular masses, but the strain at the location was much higher. After looking further into the results, a probable cause for the plastic deformations in the pipes turned out to be the soil failing downwards significantly under the pipe in the sagbends.

The pipes that ended up with plastic deformations were not useable for further experiments. As the strain gauges mounted on these pipes only could be mounted once, these were also of no use. Because of this further experiments were carried with precaution, as mounting of new strain gauges demanded a lot of time, and a limited amount was available. The new approach

was to add a certain axial force to the pipe with various cover heights, but without trying to make the pipe buckle.

When the pipe was buried in clay, it was exposed to axial forces above 1 kN without breaking through the cover. Based on this observation, it was assumed that the clay was the best option when it comes to preventing the pipe from buckling vertically. As the plastic deformations were detected, the assumption had to be reconsidered. It is beyond doubt that the clay provided more resistance upwards, but the pipe was still able to move enough to get plastic deformations, without breaking through the cover. This implied that the downward stiffness in the soil must also be taken into consideration, as the pipe deforms downwards in the sagbends until it is prevented for further deflection.

8.2.4 Creep test

The creep test performed in clay showed that the pipe regained its initial position after being exposed to an axial force, even after being exposed to an axial force a numerous times. The time aspect is clearly discussable, as the forces were applied for a relatively short amount of time. The axial force in the creep tests was in the range of 600 to 800 N.

8.2.5 Various imperfections in clay

A series of experiments were carried out for each cover height with two different imperfections. The imperfection heights were 18mm and 33mm. Because of the experience with two pipes ending up with plastic deformations, the main objectives for these tests were not fulfilled. The goal was to compare the maximum axial force for each cover height with the various imperfections and find a relation between the maximum axial force and imperfection height. The maximum axial force is reached as the pipe starts to buckle significantly upwards, but to avoid another pipe getting plastic deformations, it was not tried to achieve a displacement on the hydraulic pump sufficient for the axial force to build up to its maximum. Because of this a comparison of the axial force was not performed. The occurrence of a vertical buckle is highly depending on the profile of the seabed. Trenching and seabed intervention are commonly used methods to even out the seabed. When choosing a pipeline routing, avoiding areas with an uneven seabed is common practice. Performing tests with different imperfections in granular soils, should give comparable results, and is an area of interest that could be investigated further.

8.3 Analysis of ANSYS results

8.3.1 Gravel as cover

The ANSYS results with 10mm gravel cover buckled at practically the same axial force as for the experiments. There was documented a dramatic increase in the strains when the axial force was increased from 207 N to 210 N. In the experiment with a 10mm even formed cover height the maximum axial force was 207N. For the other cover heights the experiments gave higher strains when an equal axial force was added in ANSYS.

8.3.2 Sand as cover

As for the ANSYS results in gravel, the 10mm sand cover was close to the results in the sand experiment with 10mm even loading. An increase of 12 N gave very large strains compared to

the strains in the experiment. For the 20mm and 40mm cover heights ANSYS gave larger strains, which should be expected as safety factors was included in the calculations.

8.3.3 Clay as cover

The analysis with clay as cover gave similar results to the experiments for each scenario. The experiments for comparison were performed without the pipe breaking through the cover. The problem with the analysis has been to compare the strains in a post buckling configuration, as the maximum axial force in the analysis was not reduced after buckling had occurred. However, the results show that the analytical model gave comparable results before buckling had occurred.

8.4 Sources of errors

The lifting experiments gave uncertain results. There are several points to be made regarding the uncertainties. The lifting experiments were carried out with a manually operated reel, making it hard to pull the pipe with an even velocity. The resistance might be depending on the rotation speed of the reel as the reel controls the vertical velocity of the pipe. Sources of errors from the lifting experiment can be;

- Different lifting speed when pulling the pipe out of the soil
- Uneven cover height, especially for small cover heights
- Pipe not laying perfectly straight in relation to the load cells above
- Wear and tear of the lifting wires
- Various conditions in the soil

The upheaval buckling tests showed variations in the results, when performing tests with same cover height. There can be several causes for this, but the main cause might be difference in the initial positions. Especially in clay, forming the cover was hard work, and might have led the pipe out of its initial position. Sources of errors in the upheaval buckling experiments can be;

- Difference in initial position
- Inaccurate mounting of strain gauges
- Uneven formed cover
- Time difference when increasing axial force
- Various soil conditions

The results from the analytical calculations in ANSYS should have been comparable with the tests. There can be a number of reasons for the differences in the analytical and practical results. Preparing simulations in ANSYS is a time demanding process, and it is often difficult to detect errors in the model. It is likely that the actual experiments have not been performed properly. Some reasons for the various results in the experiments and simulations can be;

- The seabed in ANSYS was defined with equal downward stiffness along the whole seabed. In the experiments, no downward movement was allowed below the imperfection.
- The pipe element used in ANSYS was based on thin walled theory. The relation between diameter and wall thickness might have been too small.

- The preprogrammed script is normally used for full scale analysis. The small dimensions on the experiment might have been misread by the program during the analysis.
- Wrong input values.
- Incorrect soil data.

8.5 Conclusions

The experiments performed in this thesis have shown some interesting results. Some of the claims need further analysis to be verified. The general behavior based on the small scale experiment may not be directly comparable to a full scale situation. From the results it is possible to draw some conclusions.

Based on the results from the lifting tests and comparison of the different soils, conclusions are;

- Clay provides a significantly higher resistance compared to granular soils
- The resistance provided by clay is less depending on the cover height
- Burying a pipe in clay requires a lower cover height to provide sufficient resistance compared to granular soils

The results from the upheaval buckling experiments have verified the previous conclusions.

Based on the analysis of the general behavior from the upheaval buckling experiments, it is possible to claim that;

- A pipe laying over an imperfection forming sagbends will initially try to deflect downwards in the sagbends.

This claim might be verified by performing tests with a hard surface below the pipe allowing no downward movement at all and investigating the strains at the overbend.

A suggested reason for the pipes getting plastic deformations when buried in clay is that the clay allows a pipe more downward deflection in the sagbends. The clay has larger capabilities when it comes to providing resistance compared to the granular soils, but observations have proven certain weaknesses. When buckling occurred in granular soils, the pipe experienced less deformation before the buckle was initiated. A pipe buried in clay might more likely be exposed to deflections that can lead to plastic deformations and other failures, without leading the pipe into exposure on the seabed. This can make it difficult to detect occurrences of upheaval buckling and damages in the pipe. Including a hard foundation under a pipeline in areas with soft seabed might reduce such movements.

The creep tests showed that a pipe buried in clay is capable of regaining its initial position after being deformed. This subject needs further investigation with higher axial forces and longer time intervals in order to draw any conclusion.

The experiments with various imperfections failed to give the intended results. Suggestions for modifying the tests are given.

The results from the analytical simulation in ANSYS have not given comparable results. Further investigation of input values regarding soil parameters and of the model in general is needed to ensure that the experiments are simulated properly. However the analytical results were comparable before buckling occurred.

8.6 Suggestions for further work

The lifting tests were not the main task for this thesis. There are several ways to improve the lifting system used for this thesis. By including an automatic lifting devise and a distance measurer in the system, one could;

- Compare different uplift velocities impact on the resistance
- Apply a constant lifting force on the pipe while buried in clay for a longer period of time
- Derive a relation between resistance and the vertical distance the pipe has moved

The upheaval buckling tests with various imperfections failed to give a relation between maximal axial force and imperfection height. Performing the tests in granular soils should not lead to problems with a pipe getting plastically deformed. The problems with plastic deformations in pipes might be avoided by applying a hard surface under the pipe. Analyzing downward movement in sagbends with a hard surface below the pipe could be performed. The creep tests could very well be performed in granular soils. The creep tests in clay could also be performed where a pipe is exposed to loading for longer periods. Suggestions for further work are;

- Performing experiments with various imperfections in granular soils
- Performing creep tests in granular soils
- Performing creep tests with longer loading intervals in clay
- Applying a stiff bottom surface under the pipe when clay is used as cover
- Performing buckling tests with different trench scenarios

The test cabinet built for the purpose of the experiments in this thesis is well suited for the suggested experiments for further investigation.

References

[1] DNV-RP-F110, Global Buckling of Submarine Pipelines – Structural Design due to High Temperature/High Pressure. Det Norske Veritas, Recommended Practice, October 2007.

[2] Global Buckling, DNV Pipeline Technology Course. Presentation, IKM Ocean Desgn, Forus, 2008.

[3] Palmer, A. C., King R. A., Subsea Pipeline Engineering. PennWell Corporation, 2004, p379-413.

[4] DNV-OS-F101, Submarine Pipeline Systems. Det Norske Veritas, Offshore Standard, October 2007.

[5] Carr, M., Bruton, D., Leslie, D., Lateral Buckling and Pipeline Walking, a Challenge for Hot Pipelines. Offshore Pipeline Technology Conference, Amsterdam, 2003.

[6] Hobbs, R. E., In Service Buckling of Heated Pipelines. ASCE Journal of Transportation Engineering 110, p175-189.

[7] Martinet, A. Flambement des Voies Sans Joints sur Ballast et Rails de Grande Longueur (Buckling of Jointless Track on Ballast and Long Rails). Revue Generale des Chemins de Fer 55/2, p212-230.

[8] Kerr, A. D., On the Stability Track in the Vertical Plane. Rail International 9, September 1979, p759-768

[9] Sandvik, K., Thermal Buckling of Pipelines on Uneven Seabed. Master thesis, University of Stavanger, 2006.

[10] Halvorsen, F., Buckling Behaviour of Pipelines on Uneven Seabed. Master thesis, University of Stavanger, 2000.

[11] Stava, I., Design of Arctic Offshore Pipelines in Areas Subjected to Ice Ridge Gouging. Master Thesis, University of Stavanger, 2007.

Appendix

Table of contents

Table of figures

A. Geotechnical measures

Table A-1 Screening test data for density distribution curve in shingle

Screening test data			
Soiltype	Velde shingle 2-5 mm		
Date	18.03.2009		
Fineness - modulus	6,13		
Mesh width [mm]	Weight [g]	Weight [g]	Sieving residue [%]
8	0	0	0,00
5	111,3	125,9	19,90
4	289,3	305,3	49,89
2	583,7	576,8	97,37
1	591,1	587,5	98,88
0,5	591,3	588,5	98,98
0,25	591,4	589	99,04
0,125	591,7	589,7	99,12
0,063	592,2	590,5	99,23
Bottom	596	595,9	

Table A-2 Screening test for sand

Screening test data			
Type	Velde moulding sand 0-6 mm		
Date	05.05.2009		
Fineness - modulus	3,61		
Mesh width [mm]	Weight [g]	Weight [g]	Percentage passing [%]
8	7,00	6,00	0,82
4	139,0	108,0	15,52
2	244,0	190,0	27,28
1	361,0	290,0	40,92
0,5	499,0	427,0	58,20
0,25	641,0	591,0	77,44

0,125	742,0	721,0	91,95
0,063	781	771	97,55
Bottom	800	791	

Table A-3 Water containment in sand

Date	Time	Depth	Measured / Read	Water containment [%]
5/7/2009	11:30	Surface	0.4	0.40
5/7/2009		Middle	0.5	0.50
5/7/2009		Bottom	1.4	1.42
5/9/2009	12:00	Surface	0.6	0.60
5/9/2009		Middle	1.1	1.11
5/9/2009		Bottom	1.2	1.21
5/10/2009	15:00	Surface	0.2	0.20
5/10/2009		Middle	0.7	0.70
5/10/2009		Bottom	1.1	1.11

B. Upheaval buckling results

B.1 Upheaval buckling experiments in gravel

B.1.1 Upheaval buckling with no cover

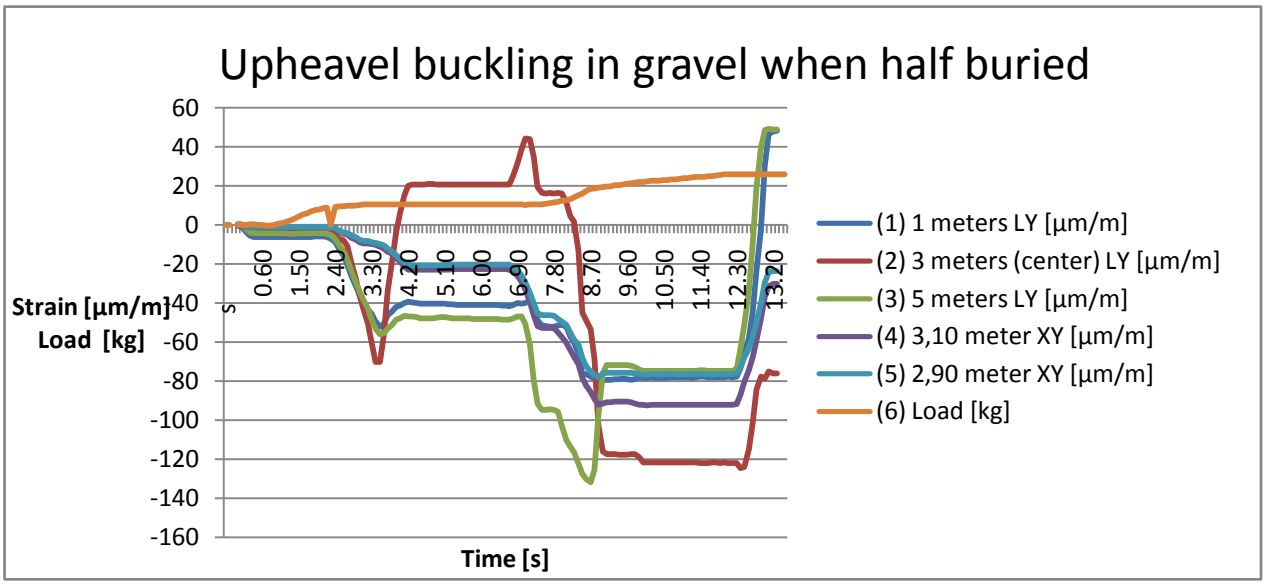

Figure B.1 Upheaval buckling in gravel when half buried

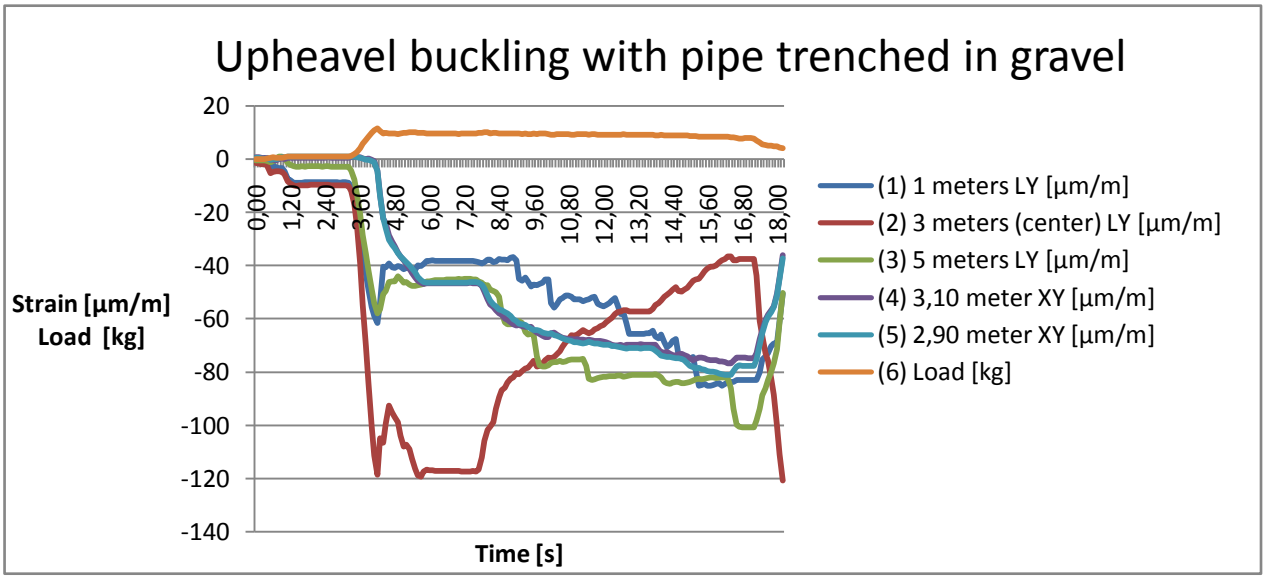

Figure B.2 Upheaval buckling with pipe trenched in gravel

B.1.2 Upheaval buckling in gravel with10mm cover

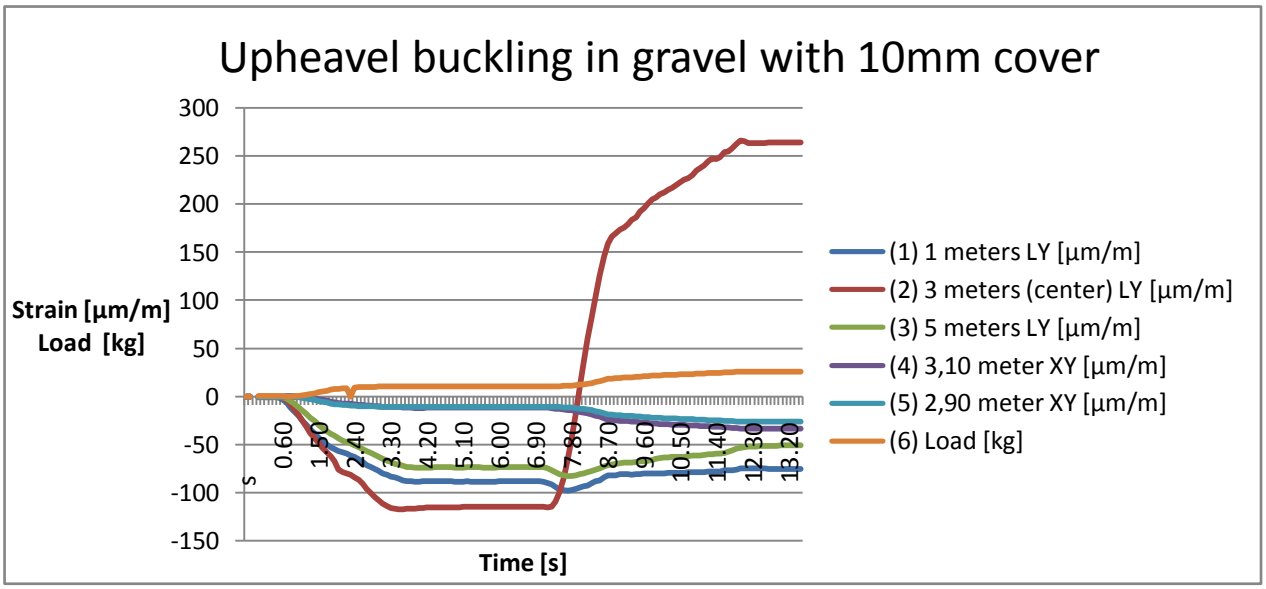

Figure B.3 Upheaval buckling in gravel with 10mm cover

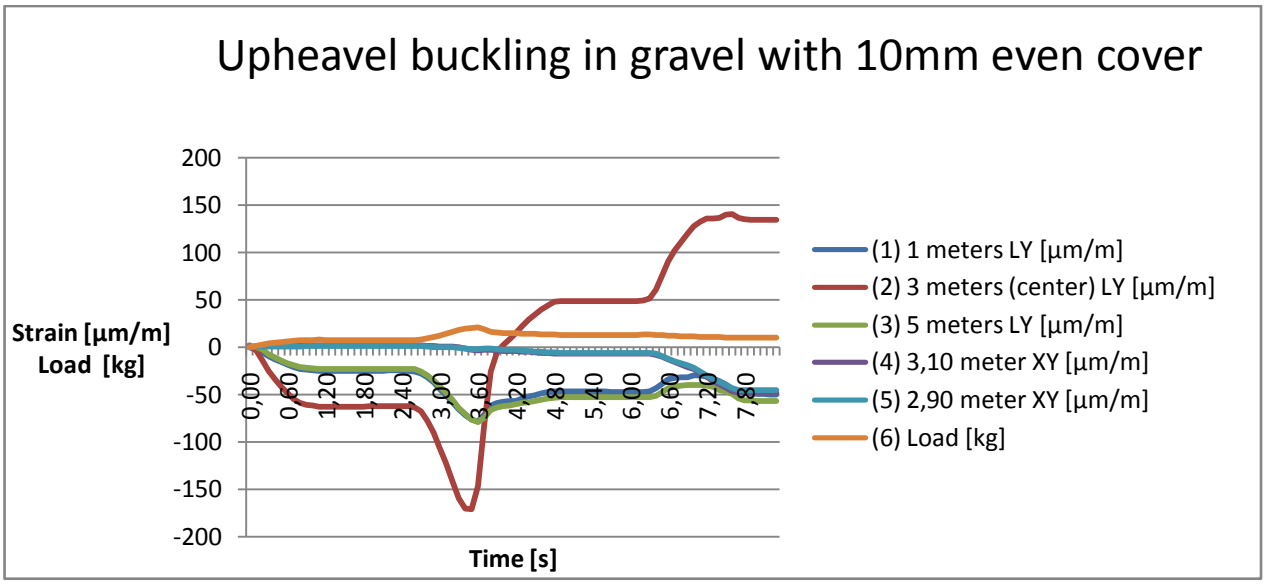

Figure B.4 Upheaval buckling in gravel with 10mm even cover

B.1.3 Upheaval buckling in gravel with 20 mm cover

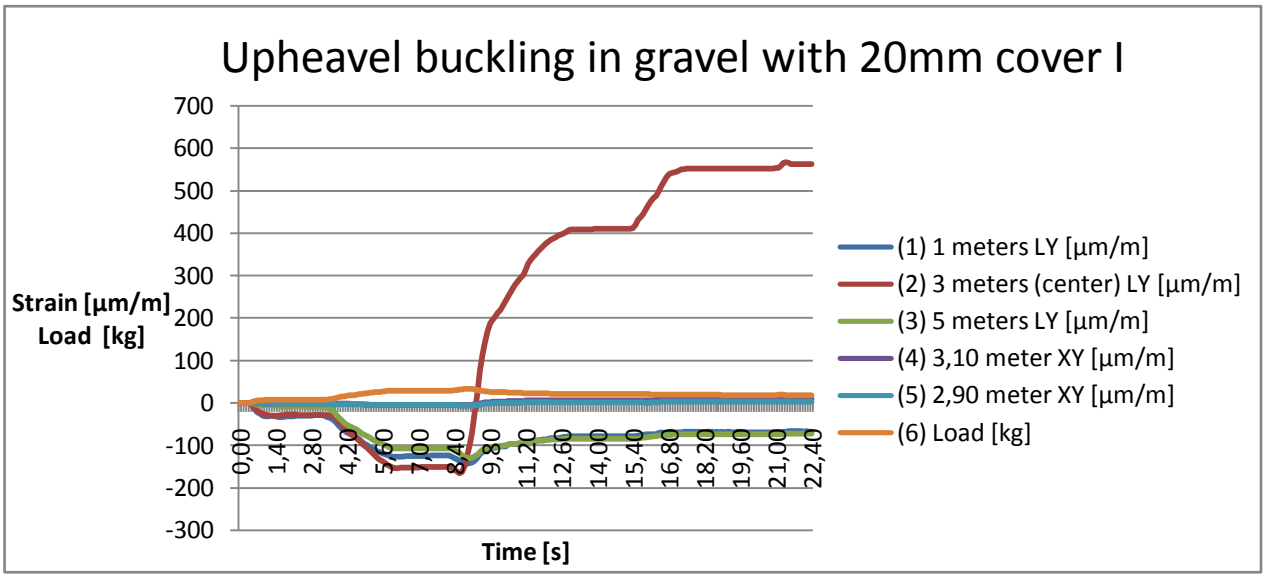

Figure B.5 Upheaval buckling in gravel with 20mm cover I

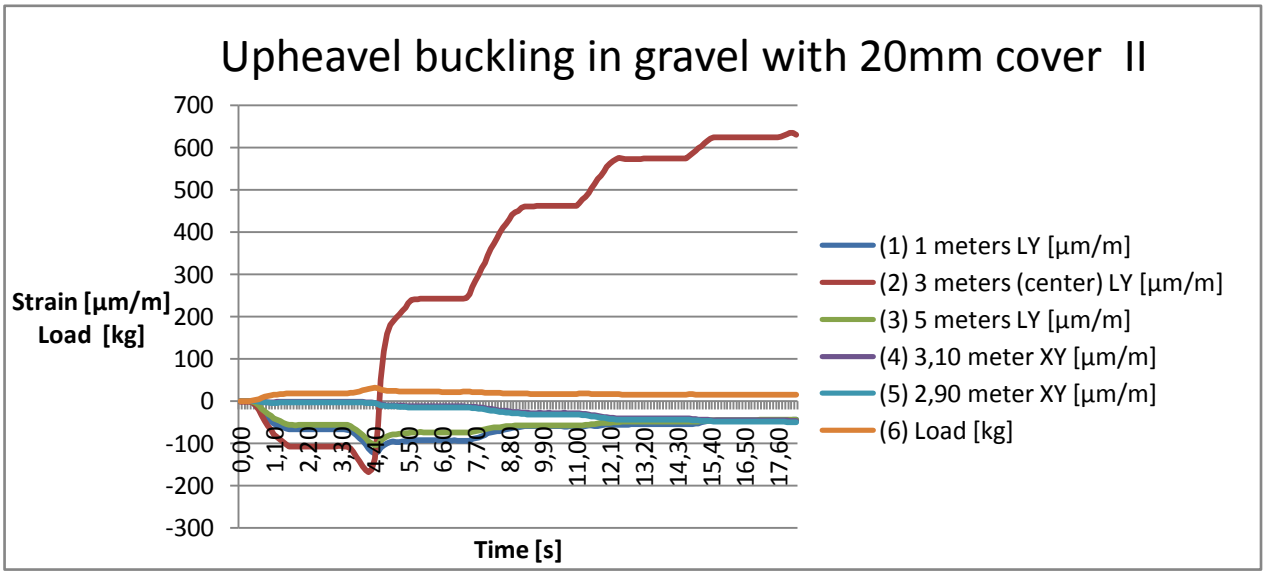

Figure B.6 Upheaval buckling in gravel with 20mm cover II

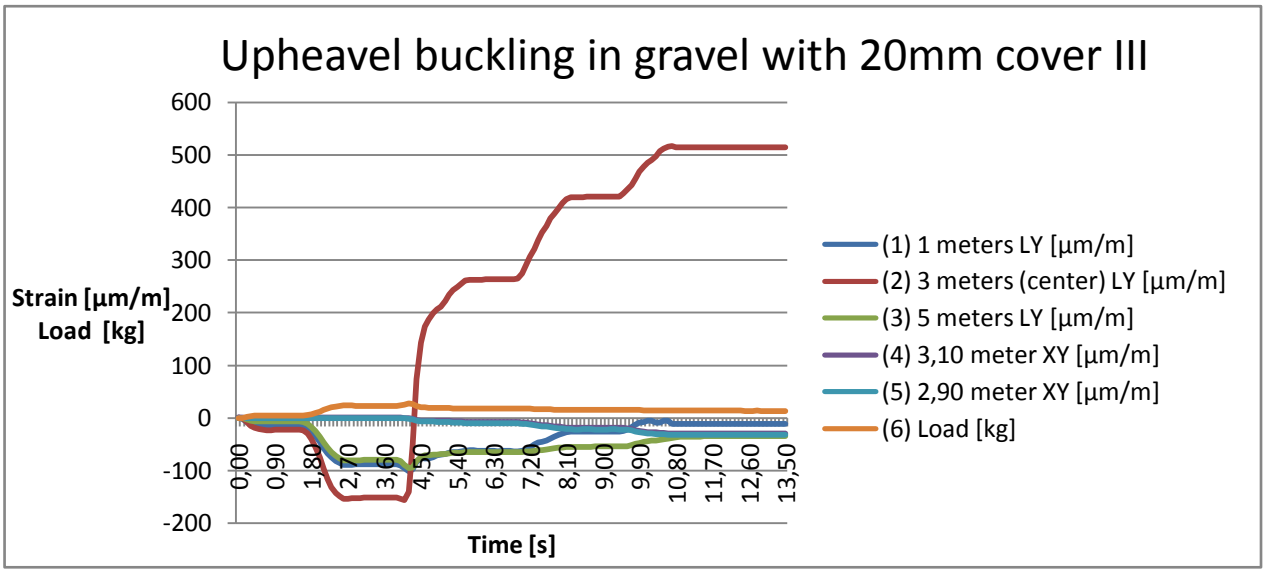

Figure B.7 Upheaval buckling in gravel with 20mm cover III

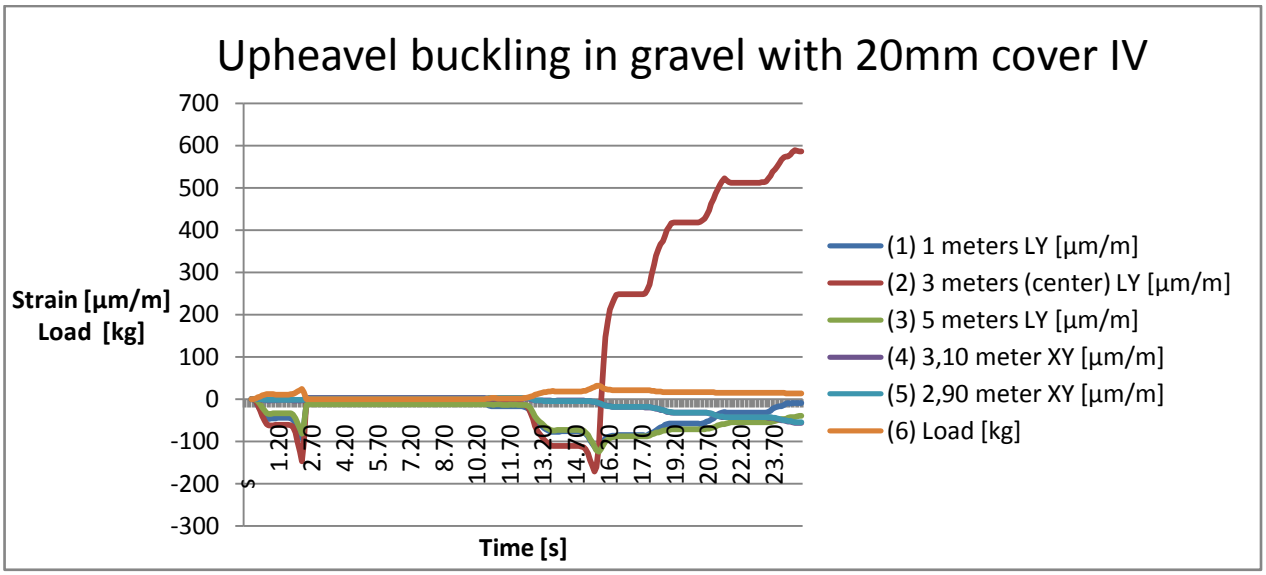

Figure B.8 Upheaval buckling in gravel with 20mm cover IV

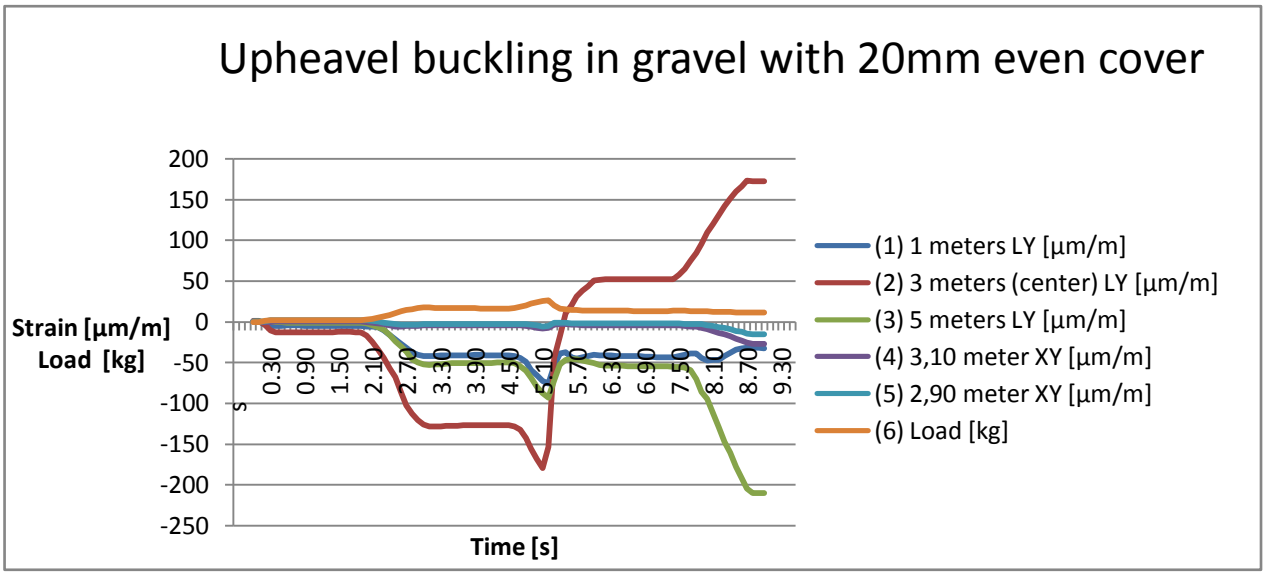

Figure B.9 Upheaval buckling in gravel with 20mm even cover

B.1.4 Upheaval buckling in gravel with 40mm cover

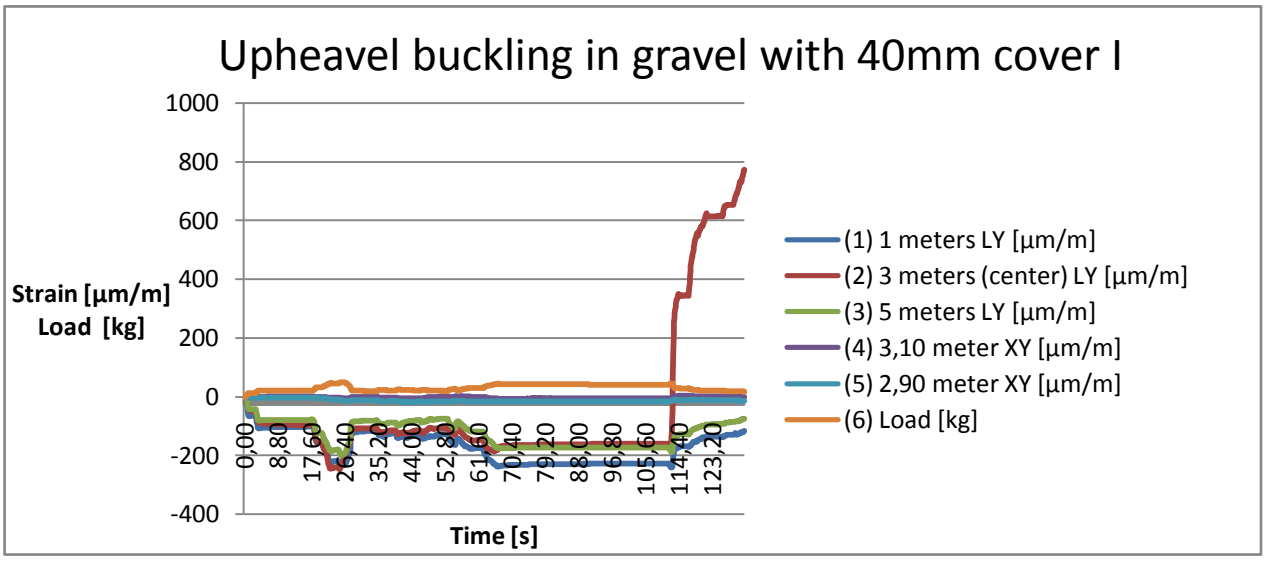

Figure B.10 Upheaval buckling in gravel with 40mm cover I

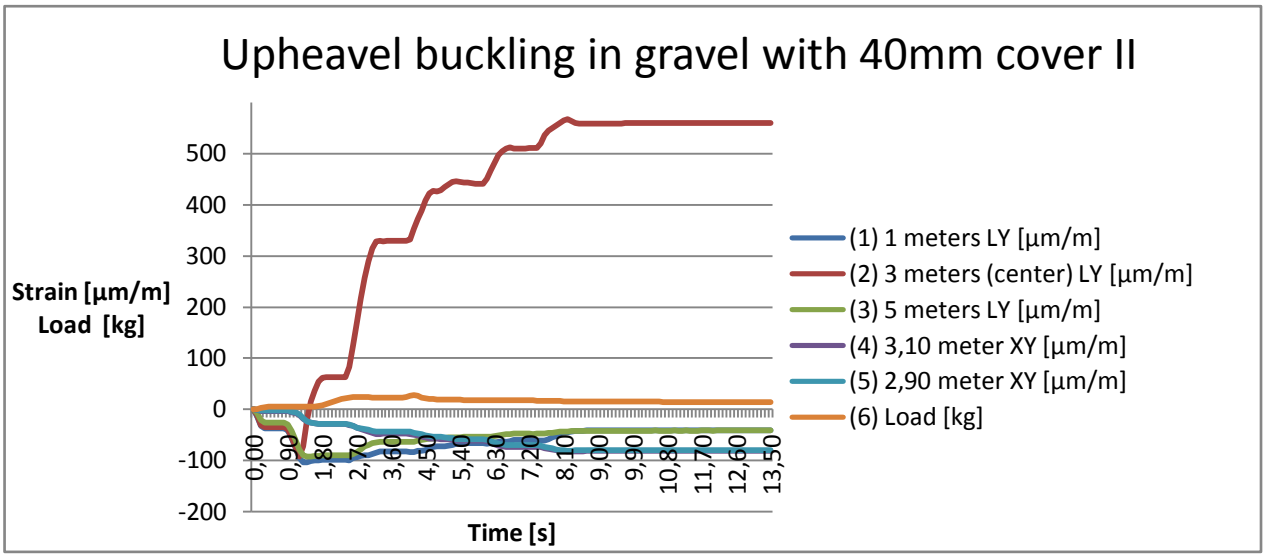

Figure B.11 Upheaval buckling in gravel with 40mm cover II

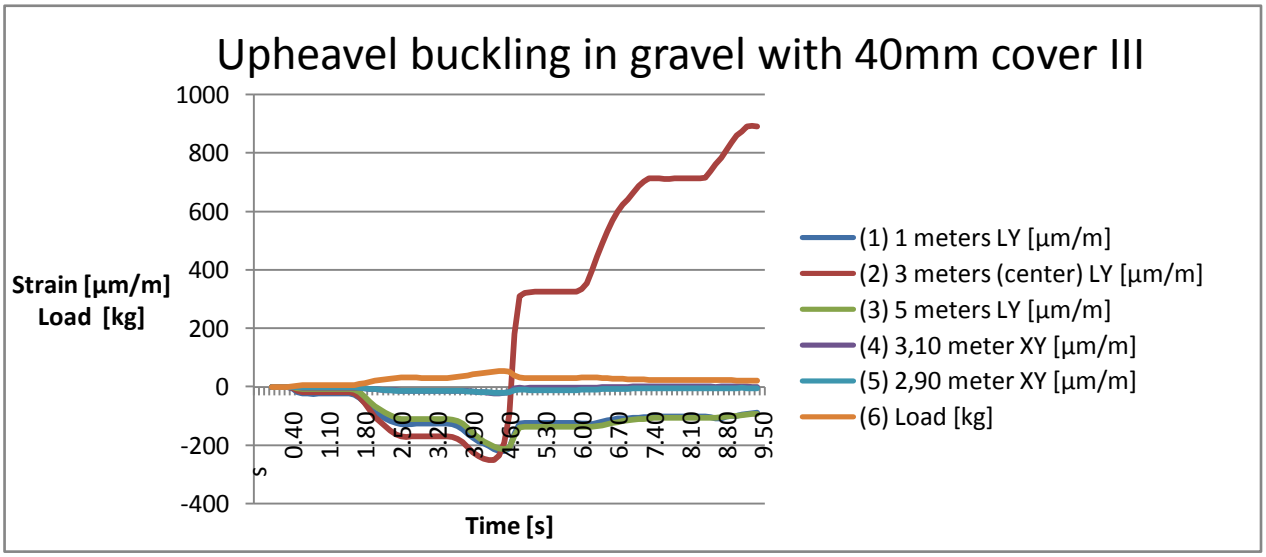

Figure B.12 Upheaval buckling in gravel with 40mm cover III

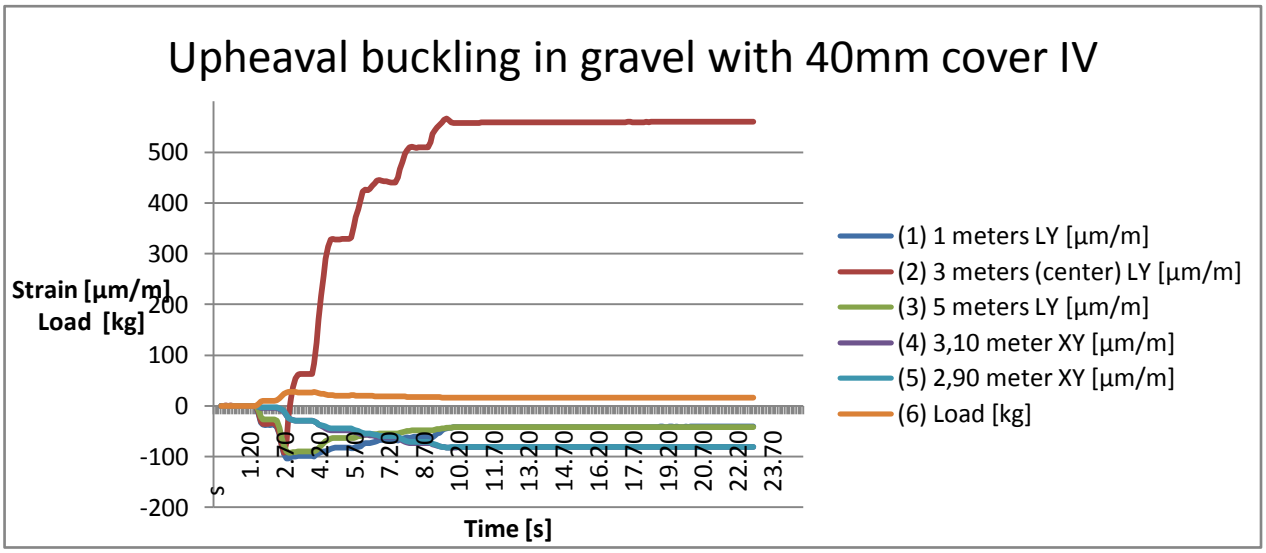

Figure B.13 Upheaval buckling in gravel with 40mm cover IV

B.2 Upheaval buckling in sand

B.2.1 Upheaval buckling in sand without cover

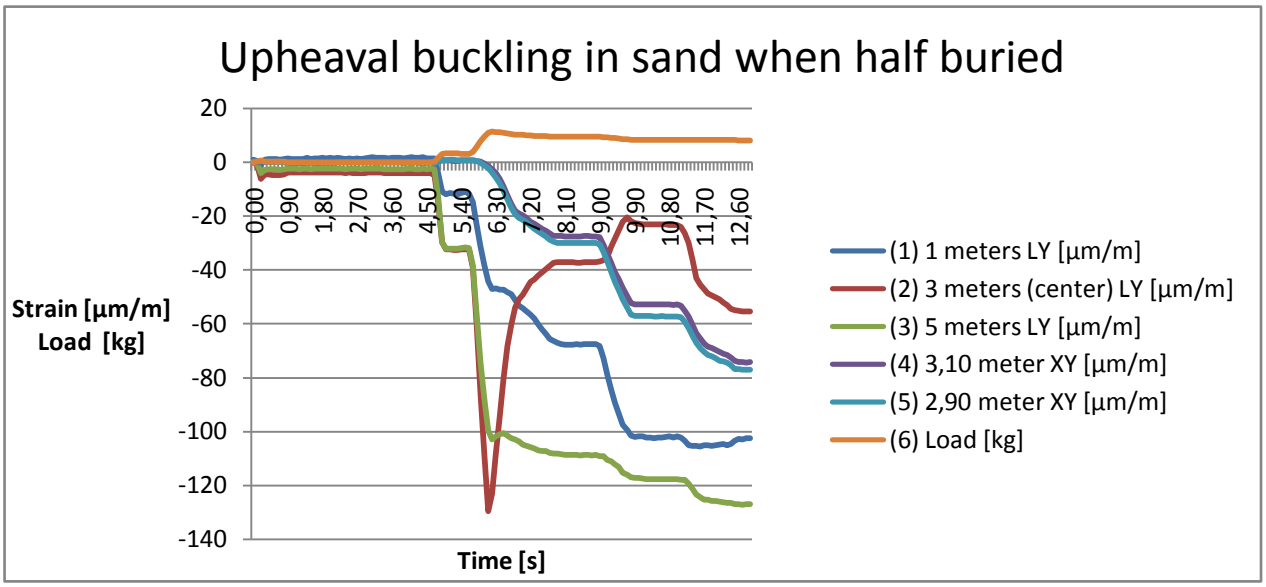

Figure B.14 Upheaval buckling in sand when half buried

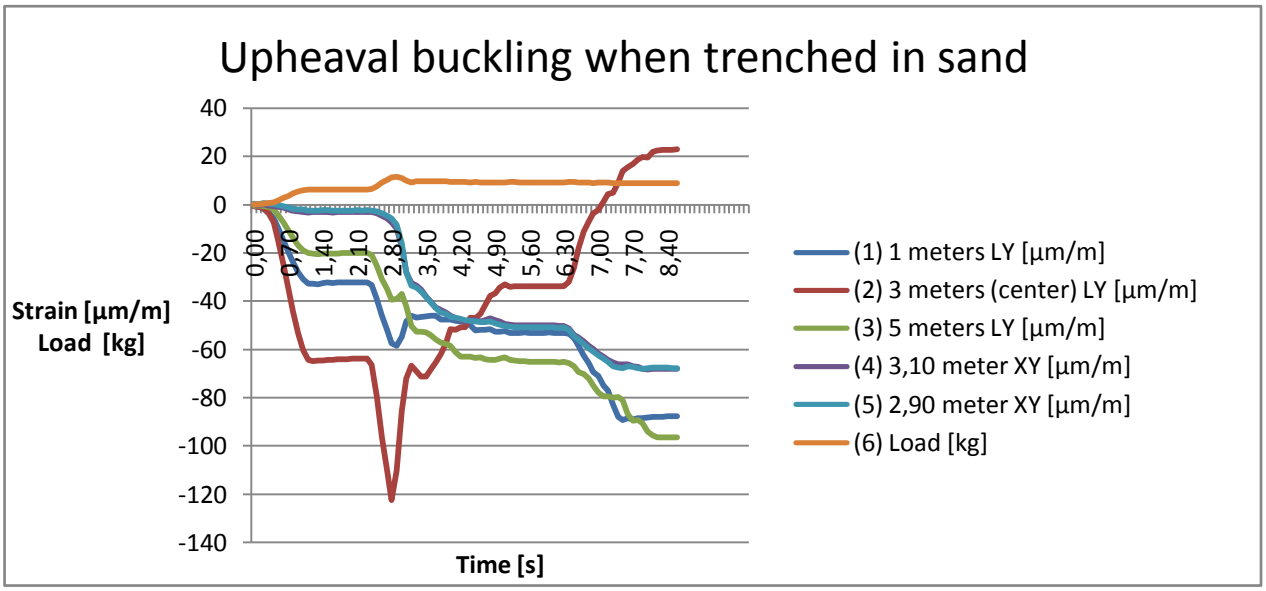

Figure B.15 Upheaval buckling when trenched in sand

B.2.2 Upheaval buckling in sand with 10mm cover

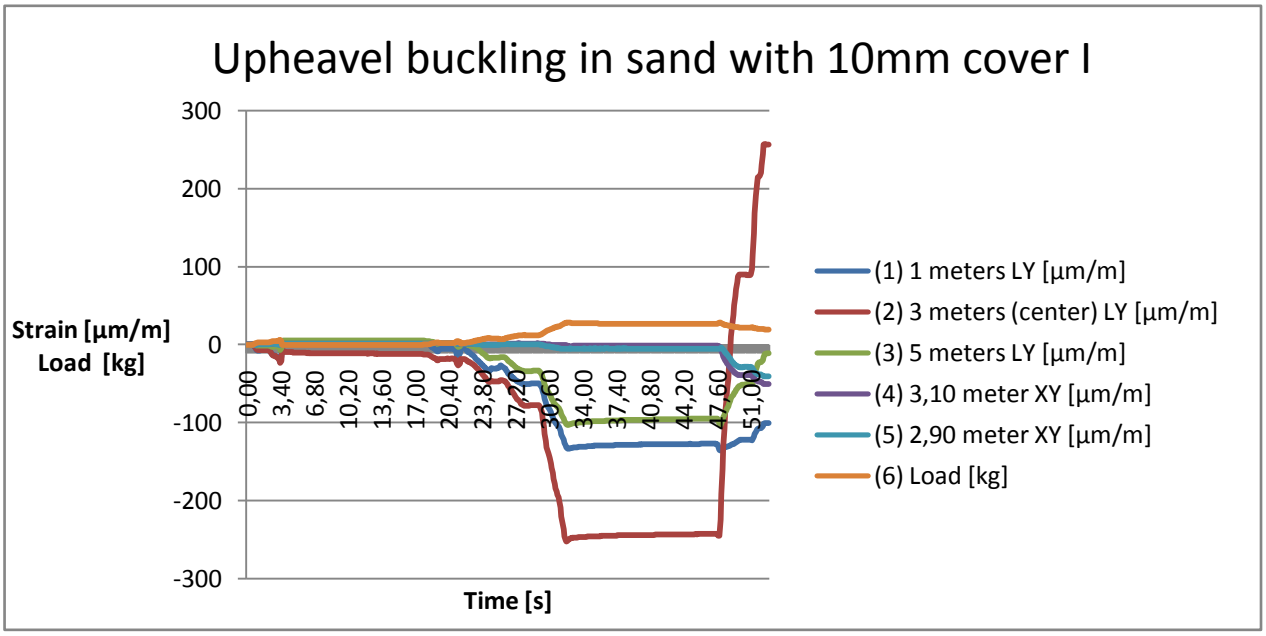

Figure B.16 Upheaval buckling in sand with 10mm cover I

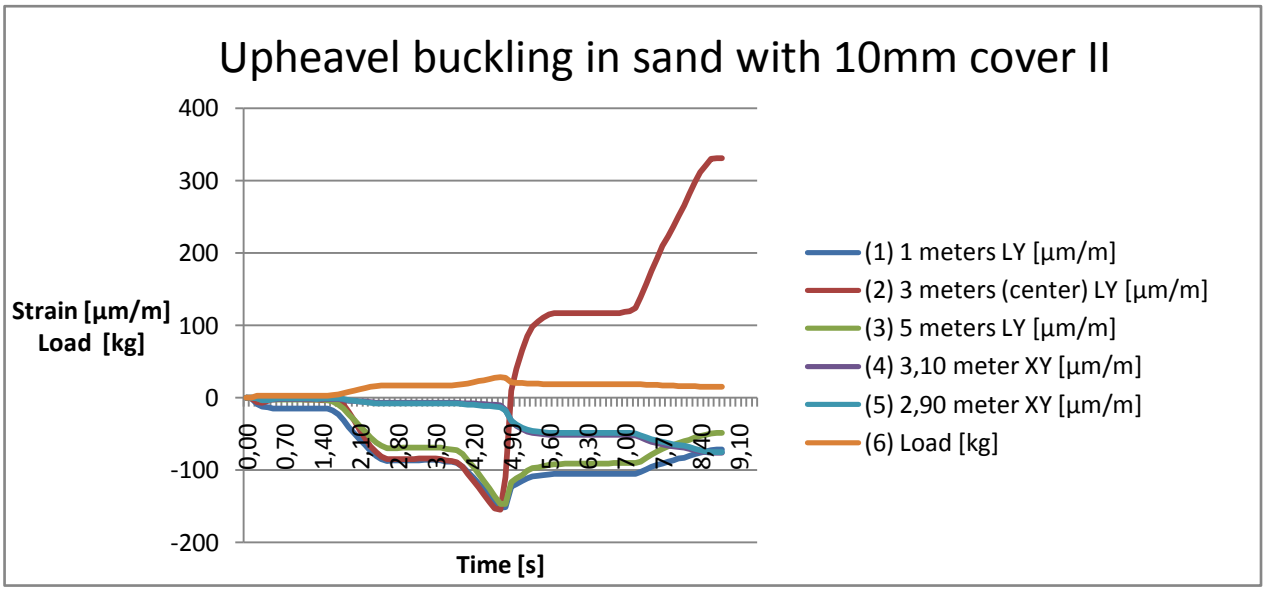

Figure B.17 Upheaval buckling in sand with 10mm cover II

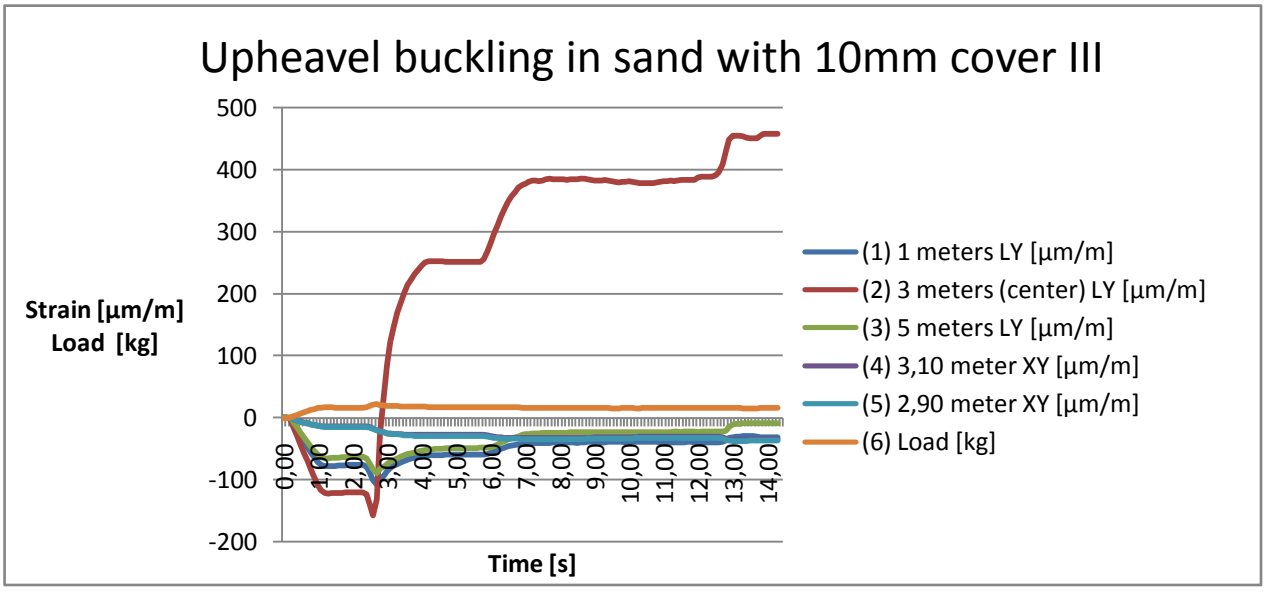

Figure B.18 Upheaval buckling in sand with 10mm cover III

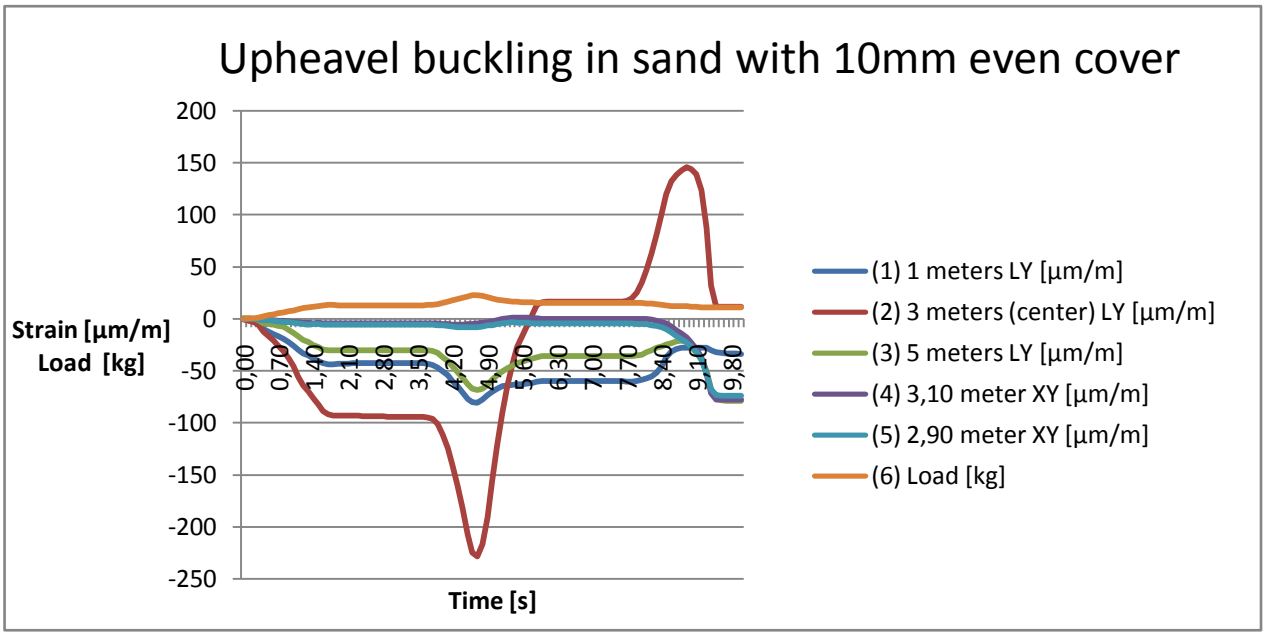

Figure B.19 Upheaval buckling in sand with 10mm even cover

B.2.3 Upheaval buckling in sand with 20mm cover

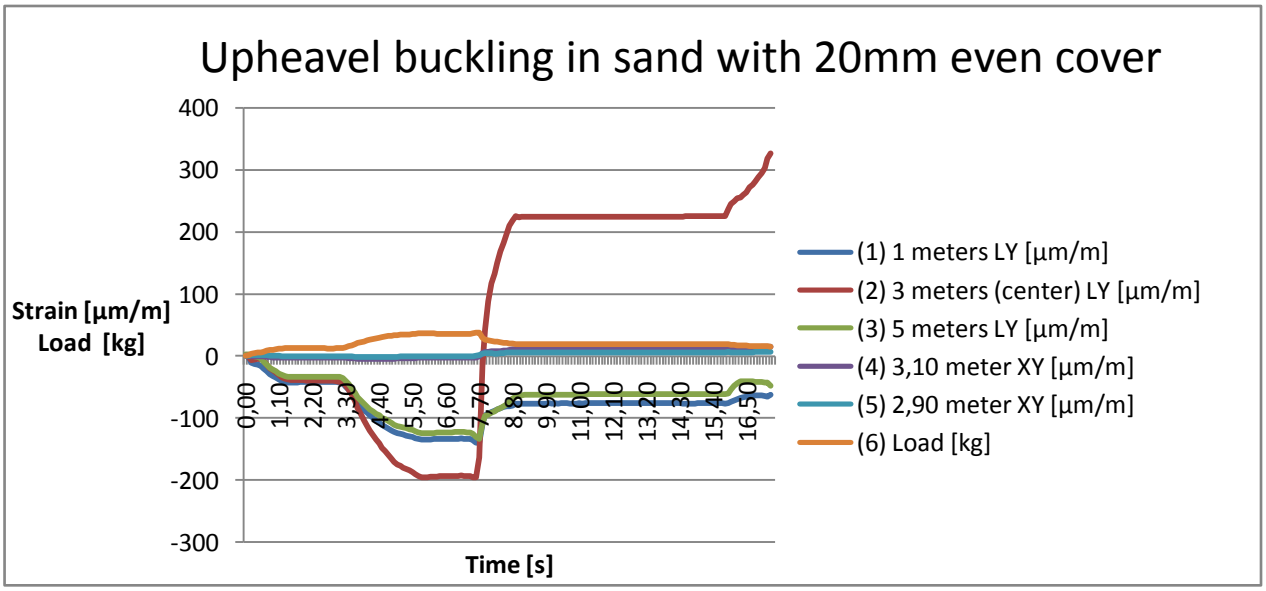

Figure B.20 Upheaval buckling in sand with 20mm even cover

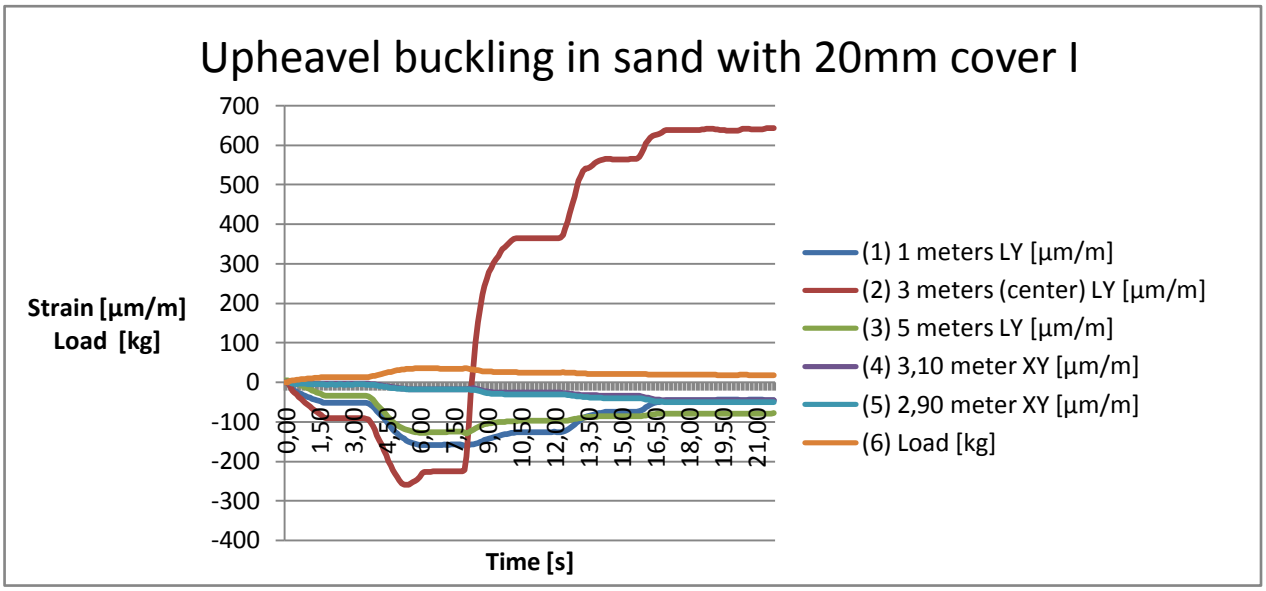

Figure B.21 Upheaval buckling in sand with 20mm cover I

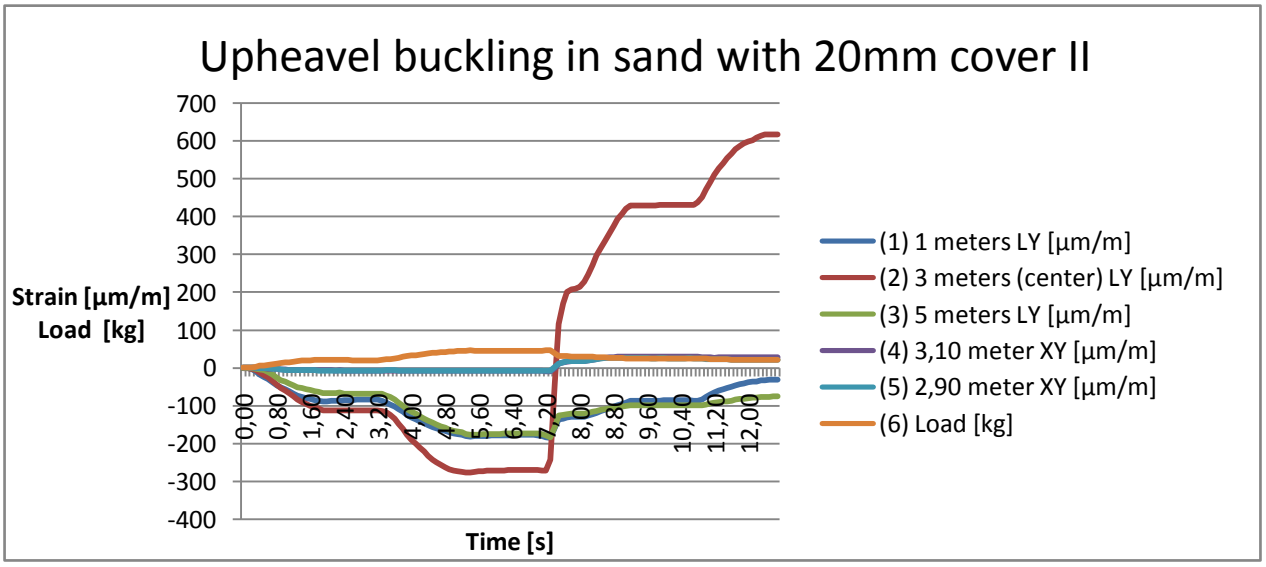

Figure B.22 Upheaval buckling in sand with 20mm cover II

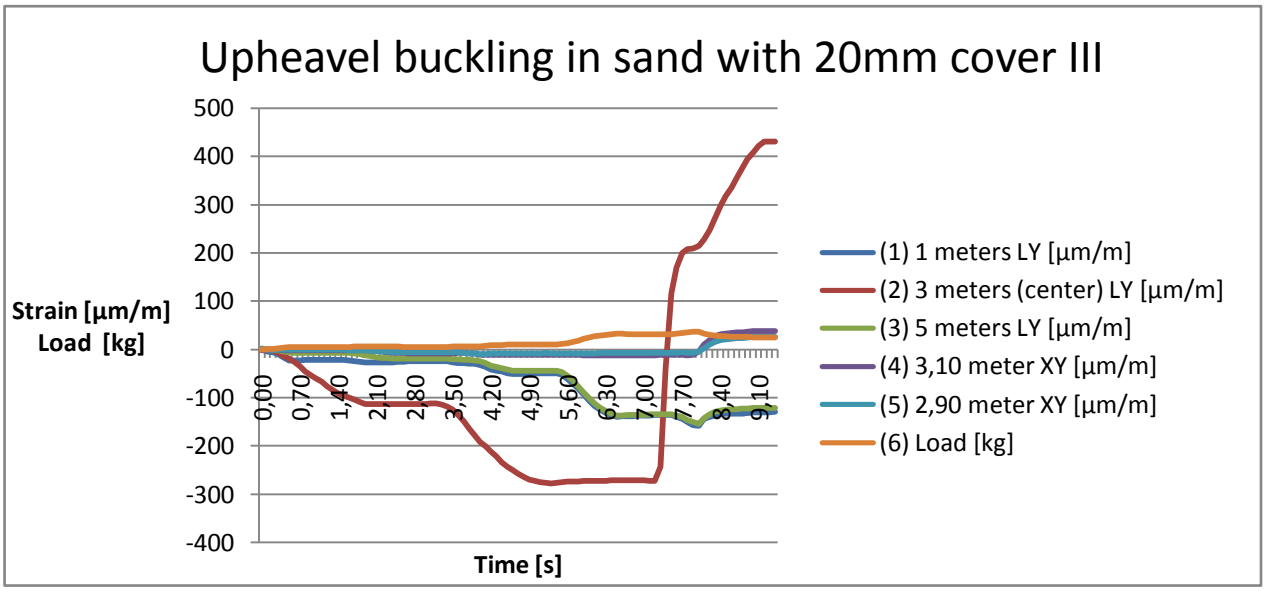

Figure B.23 Upheaval buckling in sand with 20mm cover III

B.2.4 Upheaval buckling in sand with 40mm cover

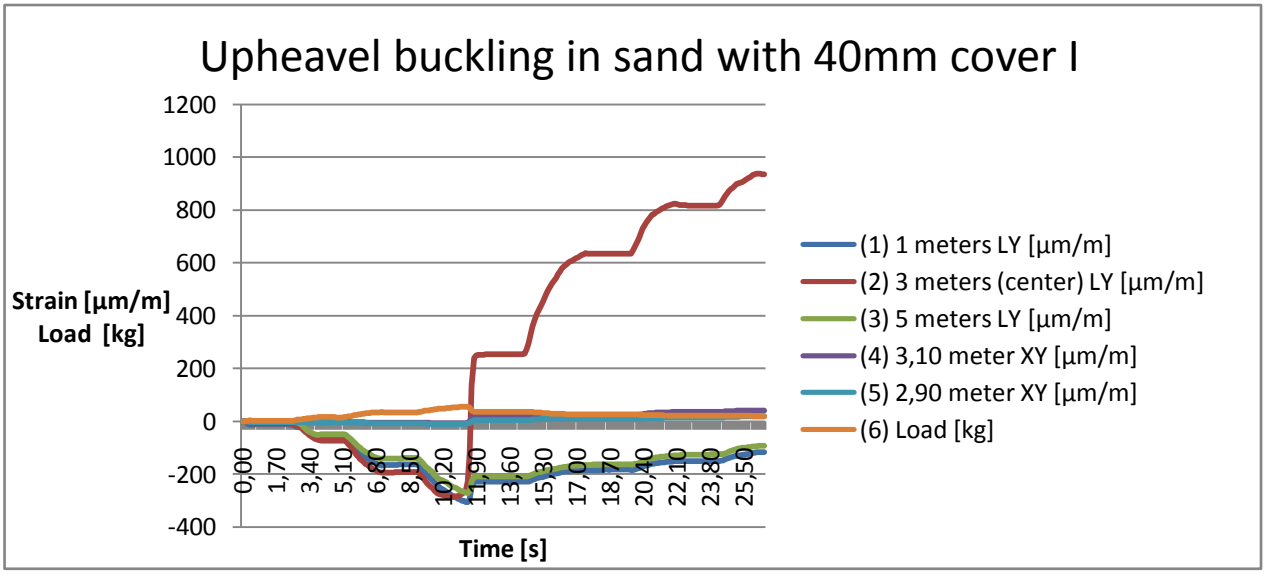

Figure B.24 Upheaval buckling in sand with 40mm cover I

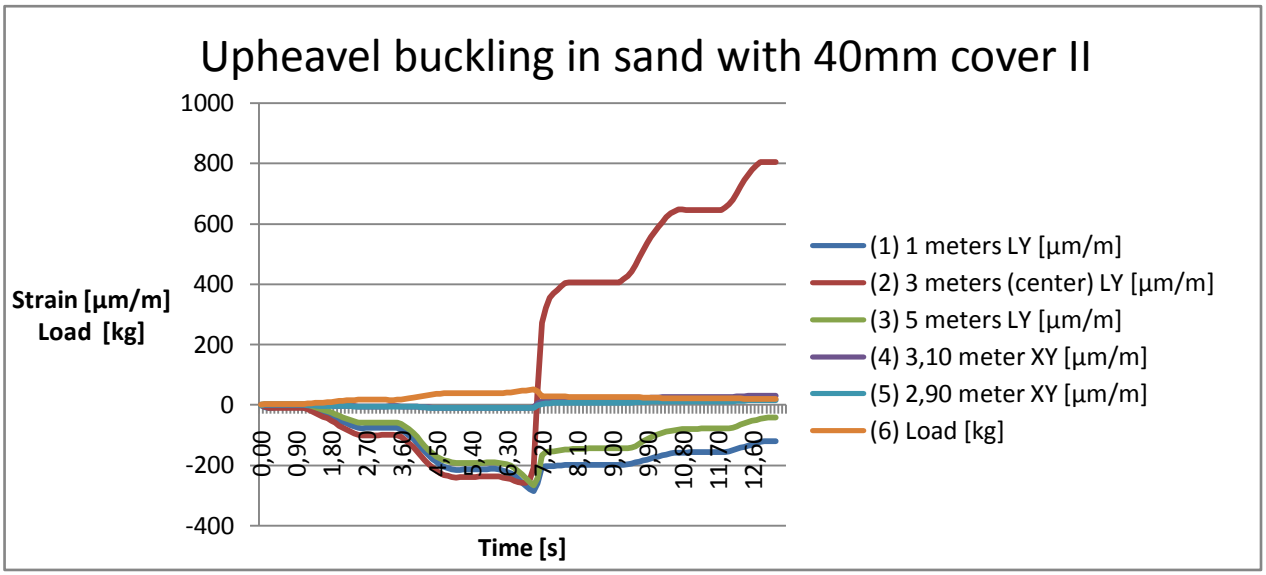

Figure B.25 **Upheaval buckling in sand with 40mm cover II**

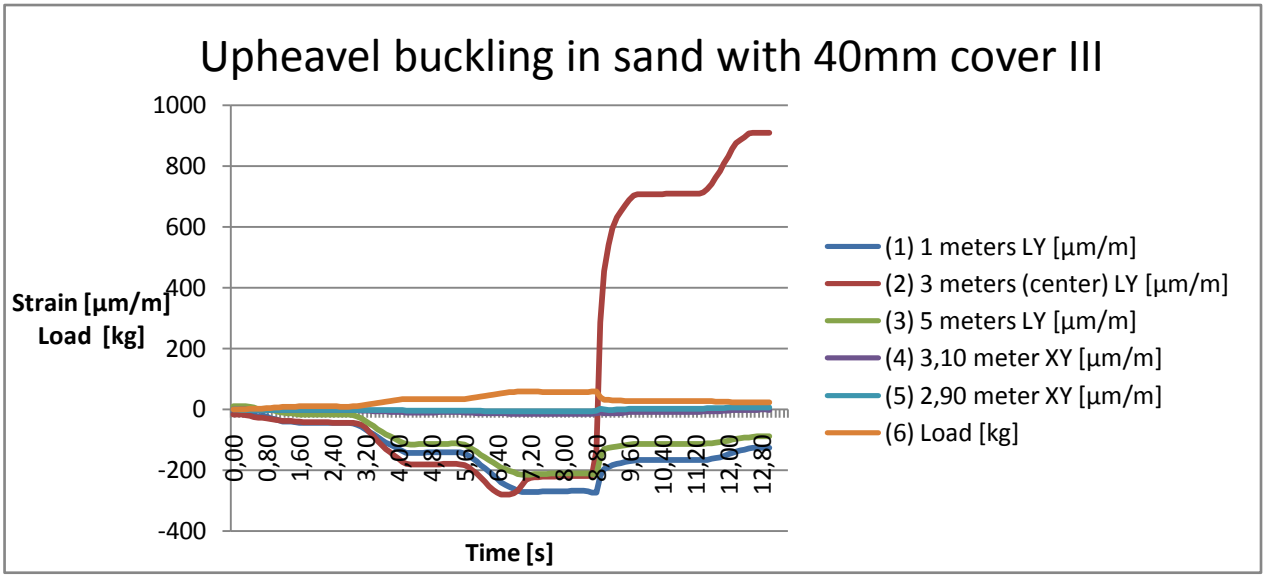

Figure B.26 **Upheaval buckling in sand with 40mm cover III**

B.3 Upheaval buckling in clay

B.3.1 20mm cover – plastic deformation in pipe

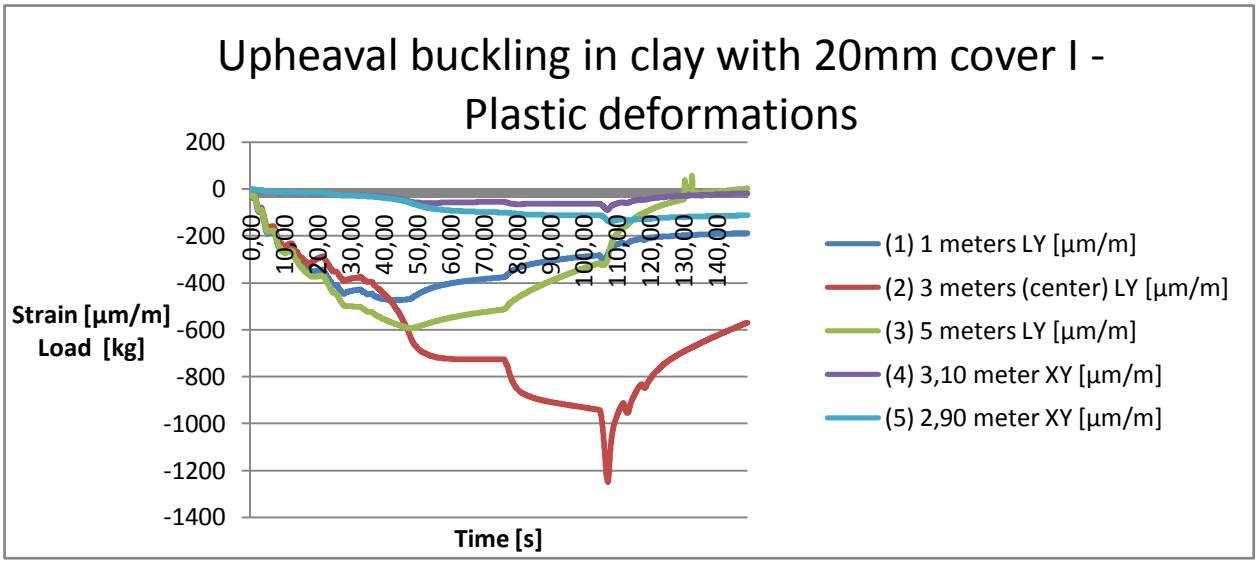

Figure B.27 Upheaval buckling in clay with 20mm cover I - Plastic deformations

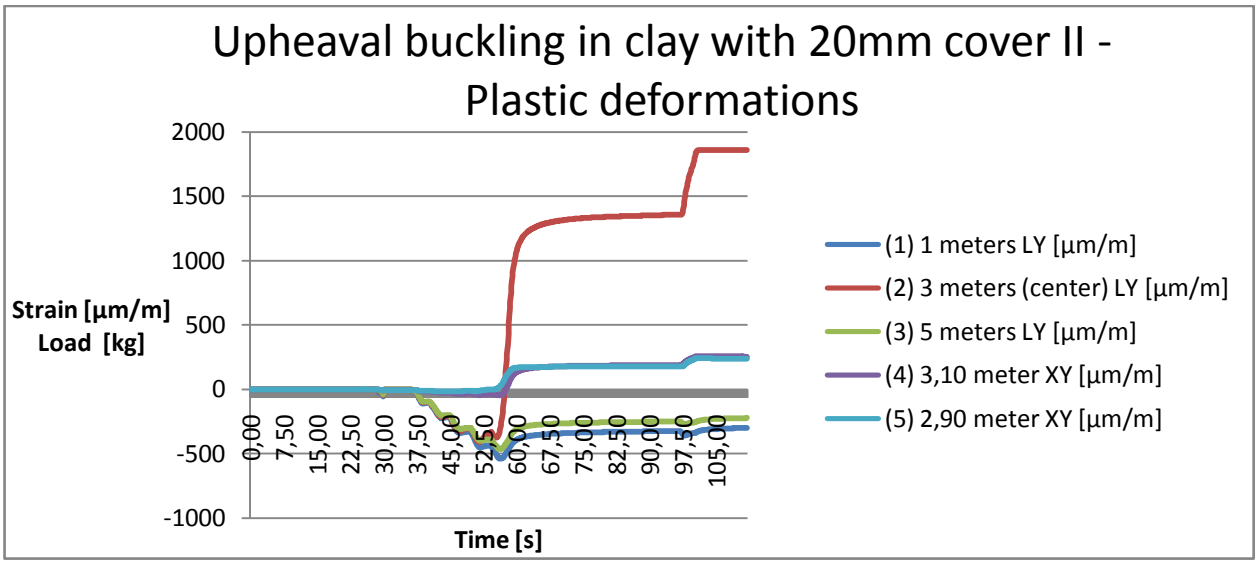

Figure B.28 Upheaval buckling in clay with 20mm cover II - Plastic deformations

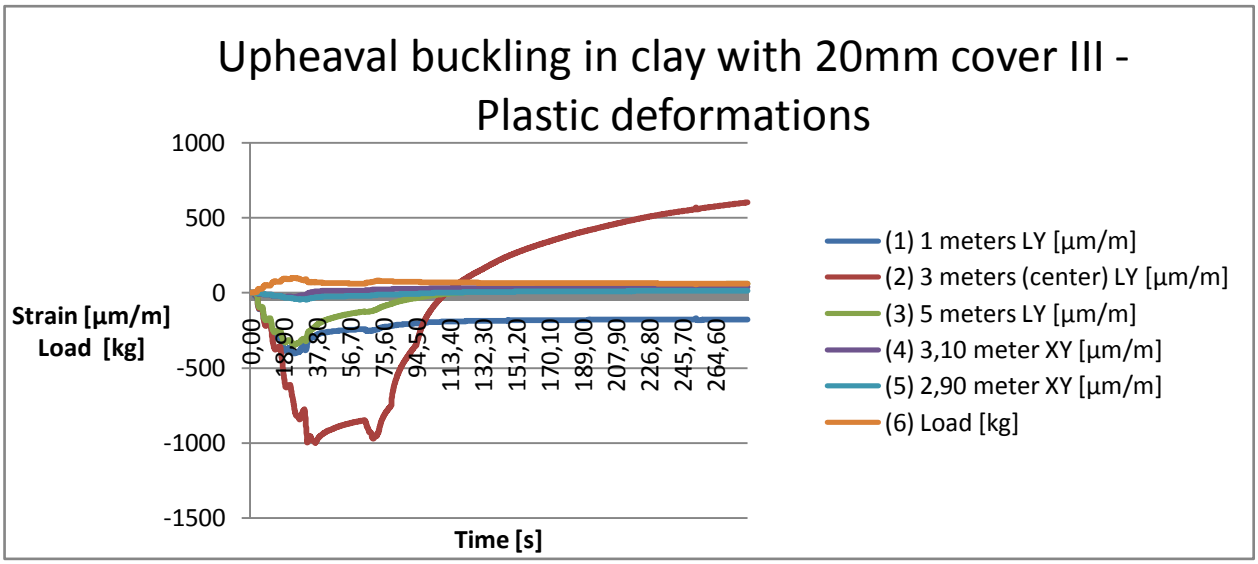

Figure B.29 Upheaval buckling in clay with 20mm cover III - Plastic deformations

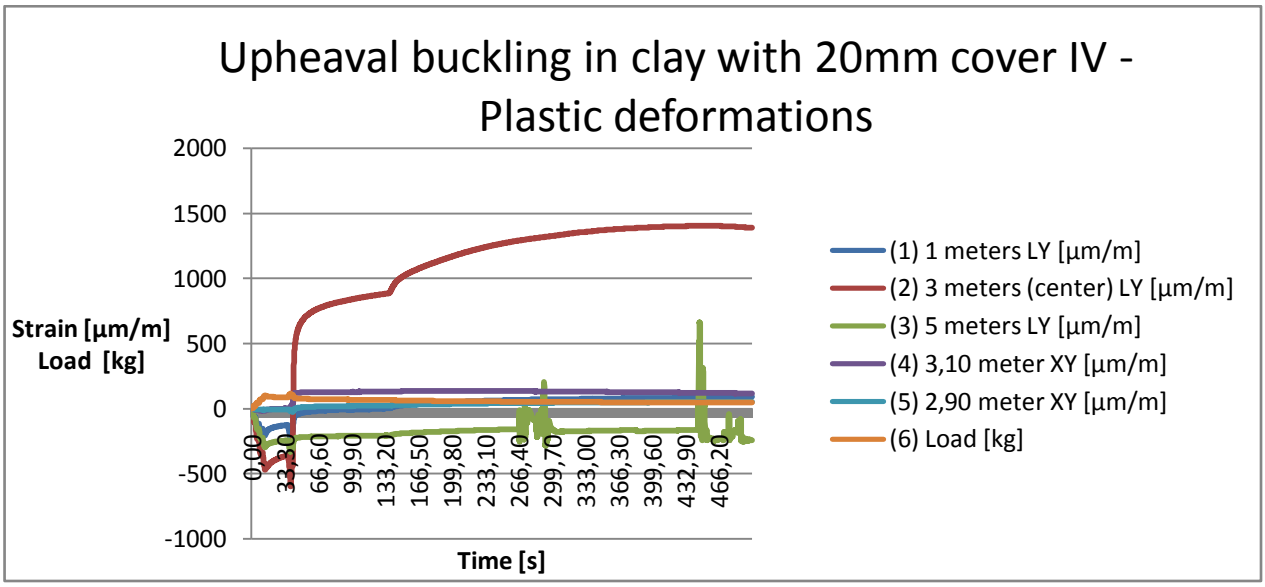

Figure B.30 Upheaval buckling in clay with 20mm cover IV - Plastic deformations

B.3.2 40mm cover – plastic deformation in pipe

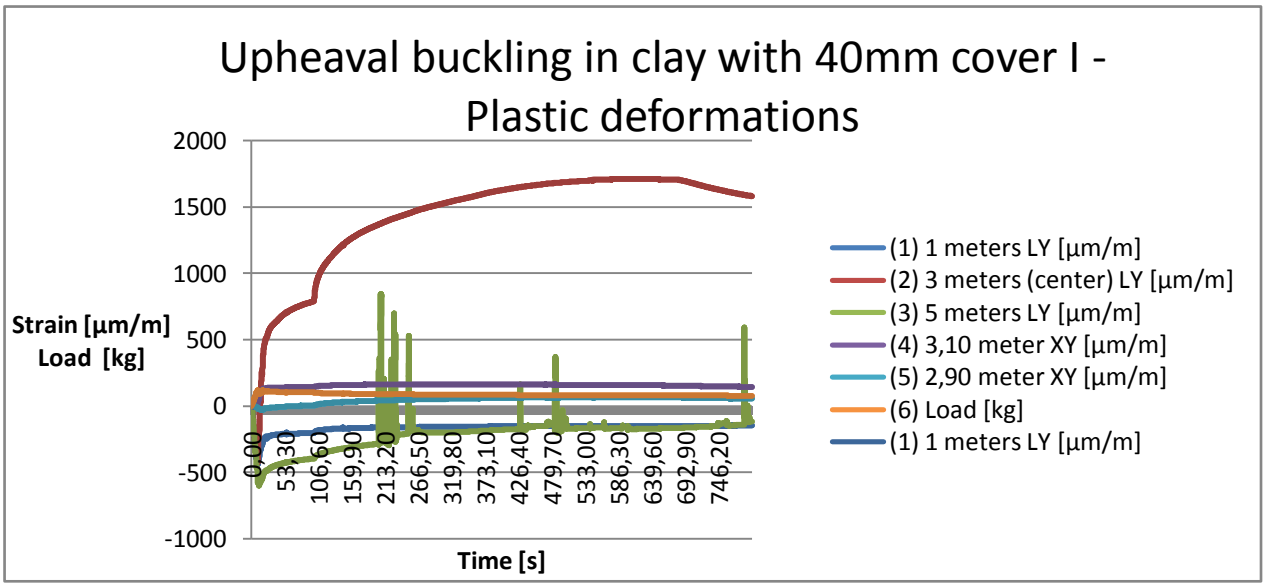

Figure B.31 Upheaval buckling in clay with 40mm cover I - Plastic deformations

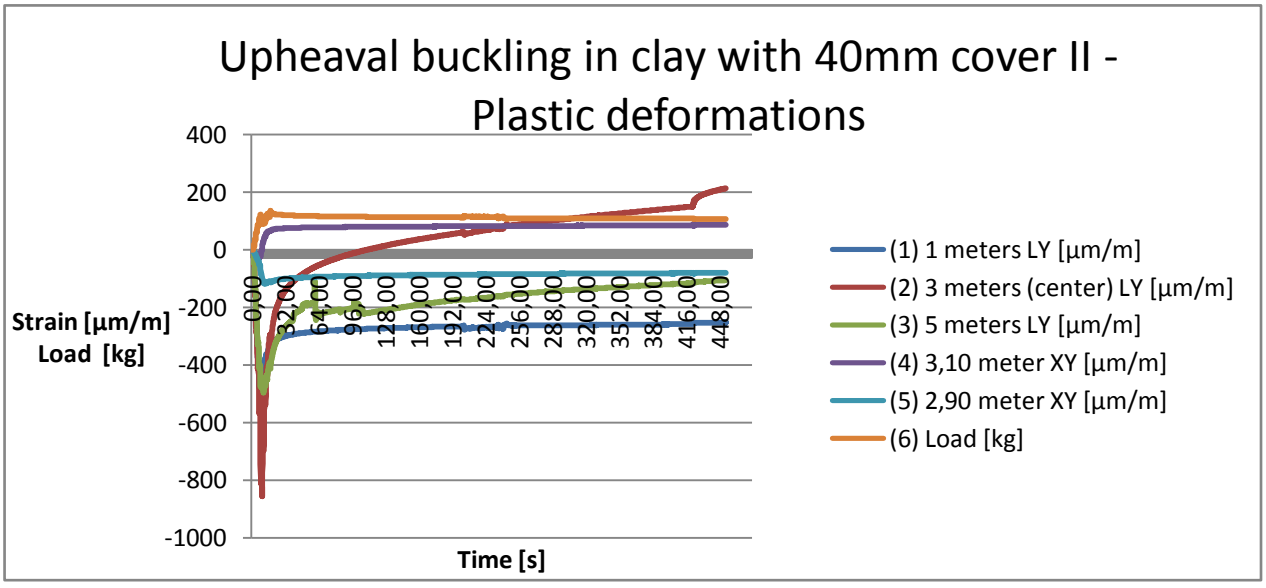

Figure B.32 Upheaval buckling in clay with 40mm cover II - Plastic deformations

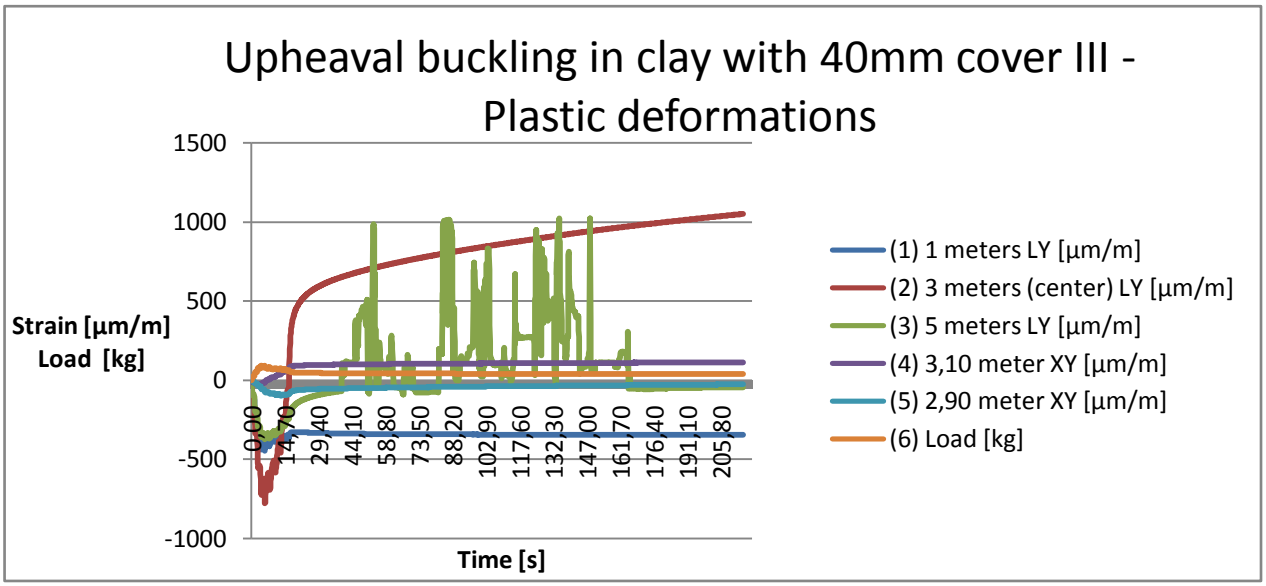

Figure B.33 **Upheaval buckling in clay with 40mm cover III - Plastic deformations**

B.3.3 10mm – 40mm cover – elastic deformation. Regular prop imperfection

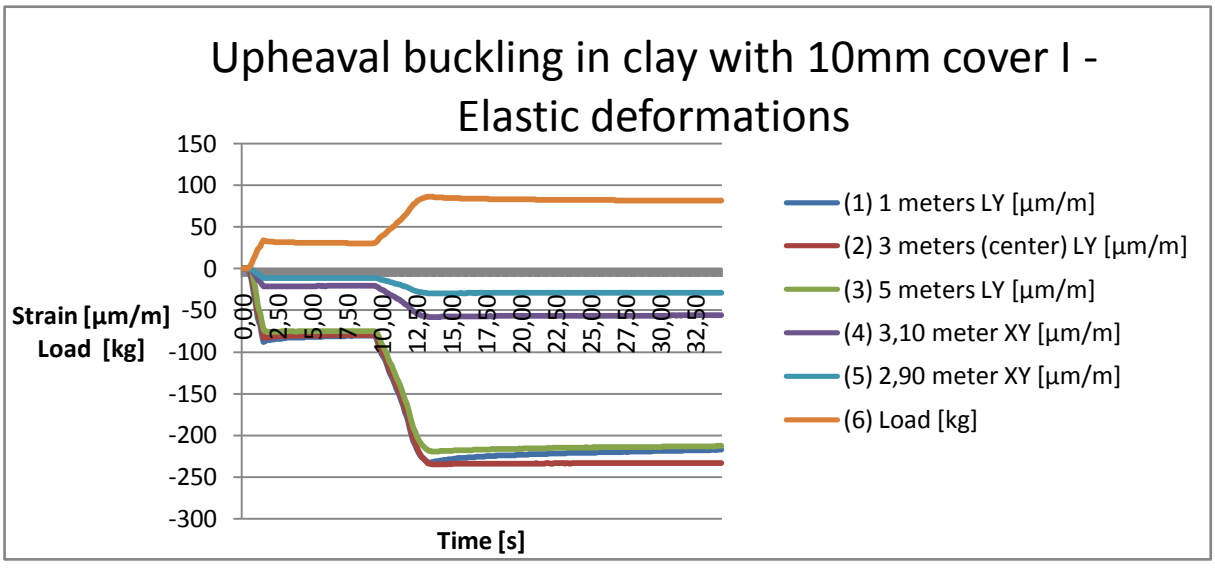

Figure B.34 **Upheaval buckling in clay with 10mm cover I - Elastic deformations**

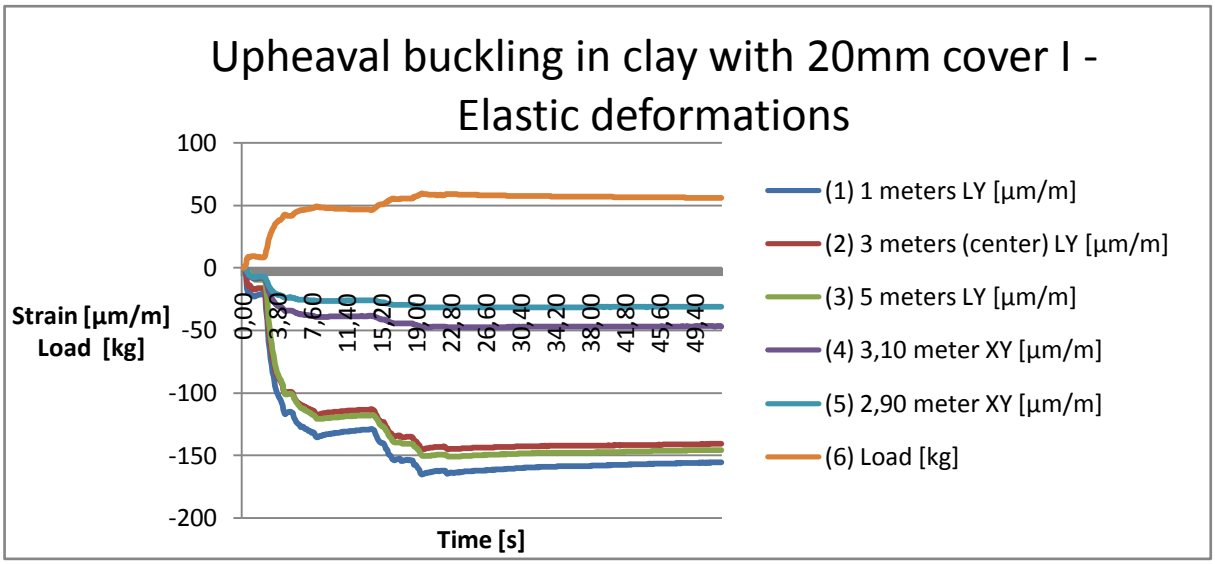

Figure B.35 Upheaval buckling in clay with 20mm cover I - Elastic deformations

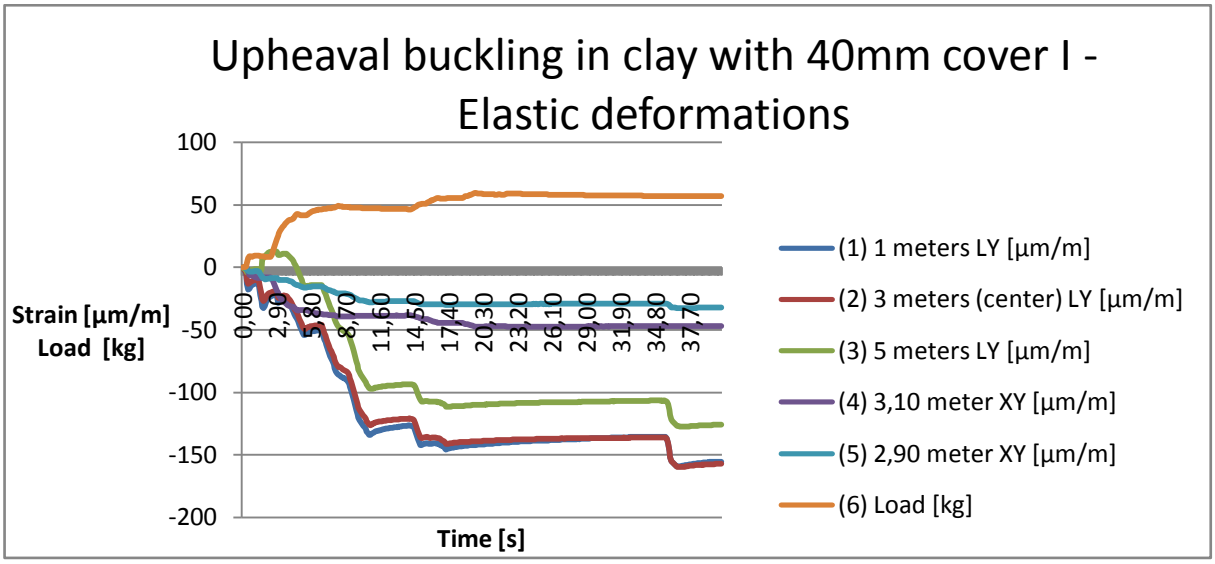

Figure B.36 Upheaval buckling in clay with 40mm cover I - Elastic deformations

B.3.4 10mm – 40mm cover. Reduced prop imperfection.

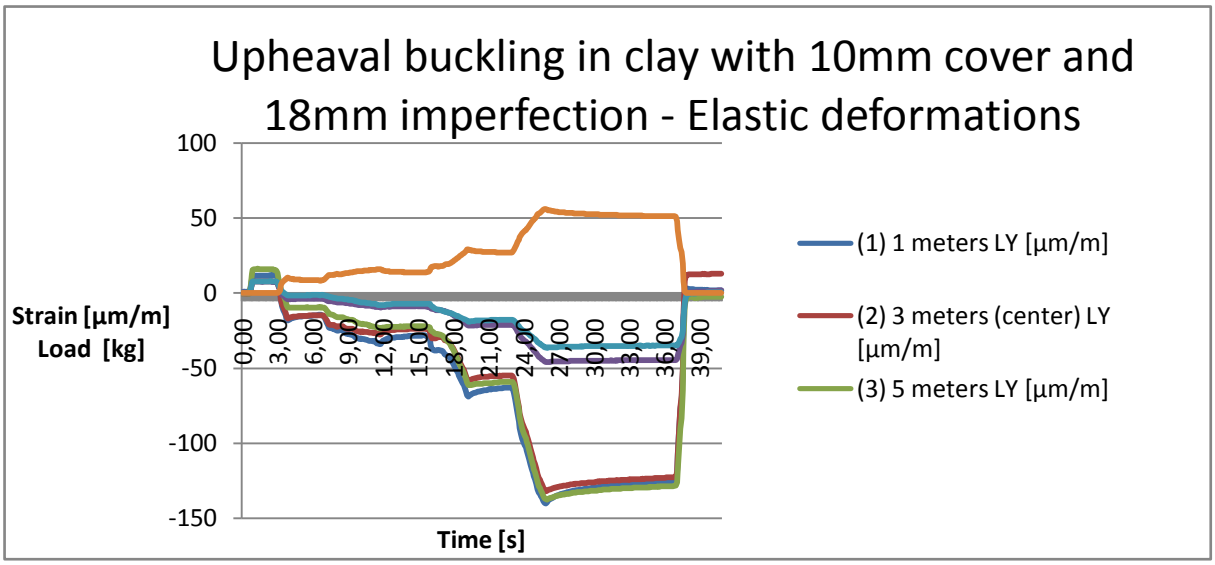

Figure B.37 **Upheaval buckling in clay with 10mm cover and 18mm imperfection - Elastic deformations**

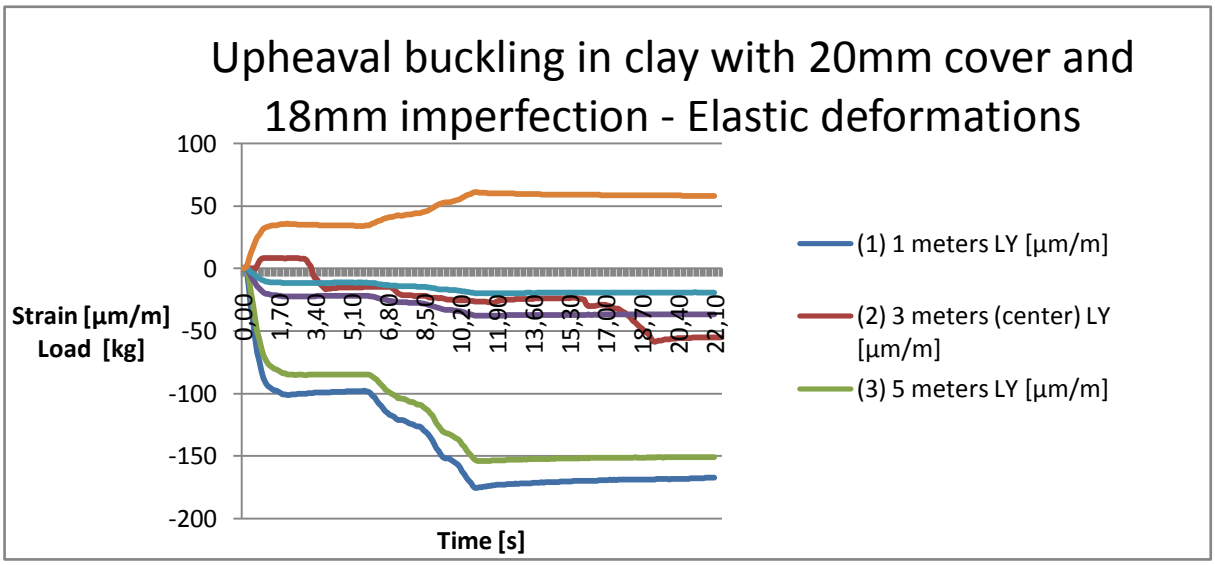

Figure B.38 **Upheaval buckling in clay with 20mm cover and 18mm imperfection - Elastic deformations**

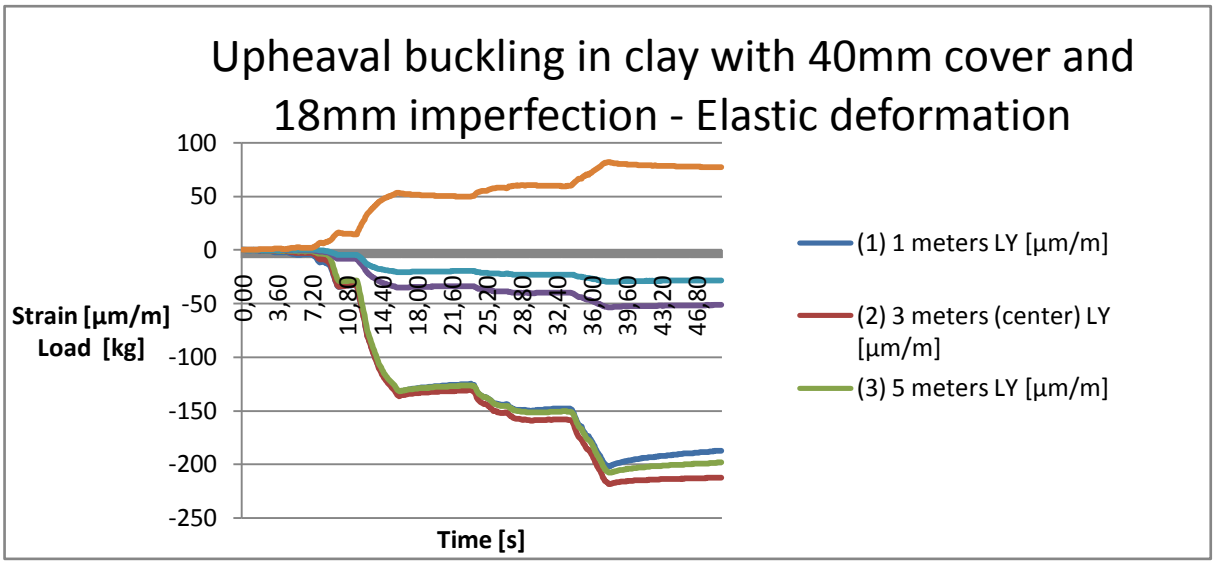

Figure B.39 **Upheaval buckling in clay with 40mm cover and 18mm imperfection - Elastic deformations**

B.3.5 Creep experiment in clay with 20mm cover

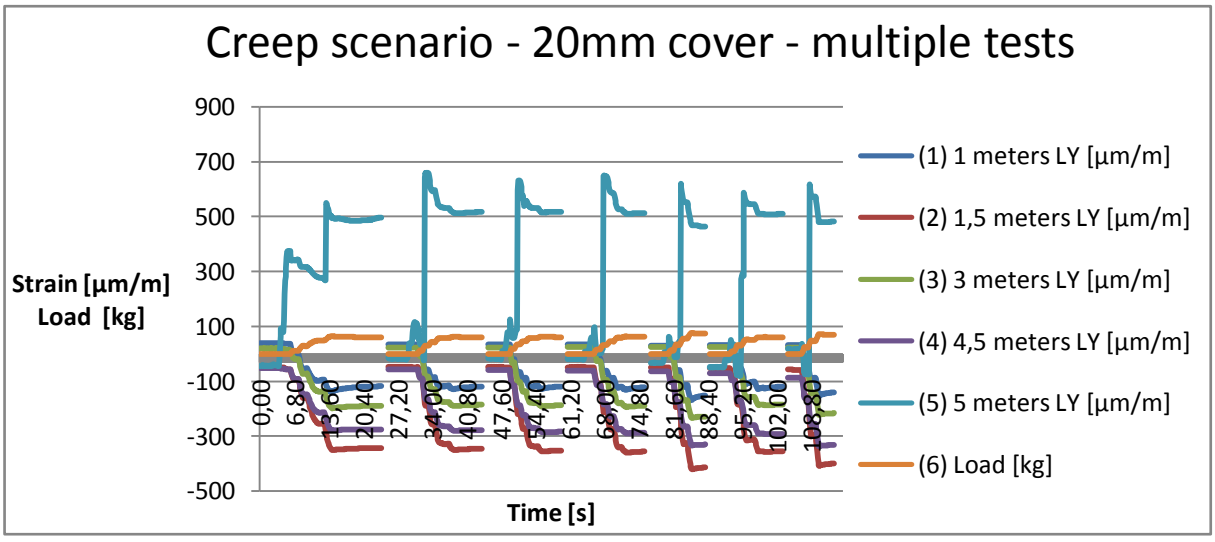

Figure B.40 **Creep scenario - 20mm cover - multiple tests**

C. Lifting experiment results

C.4 Lifting experiments in gravel

C.4.1 10mm OD copper pipe with 10mm overburden

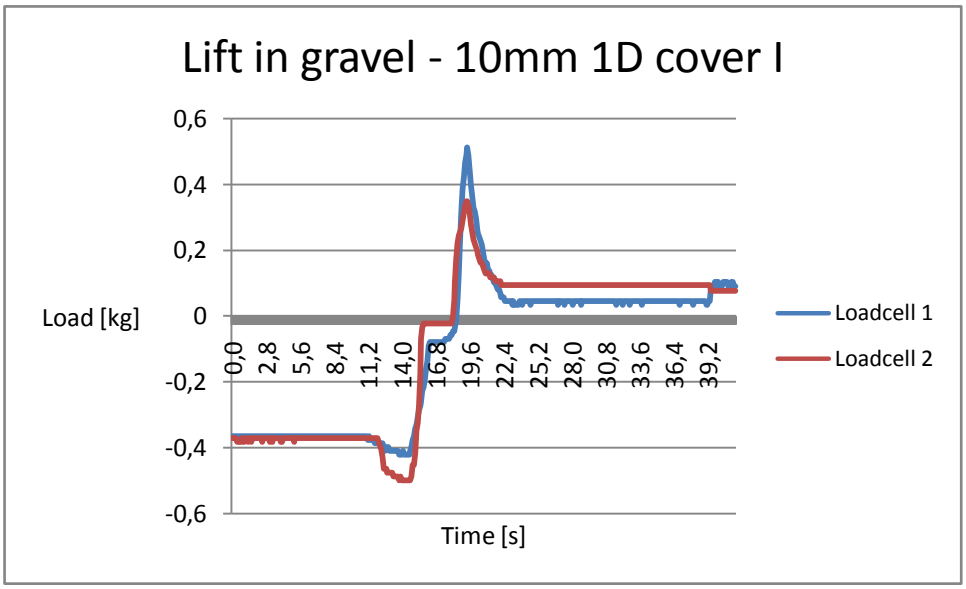

Figure C.1 Lift in gravel - 10mm 1D cover I

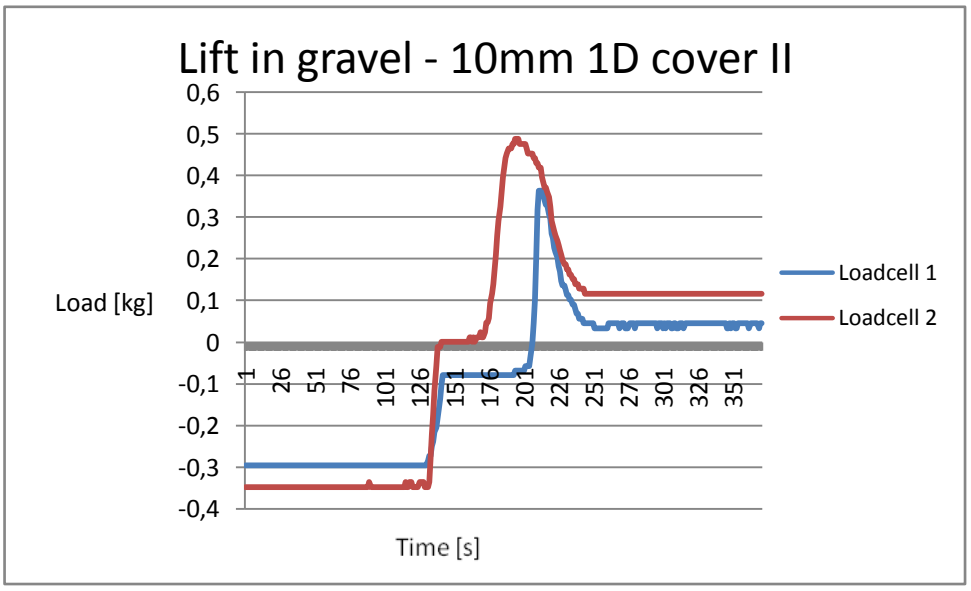

Figure C.2 Lift in gravel - 10mm 1D cover II

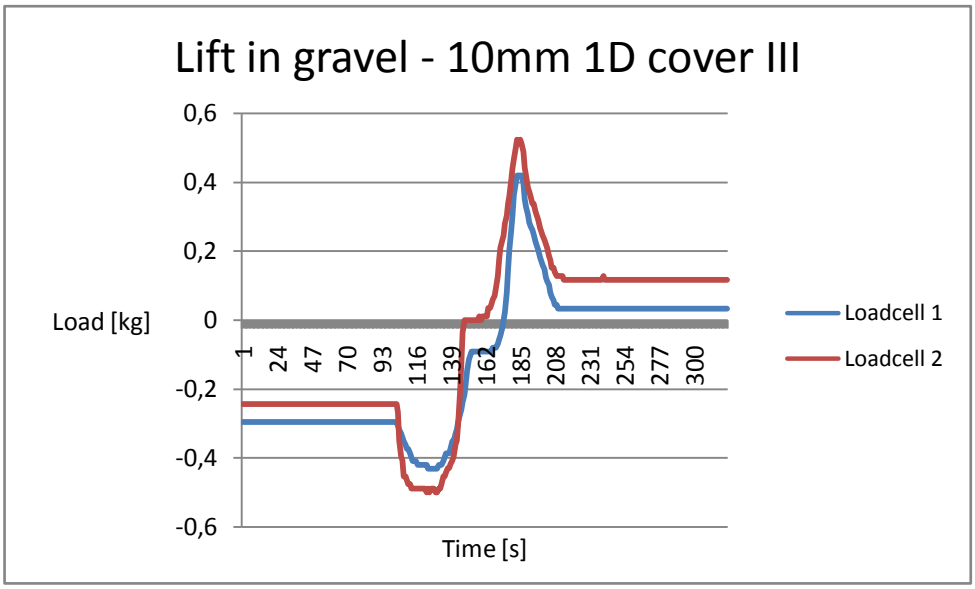

Figure C.3 Lift in gravel - 10mm 1D cover III

C.4.2 10mm OD Copper pipe with 20mm overburden

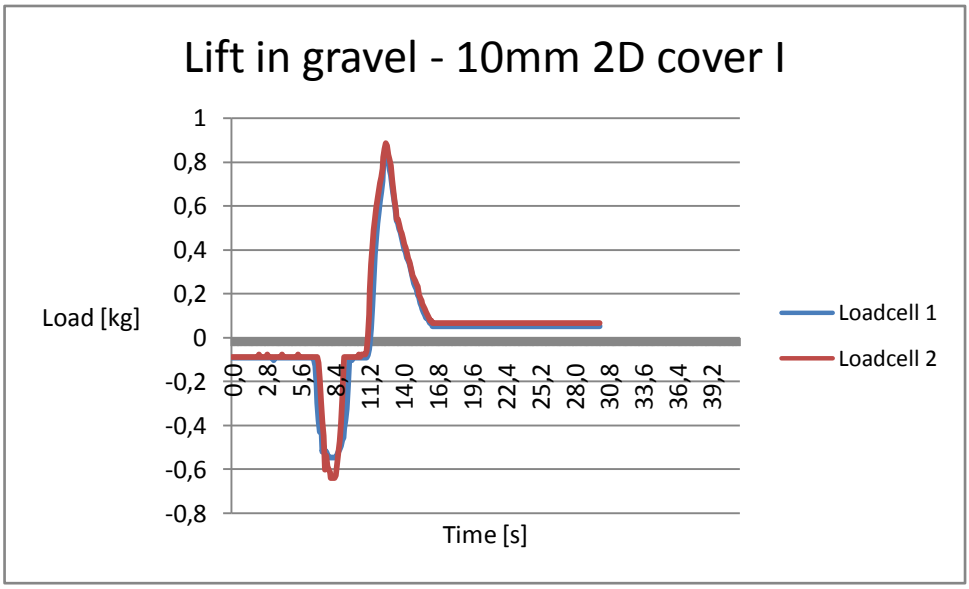

Figure C.4 Lift in gravel - 10mm 2D cover I

C.4.3 22mm OD Copper pipe with 22mm overburden

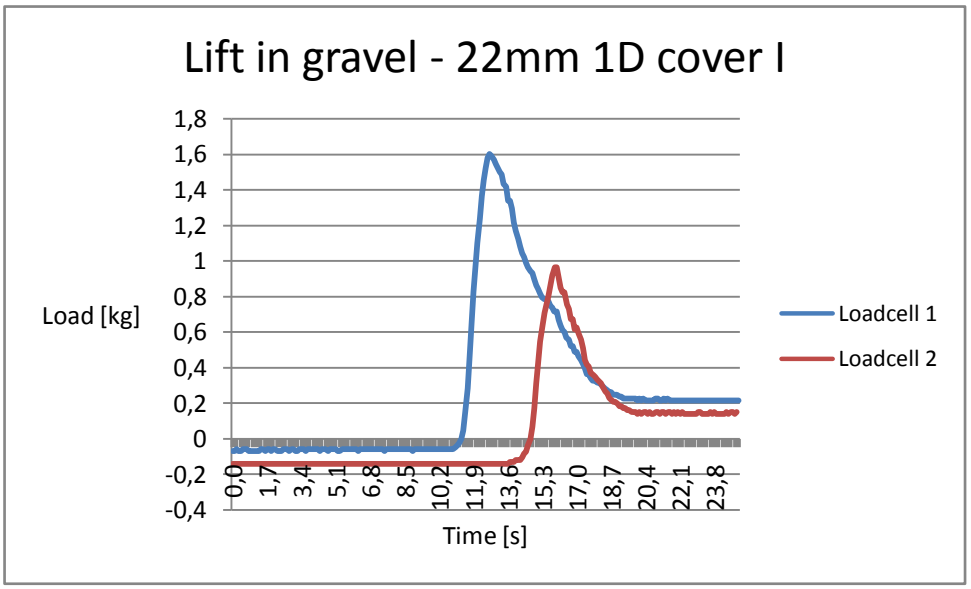

Figure C.5 **Lift in gravel - 22mm 1D cover I**

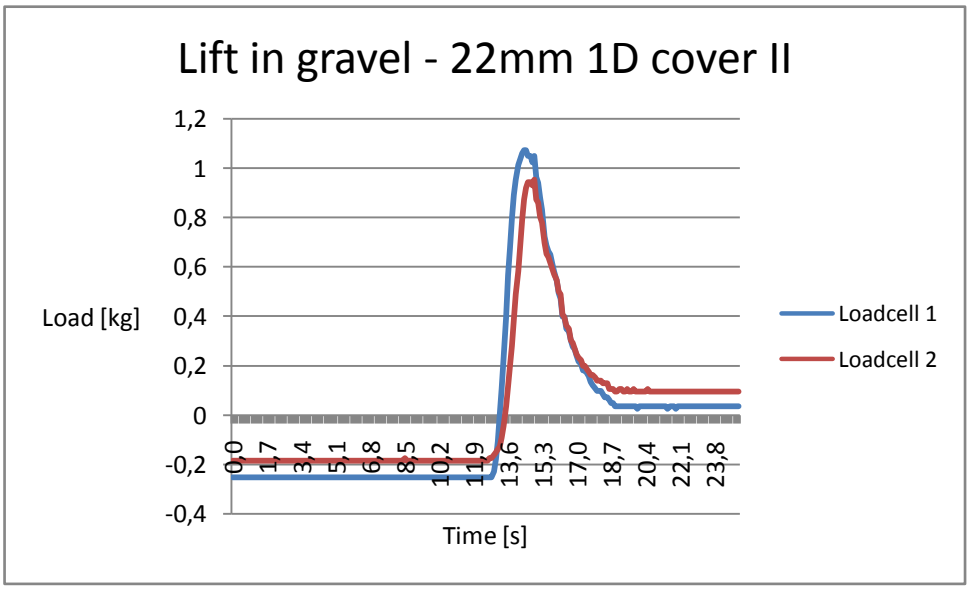

Figure C.6 **Lift in gravel - 22mm 1D cover II**

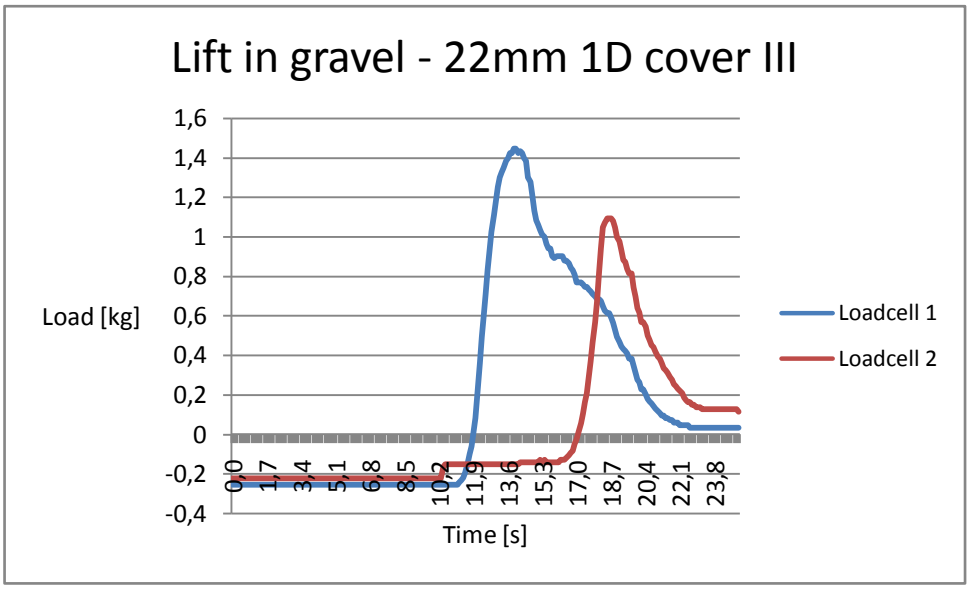

Figure C.7 Lift in gravel - 22mm 1D cover III

C.4.4 22mm OD Copper pipe with 44mm overburden

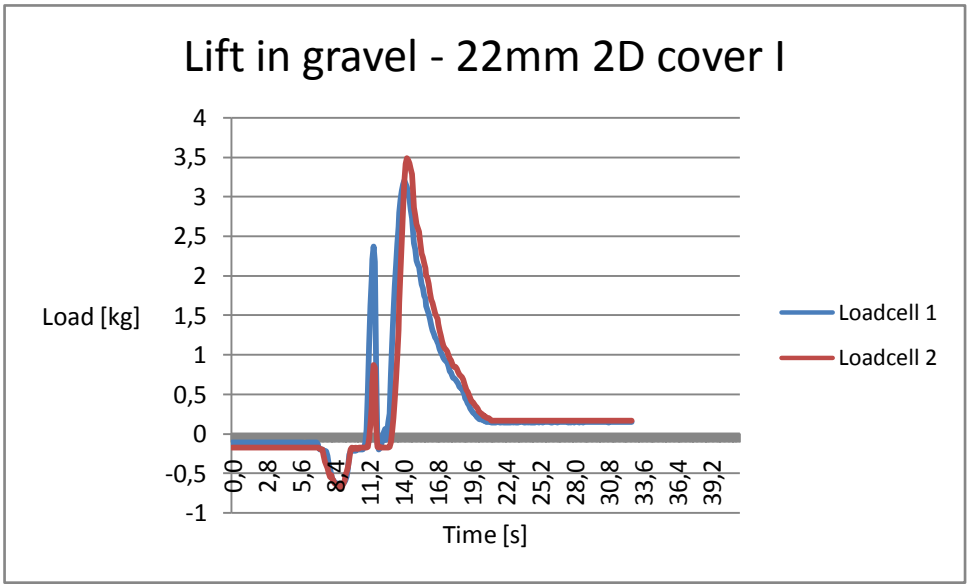

Figure C.8 Lift in gravel - 22mm 2D cover I

C.4.5 28mm OD Copper pipe with 28mm overburden

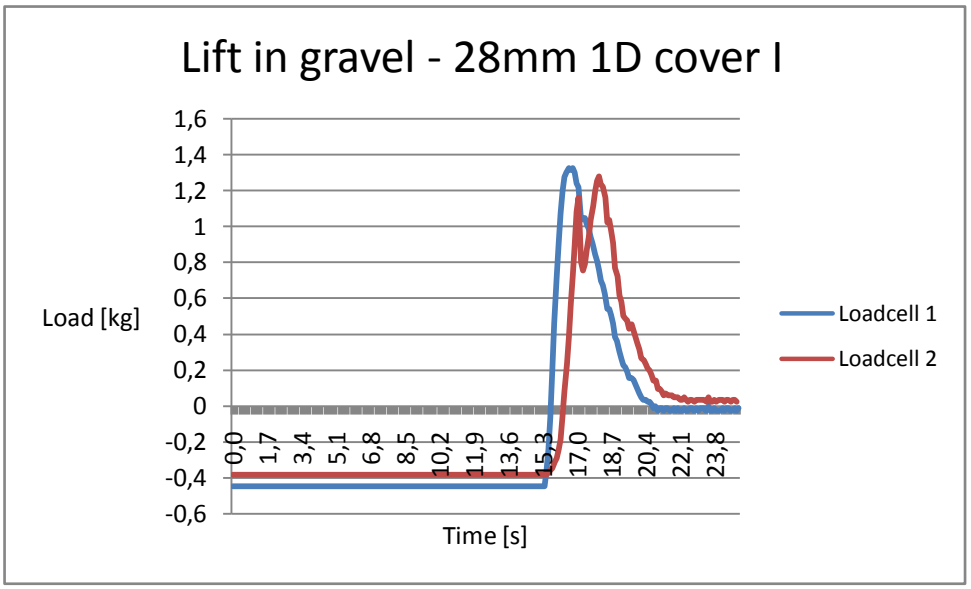

Figure C.9 **Lift in gravel - 28mm 1D cover I**

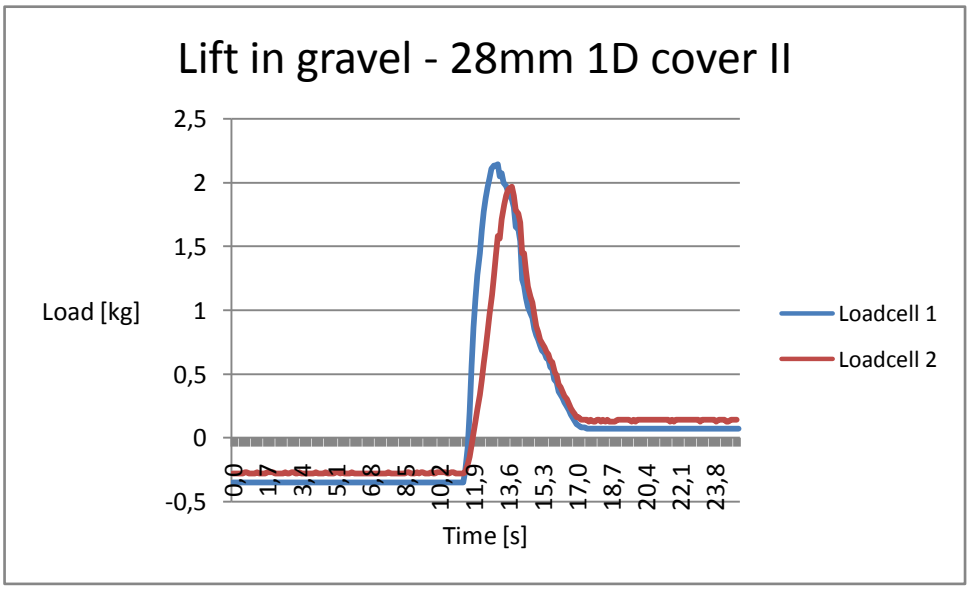

Figure C.10 **Lift in gravel - 28mm 1D cover II**

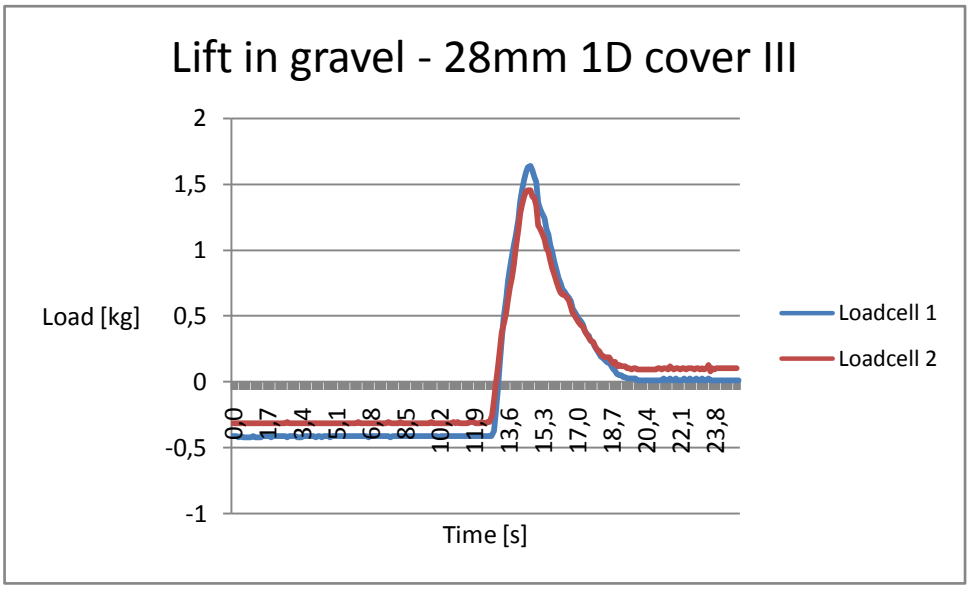

Figure C.11 Lift in gravel - 28mm 1D cover III

C.4.6 28mm OD Copper pipe with 56mm overburden

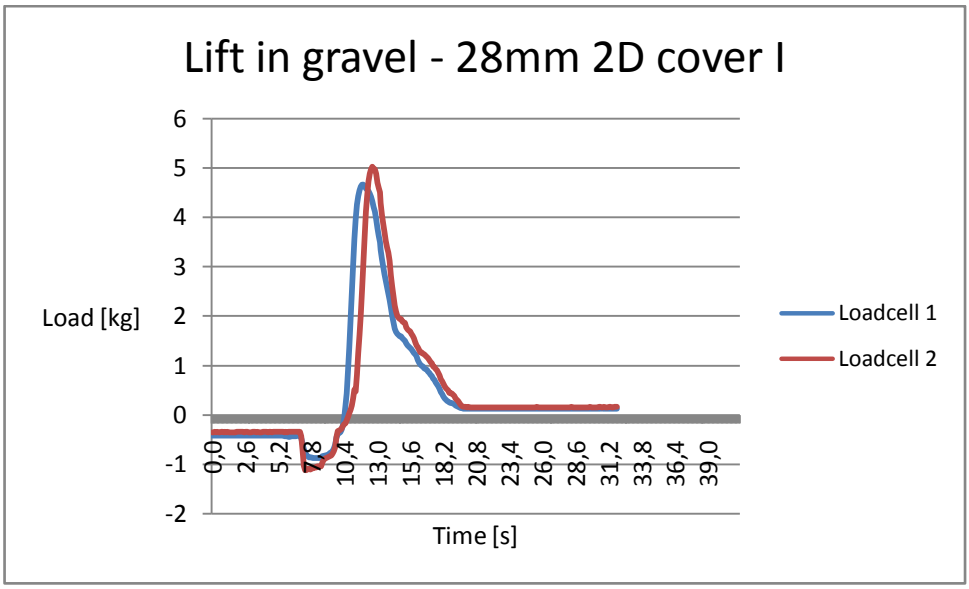

Figure C.12 Lift in gravel - 28mm 2D cover I

C.5 Lifting experiments in sand

C.5.1 10mm OD Copper pipe with 10mm overburden

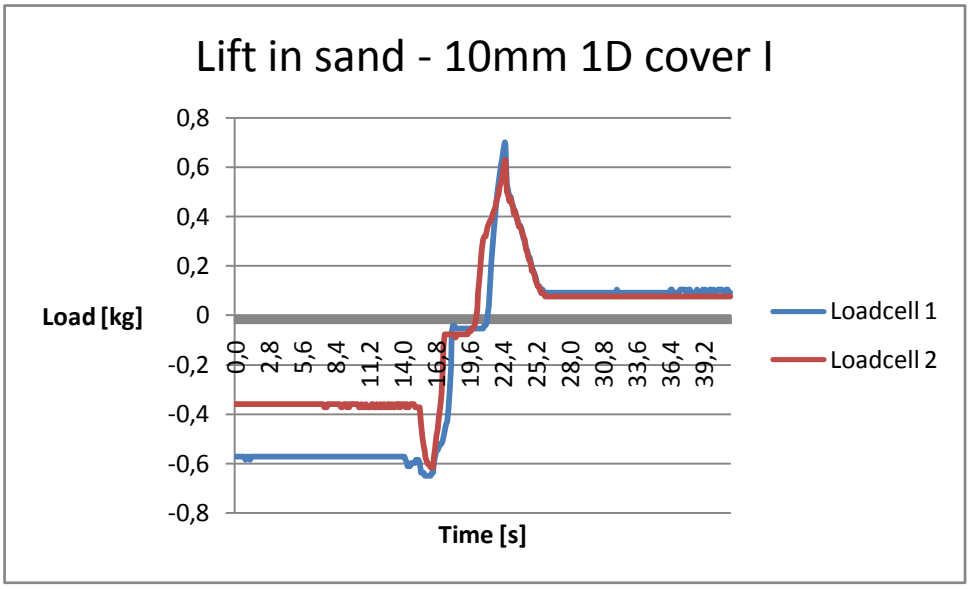

Figure C.13 Lift in sand - 10mm 1D cover I

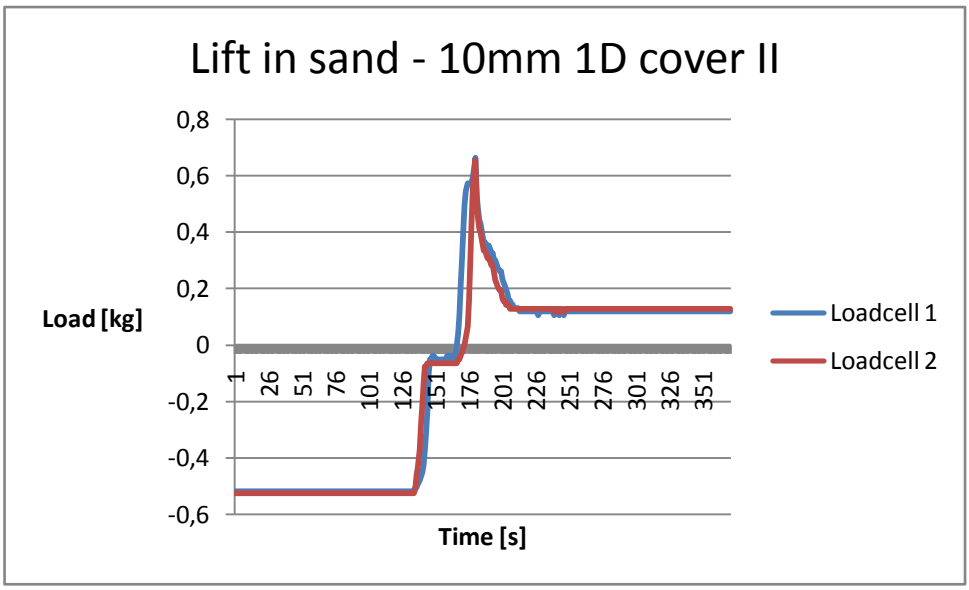

Figure C.14 Lift in sand - 10mm 1D cover II

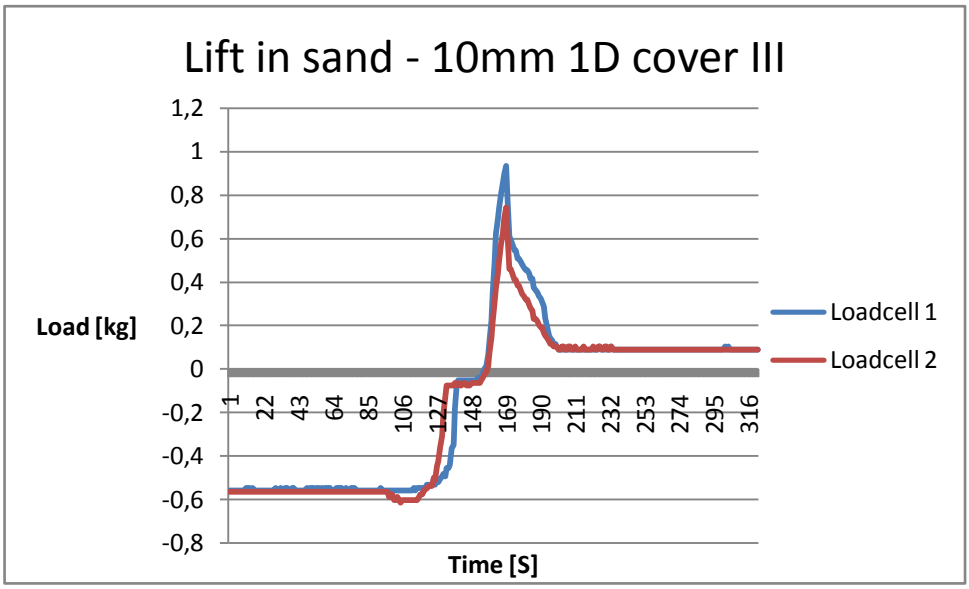

Figure C.15 **Lift in sand - 10mm 1D cover III**

C.5.2 10mm OD Copper pipe with 2D overburden

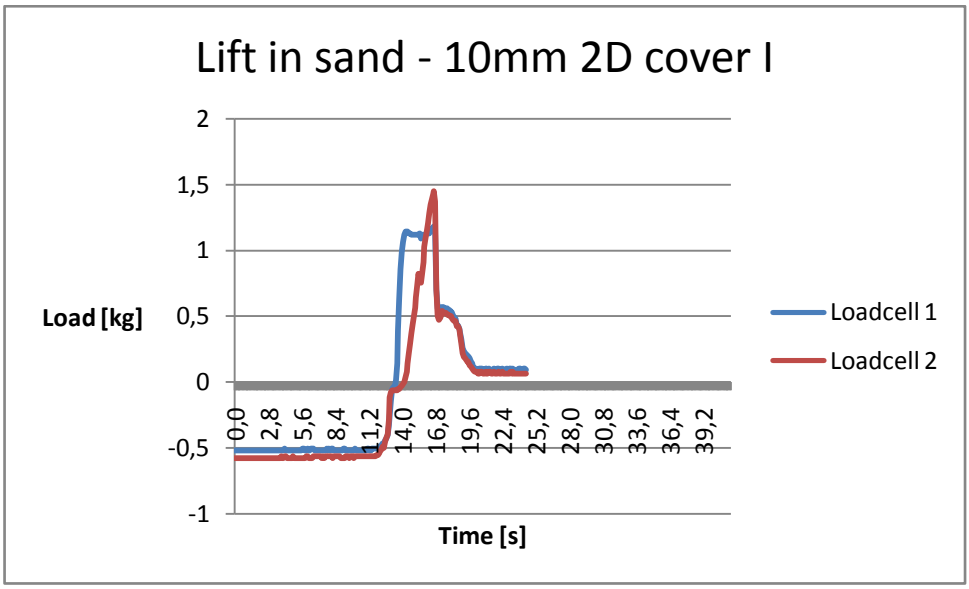

Figure C.16 **Lift in sand - 10mm 2D cover I**

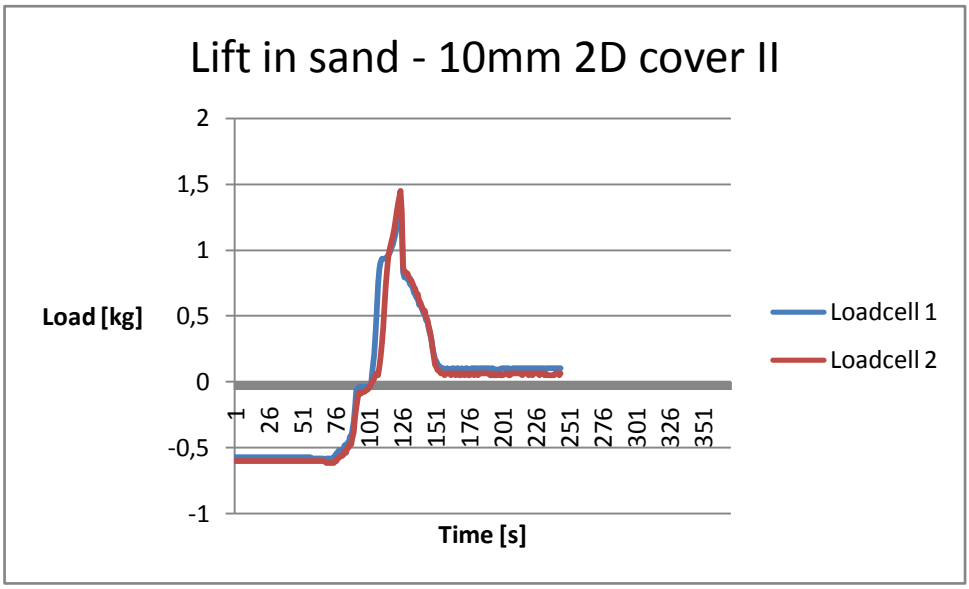

Figure C.17 **Lift in sand - 10mm 2D cover II**

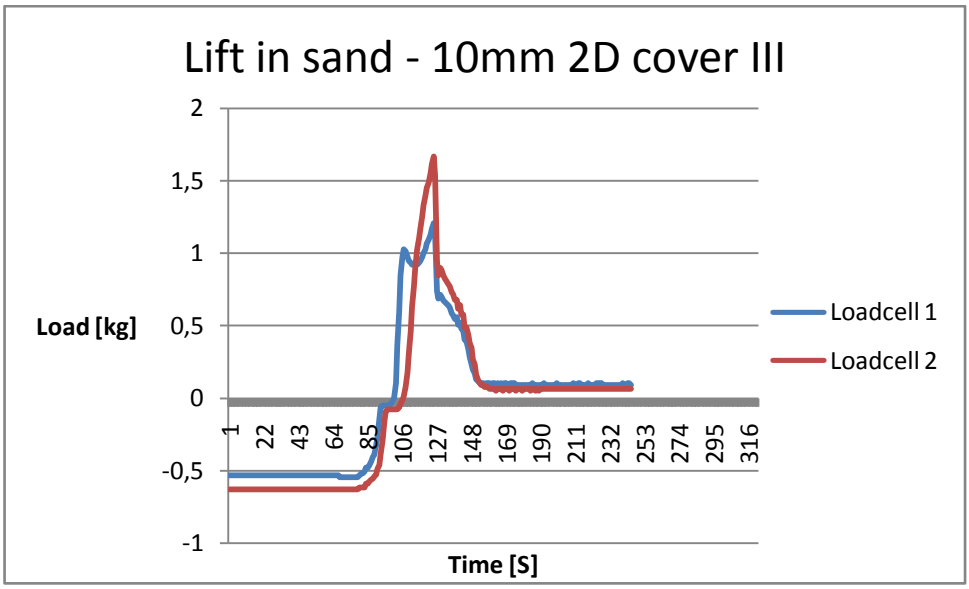

Figure C.18 **Lift in sand - 10mm 2D cover III**

C.5.3 22mm OD Copper pipe with 22mm overburden

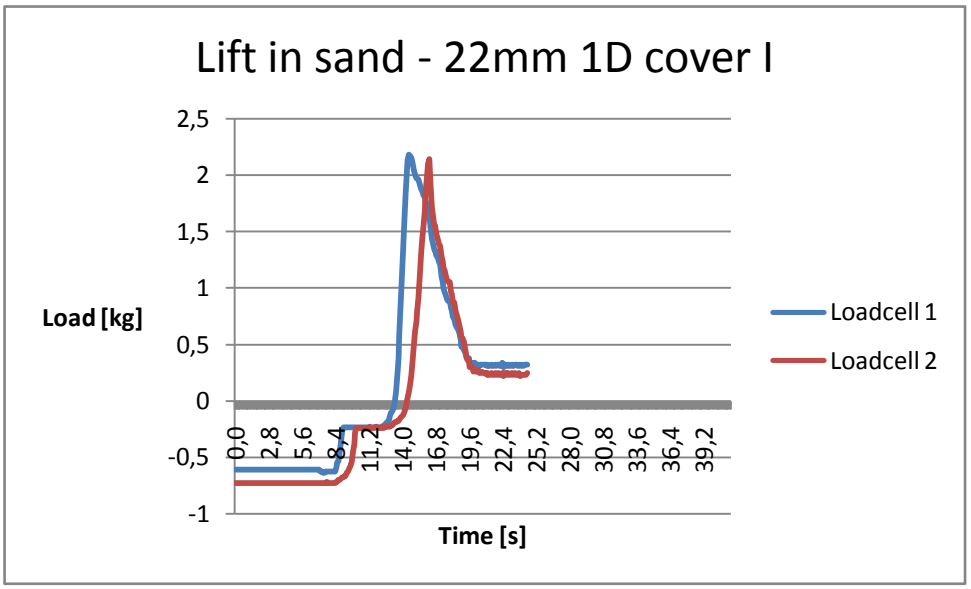

Figure C.19 Lift in sand - 22mm 1D cover I

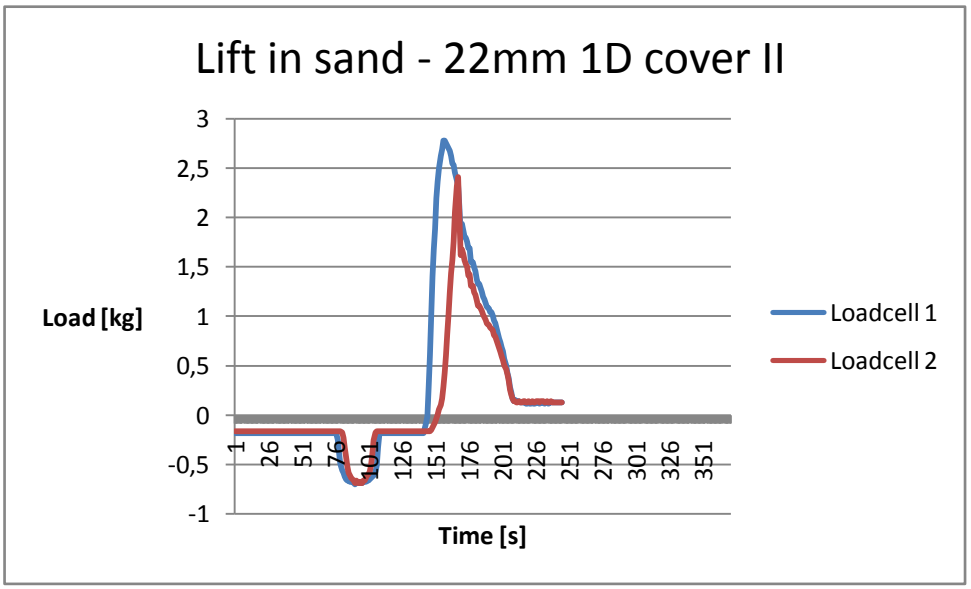

Figure C.20 Lift in sand - 22mm 1D cover II

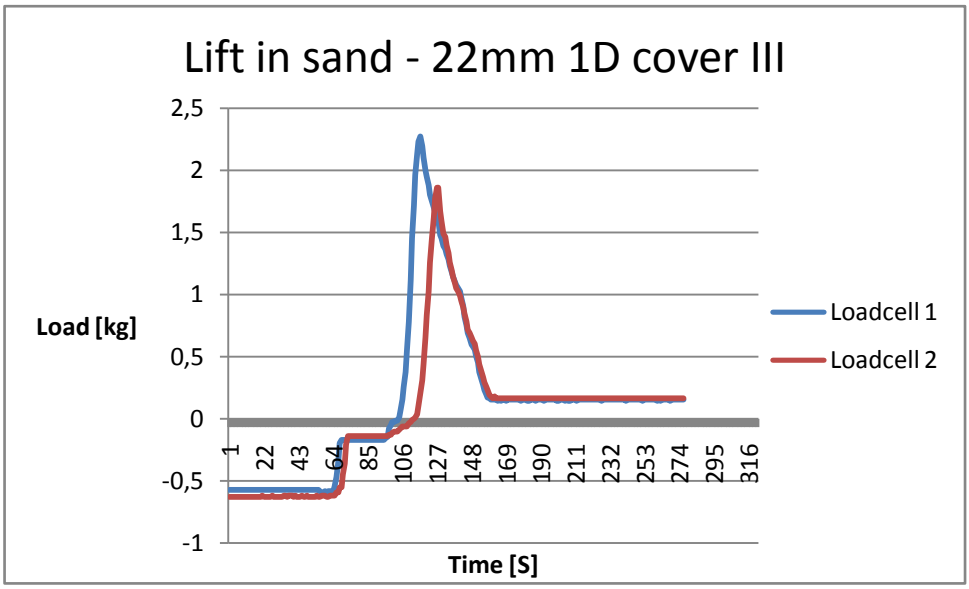

Figure C.21 Lift in sand - 22mm 1D cover III

C.5.4 22mm OD Copper pipe with 44mm overburden

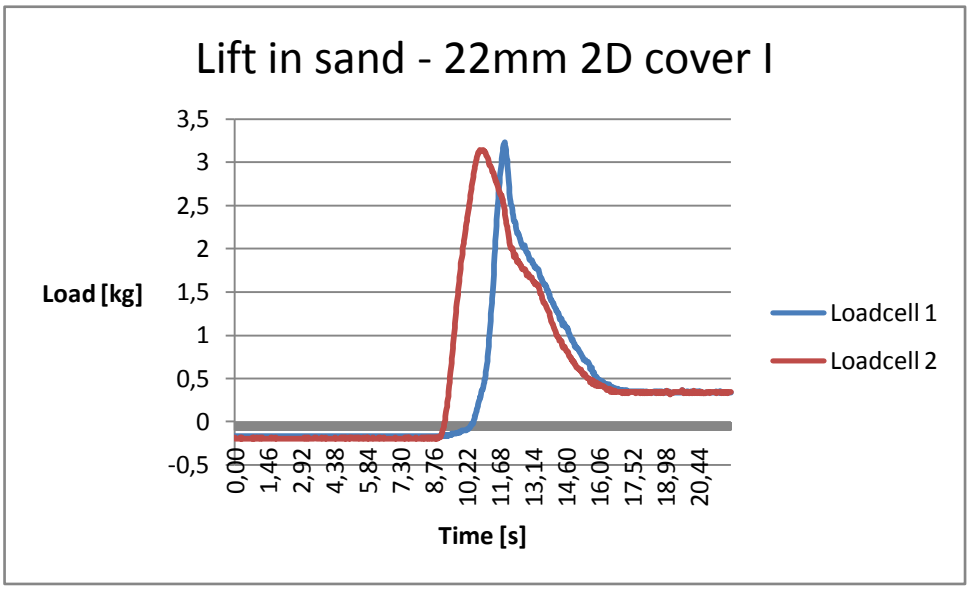

Figure C.22 Lift in sand - 22mm 2D cover I

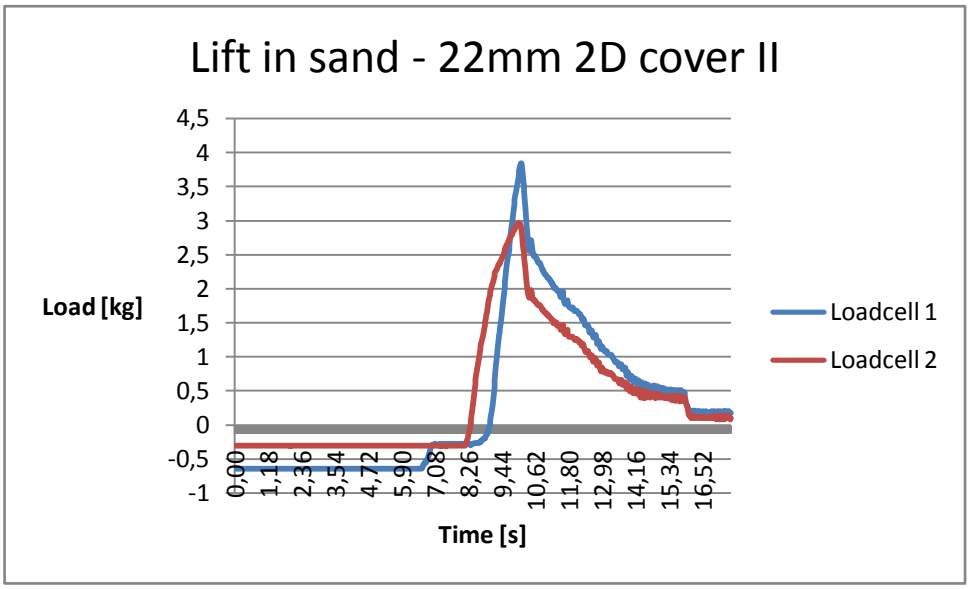

Figure C.23 **Lift in sand - 22mm 2D cover II**

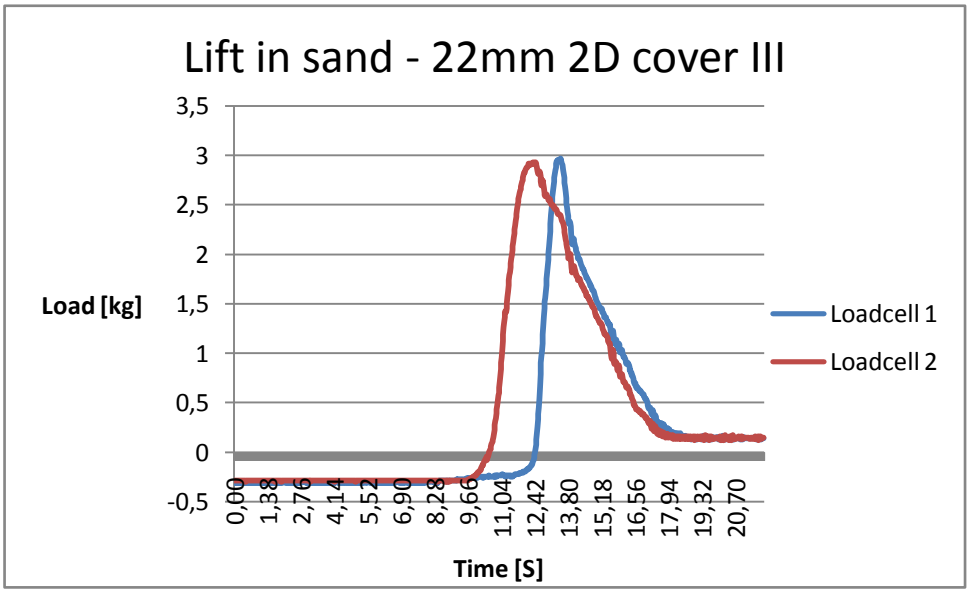

Figure C.24 **Lift in sand - 22mm 2D cover III**

C.5.5 28mm OD Copper pipe with 28mm overburden

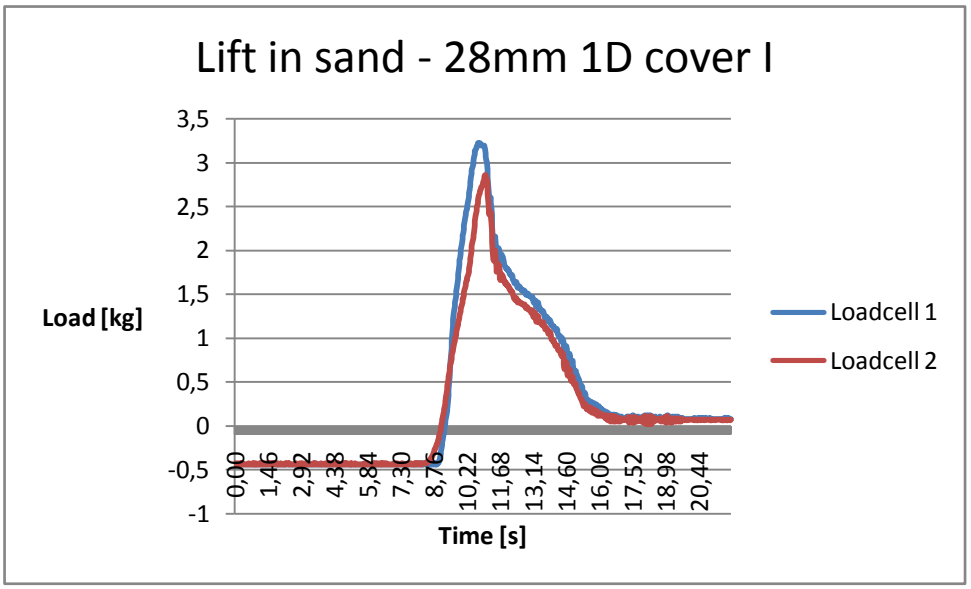

Figure C.25 Lift in sand - 28mm 1D cover I

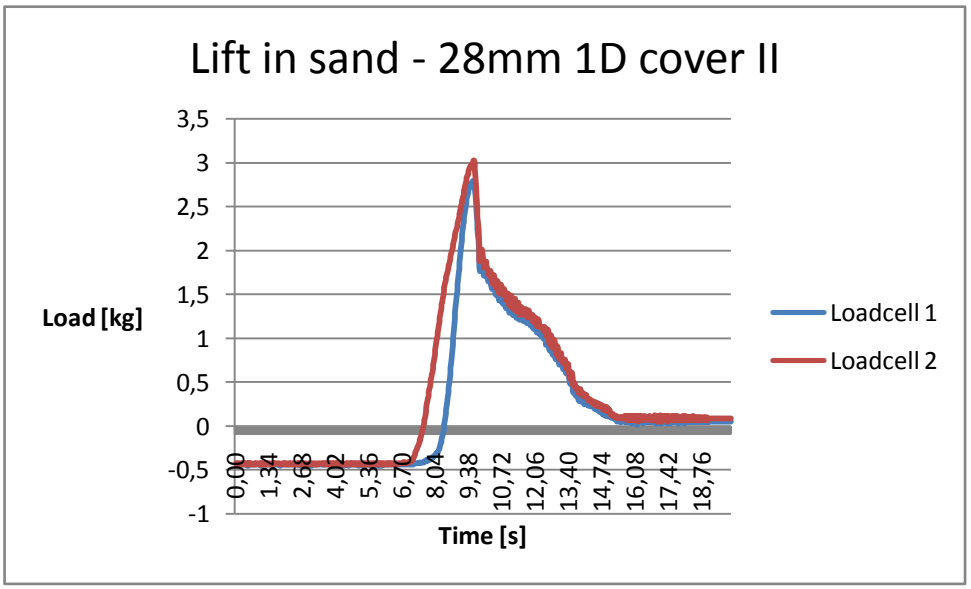

Figure C.26 Lift in sand - 28mm 1D cover II

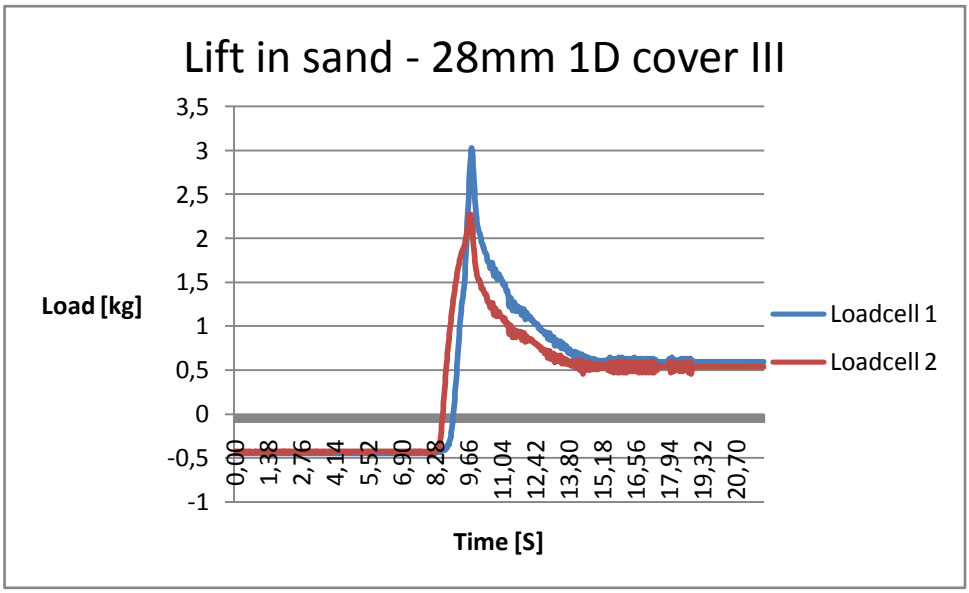

Figure C.27 Lift in sand - 28mm 1D cover III

C.5.6 28mm OD Copper pipe with 56mm overburden

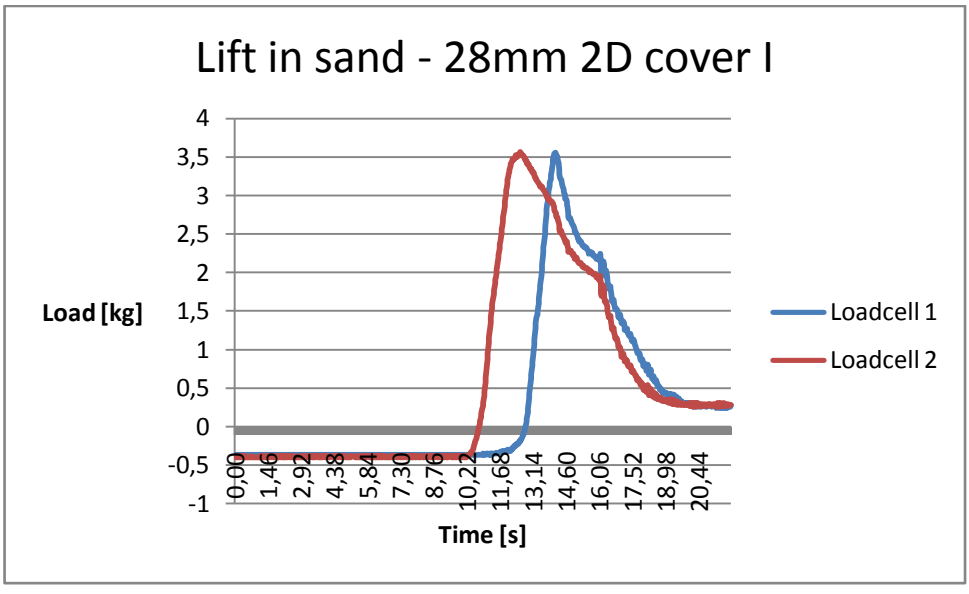

Figure C.28 Lift in sand - 28mm 2D cover I

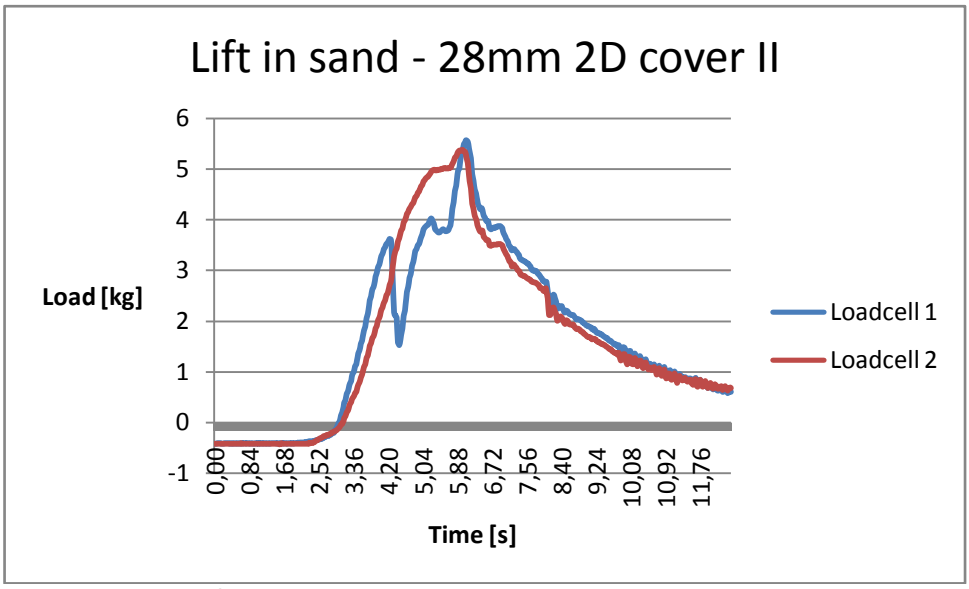

Figure C.29 **Lift in sand - 28mm 2D cover II**

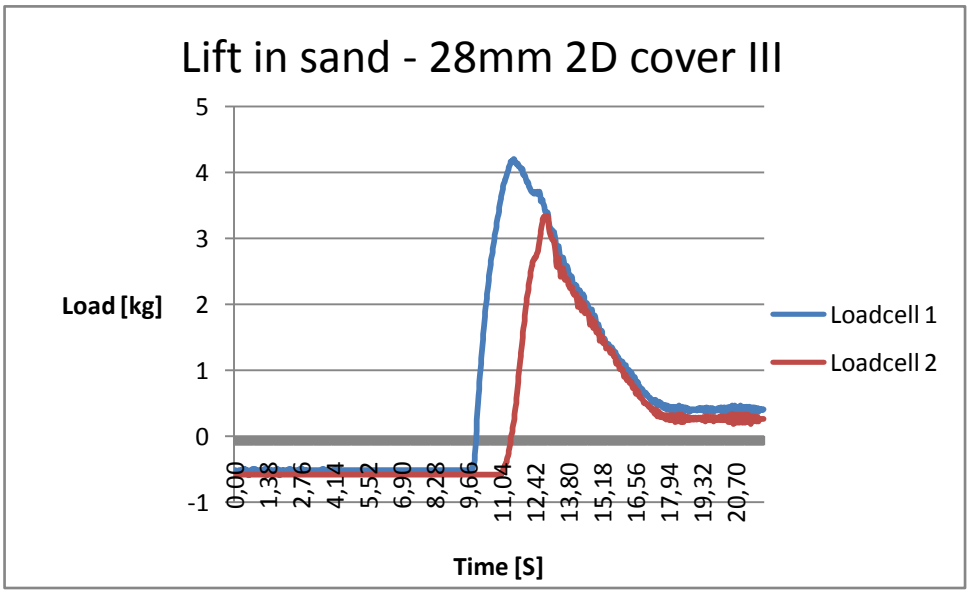

Figure C.30 **Lift in sand - 28mm 2D cover III**

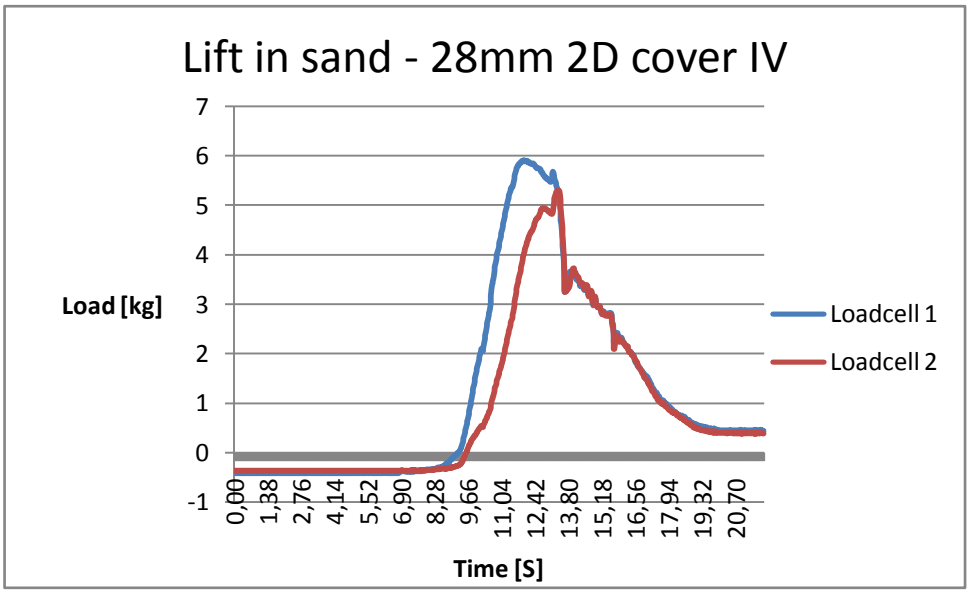

Figure C.31 **Lift in sand - 28mm 2D cover IV**

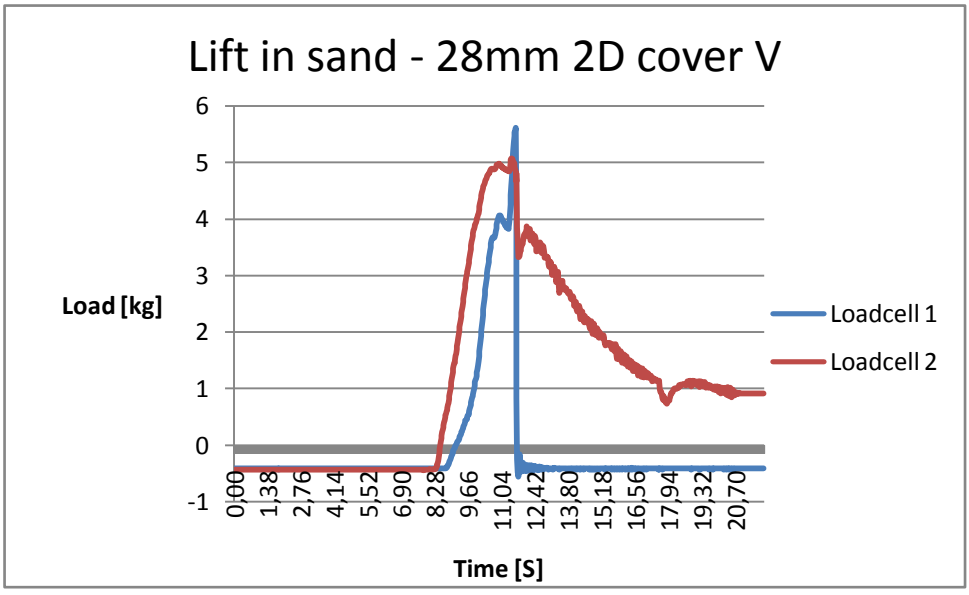

Figure C.32 **Lift in sand - 28mm 2D cover V**

C.6 Lifting experiments in clay

C.6.1 10mm OD copper pipe with 10mm overburden

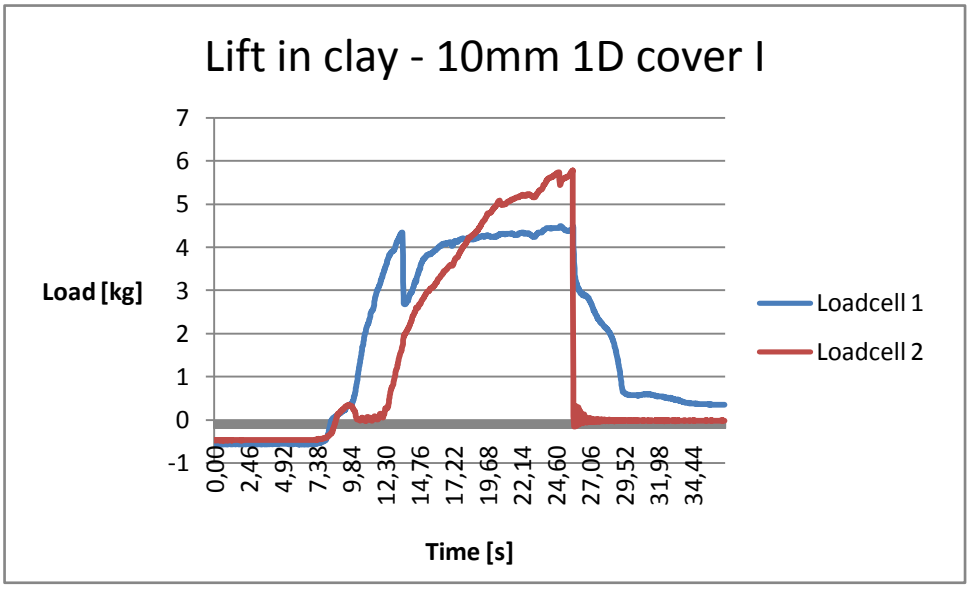

Figure C.33 Lift in clay - 10mm 1D cover I

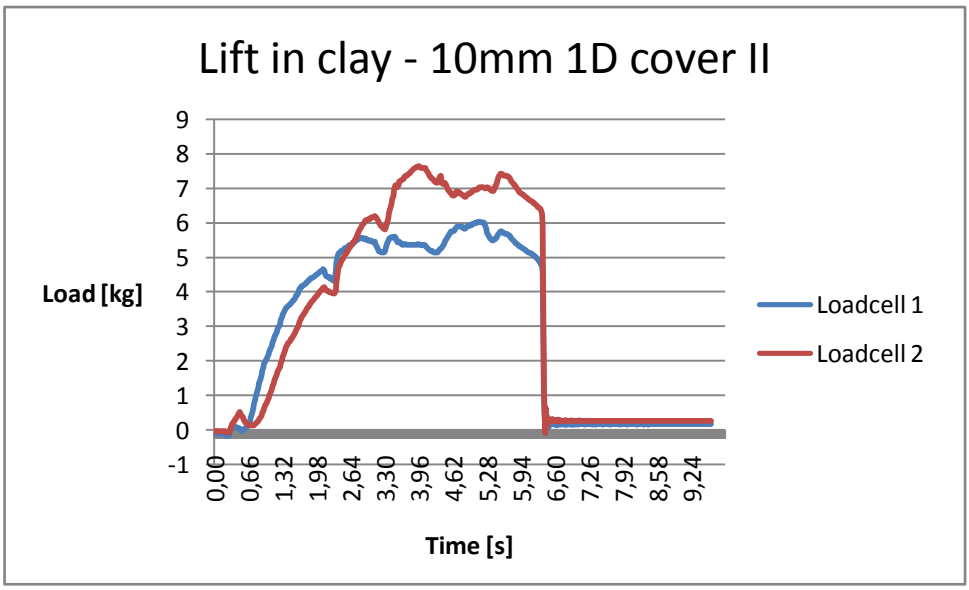

Figure C.34 Lift in clay - 10mm 1D cover II

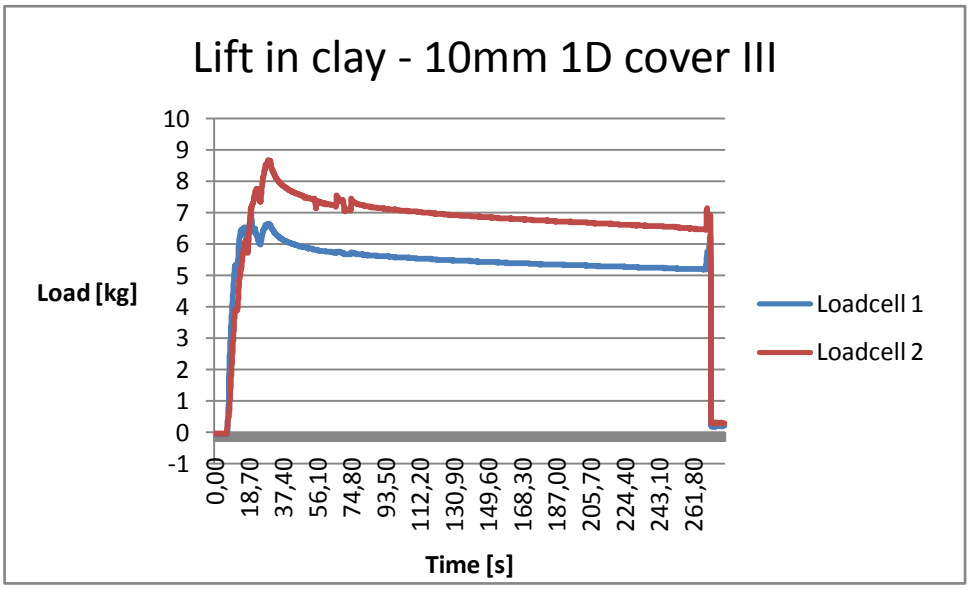

Figure C.35 Lift in clay - 10mm 1D cover III

C.6.2 10mm OD copper pipe with 20mm overburden

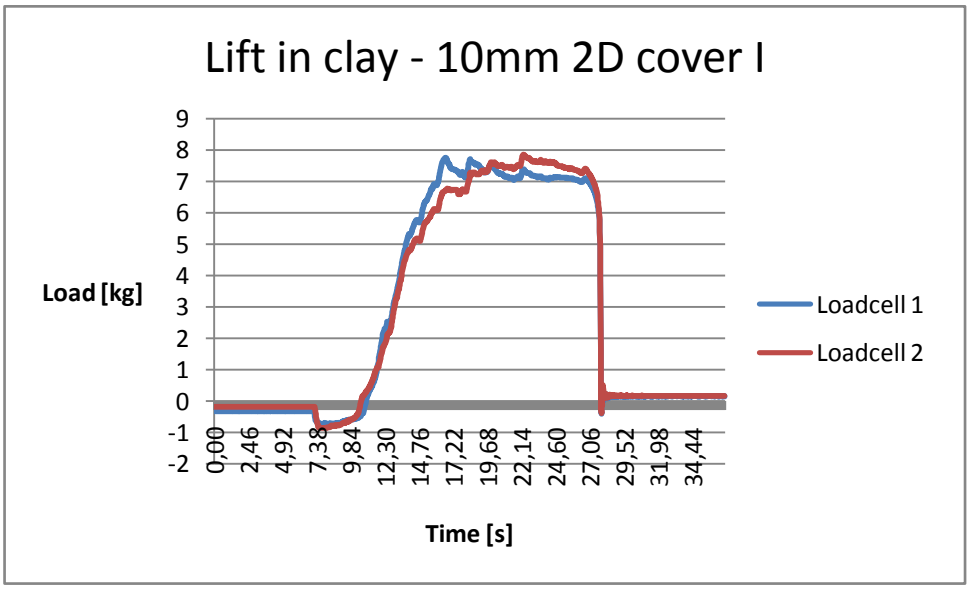

Figure C.36 Lift in clay - 10mm 2D cover I

C.6.3 22mm OD copper pipe with 22mm overburden

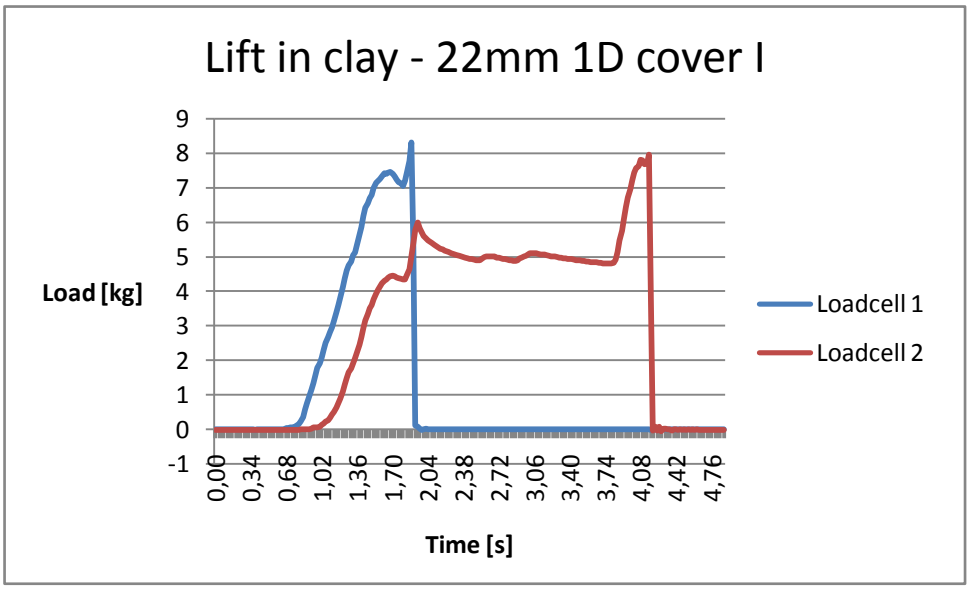

Figure C.37 **Lift in clay - 22mm 1D cover I**

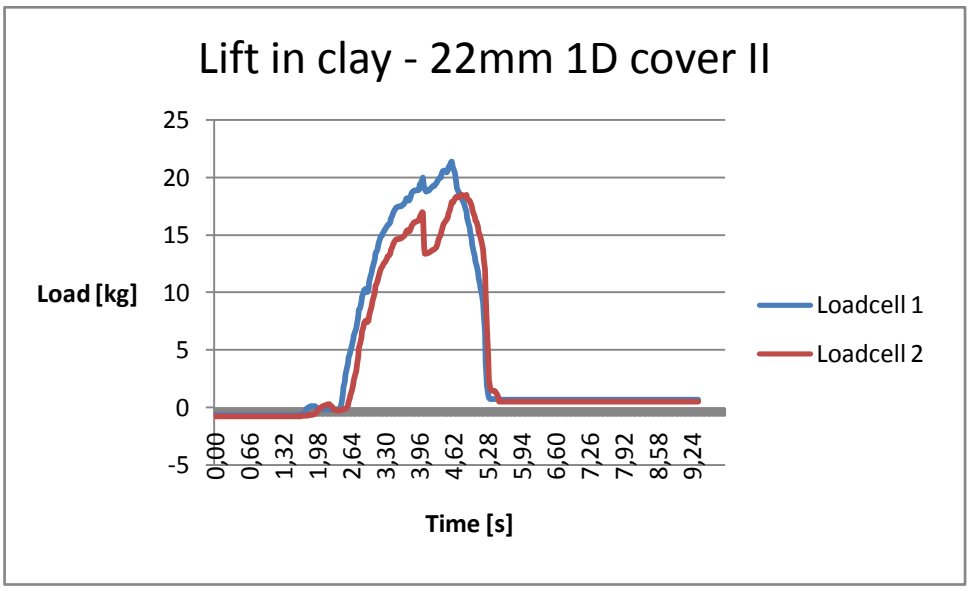

Figure C.38 **Lift in clay - 22mm 1D cover II**

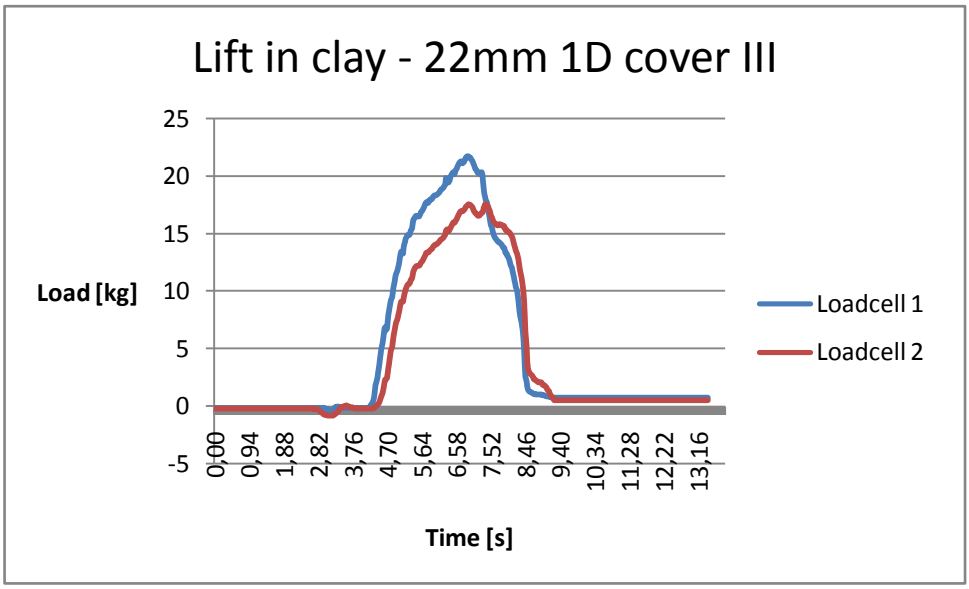

Figure C.39 Lift in clay - 22mm 1D cover III

C.6.4 22mm OD copper pipe with 44mm overburden

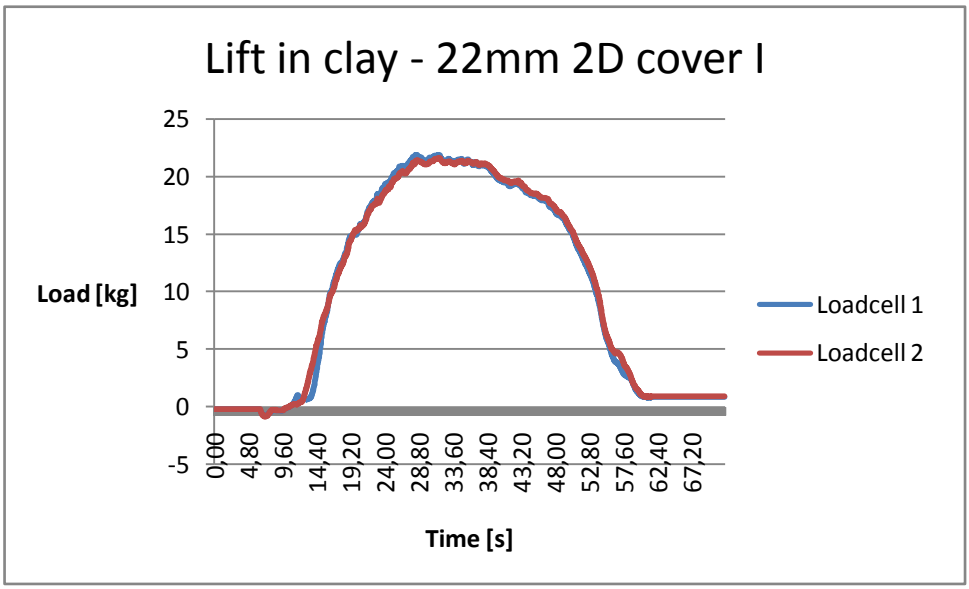

Figure C.40 Lift in clay - 22mm 2D cover I

C.6.5 28mm OD copper pipe with 28mm overburden

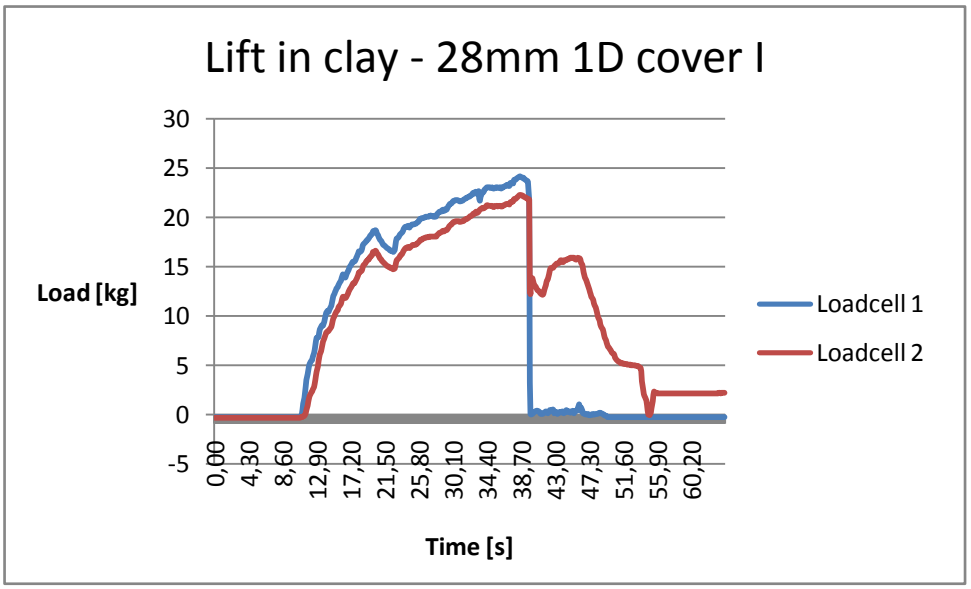

Figure C.41 **Lift in clay - 28mm 1D cover I**

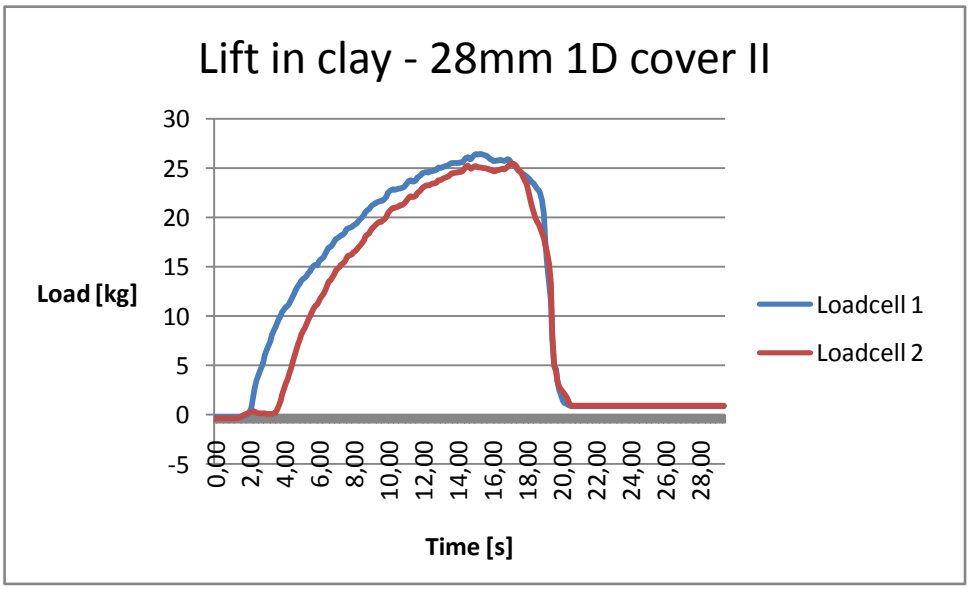

Figure C.42 **Lift in clay - 28mm 1D cover II**

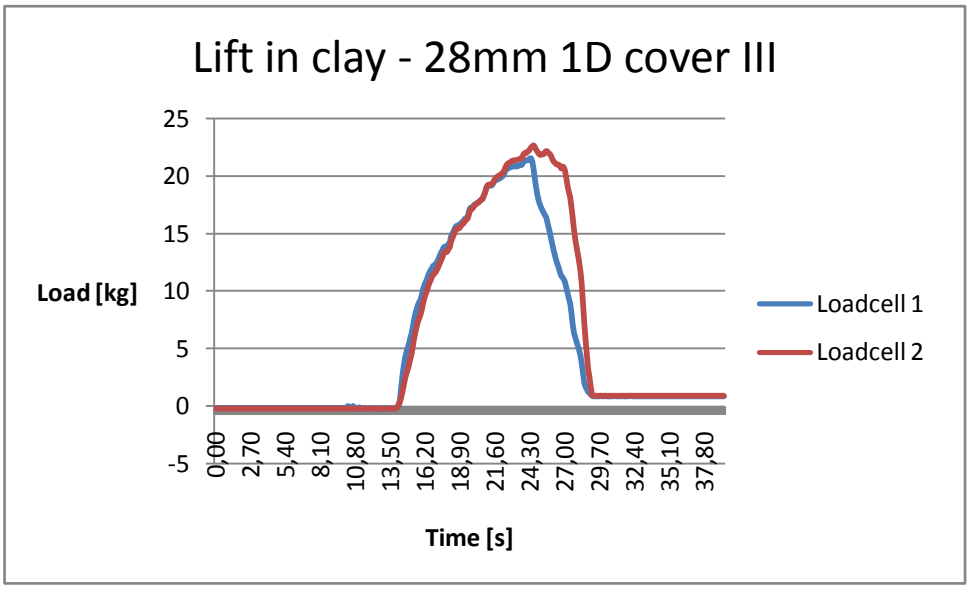

Figure C.43 Lift in clay - 28mm 1D cover III

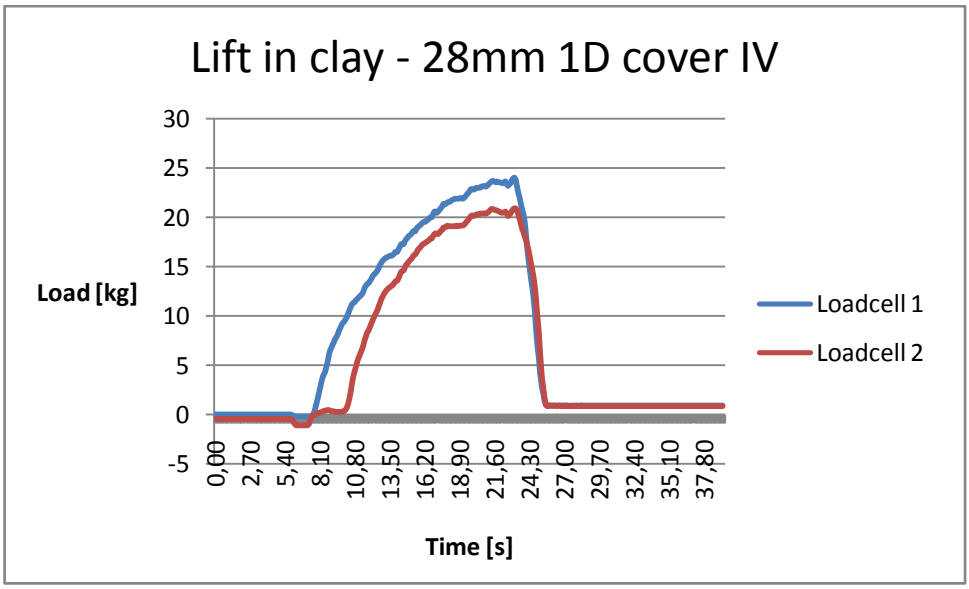

Figure C.44 Lift in clay - 28mm 1D cover IV

C.6.6 28mm OD copper pipe with 28mm overburden

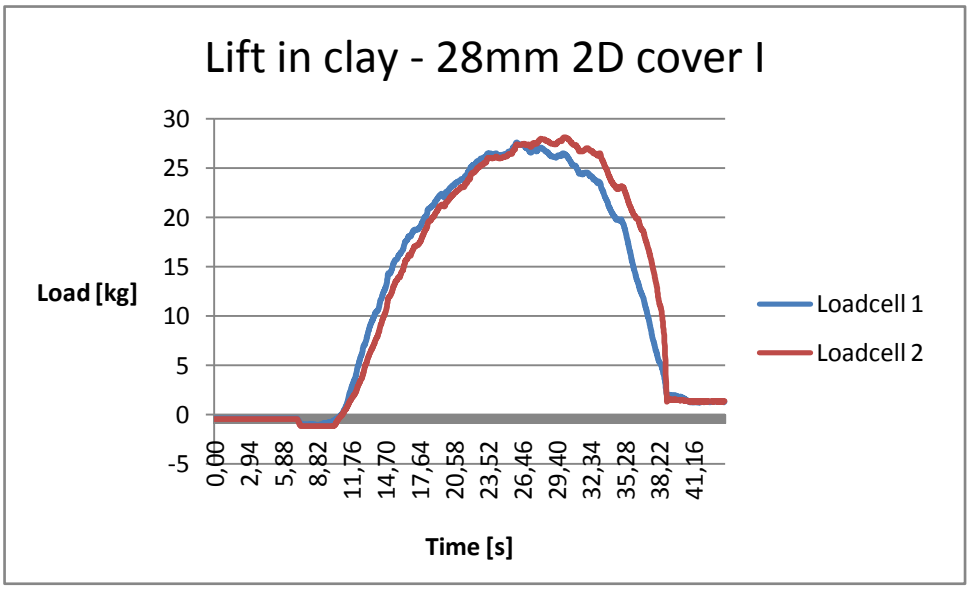

Figure C.45 Lift in clay - 28mm 2D cover I